

**THE STUDY OF COPPER BIOAVAILABILITY AND
MECHANISM OF UPTAKE IN THE TYPE I
METHANOTROPH *METHYLOMICROBIUM ALBUS* BG8**

**Thesis by
Olga Berson**

**In Partial Fulfillment of the Requirements
for the Degree of
the Doctor of Philosophy**

**California Institute of Technology
Pasadena, California**

1996

(Defended May 30, 1996)

© 1996

Olga Berson

All Rights Reserved

Science has 'explained' nothing;
the more we know the more fantastic world becomes
and the profounder surrounding darkness.

– Aldous Huxley

I expect I shall be a student to the end of my days.

– Anton Chechov

Acknowledgments

I am very grateful to my advisor, Dr. Mary E. Lidstrom, who cordially invited me to work in her lab, and who introduced me to the fascinating world of microbiology, genetics and molecular biology. She gave me a lot of support and counsel with my research, career, and even parenting. Dr. Jim J. Morgan was of great assistance in discussion of the results of my experiments and advising on presenting the data for publication. I am also thankful to Dr. Sunney I. Chan for his helpful comments on my paper. Dr. Peter Green was invaluable with his willingness to ensure smooth running of ICP-MS. I cannot thank enough my fellow Russians: Mila Chistoserdova, Andrey Chistoserdov and Sergei Stolar for their support, numerous advise, and, the most important, their friendship. I also appreciate the input of all other members of Lidstrom lab into my research.

Thomas Lloyd was a pleasure to work with on the siderophore project, and I wish him a very successful completion of his thesis. Anna E. Arreola, Jennifer Miller, Elizabeth Price and Wai Kwan were all great MURF/SURF students and I appreciate their help with experiments essential for completion of this project. I must thank Fran Matzen for her inestimable assistance with paperwork .

I would like to dedicate this thesis to the people I love the most: my husband, son, parents and parents-in-law. I treasure their encouragement, I cherish their unconditional love and friendship.

Abstract

Two aspects of copper uptake by the type I methanotroph *Methylomicrobium albus* BG8 were investigated – the effect of copper speciation in the growth medium on copper accumulation and mechanisms of copper transport in this microorganism.

Copper accumulation in *M. albus* BG8 consisted of nonspecific sorption of copper to outer cell layers and copper internalization. Most of the copper accumulated by the cells was nonspecifically sorbed to the cellular surface and was removable by EDTA. This phenomenon was especially prominent when cultures were grown at high total copper concentrations in the growth medium. This reversible binding of copper to external sites (e.g., amino acid, carboxylic, hydroxy groups, etc.) was described by a hyperbolic model with a mean maximum binding capacity of $(1.54 \pm 0.06) \times 10^{-15}$ moles/cell and an apparent half saturation constant of $(1.43 \pm 0.05) \times 10^{-7}$ moles/l. Copper availability to *M. albus* BG8 was related to the cupric ion concentration rather than to that of total copper added to the growth medium. Total internalized copper (total copper not removable by EDTA) was relatively constant at $1\text{--}3 \times 10^{-17}$ moles of copper per cell despite a 100-fold variation in medium total copper and cupric ion concentrations, indicating the presence of a specific homeostasis mechanism for copper.

A specific copper uptake system is expected to be copper-regulated. Several copper-regulated polypeptides were identified in both soluble and membrane cellular

fractions. The corresponding gene of one copper-repressible polypeptide, *corA*, was cloned and sequenced. CorA appeared to be vital for *M. albus* BG8 since an insertion mutant defective in the gene grew very poorly on plates or in liquid culture. It was suggested that CorA might be a divalent metal porin.

Three putative copper ATPase genes, *atpA*, *atpB*, *atpC*, were cloned and the complete sequence of *atpA* was obtained. The gene product of *atpA* contained a copper-binding signature motif, suggesting that AtpA does play a role in copper transport in *M. albus* BG8.

A hypothesis for copper uptake in *M. albus* BG8 was suggested by this research. A copper-repressible protein (CorA) described in Chapter Three may be an outer membrane porin that works in tandem with the putative copper ATPase(s) (Chapter Four). Such a porin would not necessarily be specific for copper, and might be overexpressed under conditions of any divalent metal limitation to facilitate the metal diffusion into periplasm.

List of Abbreviations

ddH₂O, double distilled water

GCG, Genetic Computer Group

ICP/MS, inductively coupled plasma/mass spectrometer

ISE, ion selective electrode

MMO, methane mono-oxygenase

NAD⁺, nicotinamide-adenine dinucleotide

NADH, nicotinamide-adenine dinucleotide, carrying a proton

NMS, nitrate mineral salts medium

PCR, polymerase chain reaction

pMMO, particulate methane mono-oxygenase

sMMO, soluble methane mono-oxygenase

TCE, trichloroethylene

Table of Contents

<i>ACKNOWLEDGMENTS</i>	<i>IV</i>
<i>ABSTRACT</i>	<i>V</i>
<i>LIST OF ABBREVIATIONS</i>	<i>VII</i>
<i>TABLE OF CONTENTS</i>	<i>VIII</i>
<i>LIST OF TABLES</i>	<i>XIII</i>
<i>LIST OF FIGURES</i>	<i>XIV</i>
CHAPTER ONE. INTRODUCTION AND LITERATURE REVIEW	1-1
1.1. INTRODUCTION.....	1-1
1.2. TRICHLOROETHYLENE BIODEGRADATION BY METHANOTROPHS	1-2
1.3. COPPER SPECIATION IN VARIOUS ENVIRONMENTS AND ITS BIOAVAILABILITY.....	1-4
<i>1.3.1. Copper in Seawater</i>	1-5
<i>1.3.2. Copper in Soil</i>	1-6
<i>1.3.3. Copper in Freshwater Environments</i>	1-6
<i>1.3.4. Copper Bioavailability</i>	1-7

1.4. COPPER ION SELECTIVE ELECTRODE AS A METHOD FOR MEASURING CUPRIC ION CONCENTRATION IN FRESH WATER MEDIUM	1–8
1.5. MECHANISMS OF METAL UPTAKE AND TRANSPORT ACROSS THE CELL MEMBRANE FOUND IN MICROORGANISMS.....	1–10
1.6. COPPER RESISTANCE AND METABOLISM IN BACTERIA.....	1–13
1.7. REFERENCES	1–17
1.8. FIGURES.....	1–27
 CHAPTER TWO. STUDY OF COPPER ACCUMULATION BY THE TYPE I METHANOTROPH <i>METHYLOMICROBIUM ALBUS</i> BG8.....	
2.1. INTRODUCTION.....	2–1
2.2. EXPERIMENTAL SECTION.....	2–3
2.2.1. <i>Bacterial Strain and Growth Conditions</i>	2–3
2.2.2. <i>Ion Selective Electrode (ISE) Pretreatment and Calibration</i>	2–4
2.2.3. <i>Mass Spectrometry</i>	2–5
2.2.4. <i>Optical Density Measurement and Calibration</i>	2–6
2.2.5. <i>Copper Accumulation</i>	2–6
2.2.6. <i>Copper Accumulation in <u>M. albus</u> BG8 under Different Complexation Conditions</i>	2–8
2.2.7. <i>Sorption Estimates</i>	2–8
2.2.8. <i>Study of Uptake of Cell–Surface Associated Copper</i>	2–9
2.3. RESULTS AND DISCUSSION.....	2–10
2.3.1. <i>Copper Accumulation</i>	2–10

2.3.2. Copper Accumulation in <i>M. albus</i> BG8 under Different Complexation Conditions.....	2-12
2.3.3. Sorption versus Uptake (Surface-Associated versus Internal Copper).....	2-13
2.3.4. Desorption of Cell-Surface Associated Copper and Uptake into the Cells.....	2-17
2.4. REFERENCES.....	2-20
TABLES.....	2-22
FIGURES.....	2-23
APPENDIX	2-31

CHAPTER THREE. CLONING AND CHARACTERIZATION OF *COR A*,

A GENE ENCODING A COPPER-REPRESSIBLE POLYPEPTIDE PRESUMABLY

INVOLVED IN COPPER UPTAKE BY *METHYLOMICROBIUM*

<i>ALBUS</i> BG8.....	3-1
3.1. INTRODUCTION.....	3-1
3.2. MATERIALS AND METHODS	3-3
3.2.1. Growth of <i>M. albus</i> BG8.....	3-3
3.2.2. Isolation of a Copper-repressible Protein and Sequence Determination.....	3-4
3.2.3. DNA Purification.....	3-6
3.2.4. Cloning and Sequencing of <i>CorA</i>	3-8

3.2.5. Construction of an Insertion Mutation in <i>corA</i>	3-10
3.2.6. Analysis of Insertion Mutation in <i>corA</i>	3-11
3.3. RESULTS AND DISCUSSION.....	3-13
3.3.1. Purification and Sequencing of the 29-kDa Polypeptide.....	3-13
3.3.2. Cloning and Sequencing of <i>corA</i>	3-14
3.3.3. Analysis of the Sequence Data.....	3-15
3.3.4. Mutant characterization	3-17
3.4. CONCLUSIONS	3-19
3.5. REFERENCES.....	3-20
FIGURES.....	3-23
APPENDIX.....	3-41

CHAPTER FOUR. CLONING AND SEQUENCING OF A PUTATIVE COPPER

TRANSPORTING P-TYPE ATPASE	4-1
4.1. INTRODUCTION.....	4-1
4.2. MATERIALS AND METHODS.....	4-4
4.2.1. Bacterial Strains, Culture Conditions, and Preparation of DNA.	4-4
4.2.2. Polymerase Chain Reaction.	4-4
4.2.3. Cloning and Sequencing of ATPase genes	4-8
4.2.4. Construction of Insertion Mutations in <i>atpB</i>	4-9
4.3. RESULTS AND DISCUSSION.....	4-10
4.3.1. Isolation and Cloning of Three Putative Atpase Genes, <i>atpA</i> , <i>atpB</i> and <i>atpC</i>	4-10

4.3.2. Sequencing Results And Sequence Comparison With Known Copper ATPases.....	4-12
4.3.3 Mutant Characterization.....	4-16
4.4. REFERENCES.....	4-17
TABLES.....	4-20
FIGURES.....	4-24
APPENDIX	4-46
CHAPTER FIVE. CONCLUSIONS	5-1
5.1. COPPER SPECIATION AFFECTS COPPER UPTAKE BY <i>M. ALBUS</i> BG8.	5-1
5.2. COPPER UPTAKE IN <i>M. ALBUS</i> BG8 INVOLVES MEMBRANE PROTEINS.	5-3
5.3. SUMMARY	5-7
REFERENCES	5-8
FIGURES.....	5-10

List of Tables

- Table 2.1** Results of ICP/MS and ISE measurements of the initial concentrations of total copper and cupric ion.2-22
- Table 4.1** Codon frequency statistics for *Methylomicrobium albus* BG8 calculated using the CodonPreference program of GCG Package. 4-20
- Table 4.2** The results of sequence comparison of AtpA with some other cation transporting ATPases.4-22

List of Figures

Figure 1.1 The oxidation of methane to carbon dioxide by methanotrophs.....	1–27
Figure 1.2 Major products of TCE degradation by methanotrophic bacteria.....	1–28
Figure 1.3 Examples of microbial nutrient transport systems	1–29
Figure 1.4 Secondary active transport through symports, antiports and uniports: schematic presentation.....	1–30
Figure 1.5 Model for the mechanism of copper resistance in <i>P. syringae</i>	1–31
Figure 1.6 A model of copper resistance and metabolism in <i>E. coli</i>	1–32
Figure 1.7 A diagram of the general structure of P–type ATPases.....	1–33
Figure 1.8 A schematic diagram of the reaction cycle of the Na ⁺ , K ⁺ –ATPase	1–34
Figure 2.1 Model for copper accumulation by <i>M. albus</i> BG8	2–23
Figure 2.2 Specific growth rate observed within a total copper concentration range from 3 to 37 μM.....	2–24
Figure 2.3 Cupric ion concentration and copper accumulation by <i>Methylomicrobium albus</i> BG8 during growth; 3μM and 37 μM total copper added to NMS.	2–25
Figure 2.4 Cellular copper content of <i>M. albus</i> BG8 versus negative logarithm of total copper added to the medium.....	2–26
Figure 2.5 Cellular copper content of <i>M. albus</i> BG8 versus negative logarithm	

of the cupric ion concentration (pCu) in the medium at different EDTA concentrations.	2-27
Figure 2.6 Copper accumulation in cells either untreated or incubated with EDTA and then washed.	2-28
Figure 2.7 Copper accumulated in cells within 1h of inoculation during sorption experiments versus total copper concentration and cupric ion concentration.	2-29
Figure 2.8 Fate of cell-surface associated copper.	2-30
Figure A2.1 The decrease in free copper concentration during media preequilibration.	2-32
Figure A2.2 One of the cupric ion selective electrode calibrations obtained with cupric ion buffers [CuNO ₃ /EDTA/borax].	2-33
Figure A2.3 An example of ICP/MS addition calibration with copper nitrate standards.	2-34
Figure A2.4 Cupric ion concentration and copper accumulation by <i>Methylomicrobium albus</i> BG8 during growth; 4μM and 28 μM total copper added to NMS.	2-35
Figure A2.5 Cupric ion concentration and copper accumulation by <i>Methylomicrobium albus</i> BG8 during growth; 12μM and 19 μM total copper added to NMS.	2-36
Figure A2.6 Cupric ion concentration and copper accumulation by <i>Methylomicrobium albus</i> BG8 during growth; 8μM and 17 μM	

total copper added to NMS.	2-37
Figure A2.7 Total copper concentration in adsorption controls (cell-free NMS medium) versus time.....	2-38
Figure A2.8 Copper accumulation in cells either untreated or incubated with EDTA and then washed; 6 μ M and 54 μ M total copper concentration in the medium.....	2-39
Figure A2.9 Copper accumulation by <i>Methylobacterium albus</i> BG8 during sorption experiments.	2-40
Figure A2.10 Copper accumulated in cells by the end of growth (25-30 h) during sorption experiments versus total copper concentration and cupric ion concentration.....	2-41
Figure 3.1 Identification of copper-repressible and copper-inducible polypeptides in particulate and soluble fractions of <i>Methylobacterium albus</i> BG8 by sodium dodecyl sulfate-polyacrylamide [14% and 10%] gel electrophoresis.....	3-23
Figure 3.2. Comparison of the N-terminal amino acid sequence of Cu ₃ ⁺ with the N-terminal part of fructose biphosphate aldolases.	3-24
Figure 3.3 Hybridization of oligonucleotide probe OB1 to restriction enzyme digests of <i>Methylobacterium albus</i> BG8.....	3-25
Figure 3.4 Physical map of the 4.2-kb <i>Methylobacterium albus</i> BG8 chromosomal region containing <i>orf1</i> , <i>orf2</i> , <i>orf3</i> (<i>corA</i>), <i>orf4</i> , <i>orf5</i>	3-26
Figure 3.5 Nucleotide sequence and deduced amino acid sequence of	

the 4.2-kb <i>M. albus</i> BG8 chromosome region containing <i>orf2</i> , <i>orf3</i> (<i>corA</i>), <i>orf4</i> , and partially <i>orf1</i> , <i>orf5</i>	3-27
Figure 3.6 Frame-independent gene localization using the TestCode Program from the GCG Package.	3-33
Figure 3.7 Predicted structure of <i>corA</i> gene product.	3-34
Figure 3.8 Comparison of the deduced amino acid sequence of CorA with the sequence of calcium release protein.....	3-35
Figure 3.9 Sequence comparison of predicted amino acid sequence of <i>orf1</i> and <i>suhB</i> , extragenic suppressor protein.....	3-36
Figure 3.10 Predicted hydropathy plots of <i>orf1</i> , <i>orf2</i> , <i>orf4</i> and <i>orf5</i> gene products by the Kyte-Doolittle algorithm.	3-37
Figure 3.11 Construction of plasmids pOB16 and pOB17 carrying the mutated <i>corA</i> gene.	3-38
Figure 3.12 The phenotypes of wild type (w.t.), single and double crossover <i>corA</i> mutants of <i>M. albus</i> BG8.....	3-39
Figure 3.13 Characterization of OB12.7 mutant.....	3-40
Figure A3.1 Identification of copper-repressible and copper-inducible polypeptides in particulate and soluble fractions of <i>Methylomicrobium</i> <i>albus</i> BG8 by sodium dodecyl sulfate-polyacrylamide [10% and 14%] gel electrophoresis.	3-42
Figure A3.2 Identification of a copper-repressible polypeptides in particulate and soluble fractions of <i>Methylomicrobium albus</i> BG8 by sodium	

dodecyl sulfate-polyacrylamide [12%] gel electrophoresis.	3–43
Figure A3.3 Identification of copper-repressible and copper-inducible polypeptides in particulate and soluble fractions of <i>Methylomicrobium albus</i> BG8 by sodium dodecyl sulfate-polyacrylamide [16%] gel electrophoresis.	3–44
Figure 4.1 Conserved regions found in P-type ATPases.	4–24
Figure 4.2 PCR-amplified products in an agarose gel.	4–27
Figure 4.3 Construction of plasmid pOB30 carrying mutated <i>atpB</i> gene.	4–28
Figure 4.4 Nucleotide sequence and deduced amino acid sequence of 2.2-kb <i>M. albus</i> BG8 chromosome region containing <i>atpA</i>	4–29
Figure 4.5 Nucleotide sequence and deduced amino acid sequence of the 1.96-kb <i>M. albus</i> BG8 chromosome region containing a fragment of <i>atpB</i>	4–33
Figure 4.6 Nucleotide sequence and deduced amino acid sequence of 1.34-kb <i>M. albus</i> BG8 chromosome region containing a fragment of <i>atpC</i> and the beginning of an identified open reading frame <i>orf1</i>	4–36
Figure 4.7 Sequence comparison of AtpA and partially sequenced AtpB and AtpC.	4–38
Figure 4.8 Graphic representation of sequence similarities between cation transporting ATPases.	4–39
Figure 4.9 Predicted hydropathy plot of the <i>atpA</i> gene product using the Kyte and Doolittle algorithm over a span of 20 residues.	4–40

- Figure 4.10** Predicted hydropathy plot of the C-terminal fragment of the *atpB* gene product using the Kyte and Doolittle algorithm over a span of 20 residues..... 4–41
- Figure 4.11** Predicted hydropathy plot of the C-terminal fragment of the *atpC* gene product using the Kyte and Doolittle algorithm (1982) over a span of 20 residues..... 4–42
- Figure 4.12** Charge and hydrophobicity profiles of AtpA..... 4–43
- Figure 4.13** The phenotypes of wild type, single and double crossover *atpB* mutants of *M. albus* BG8.....4–45
- Figure A4.1** PCR for amplification target genes.....4–47
- Figure 5.1** Schematic representation of the different types of transport systems that might be employed in copper uptake by *Methylomonas albus* BG8.5–10

Chapter One

Introduction and Literature Review

1.1. Introduction

Almost one-half of the population of the United States relies on aquifers for their domestic water supply (Wilson *et al.* 1983). This makes groundwater pollution a critical issue, especially in regard to compounds that are poorly degraded by natural microbial populations. One of such stable and widespread contaminants that is difficult to remove from the environment, is trichloroethylene (TCE). TCE is a synthetic chlorinated hydrocarbon, extensively used for degreasing and cleaning of metals, military hardware and electronic components, dry-cleaning and fumigation. Inattentive storage, inappropriate disposal, and accidental spills of TCE combined with its relatively high water solubility has made it one of the most frequently reported groundwater pollutants in the United States (Ensley 1991; Murray 1993). It is a suspected carcinogen, and it has been designated as a priority pollutant by the US. Environmental Protection Agency (EPA, 1985; Phelps *et al.* 1990). While strong sorption of TCE onto sediments makes pump-and-treat techniques excessively lengthy and financially unfeasible, *in situ* TCE bioremediation has received increasing attention as a promising contaminant-destructive approach as opposed to contaminant-relocative approach (Bouwer and McCarty 1983; Parsons *et al.* 1984; Vogel and McCarty 1985; Ensley 1991; Halden and Chase 1991).

Partial biodegradation of TCE and other chlorinated alkenes under anaerobic conditions has been reported (Bouwer and McCarty 1983; Parsons *et al.* 1984), however, one of the products of degradation that accumulates is vinyl chloride, a known stable carcinogen (Vogel and McCarty 1985; Ensley 1991).

TCE has been shown to be aerobically co-metabolized by a variety of microorganisms in the presence of their primary growth substrate. These include toluene oxidizers (Nelson *et al.*, 1987; Folsom and Chapman, 1991), ammonia oxidizers (Arciero *et al.* 1989), propane oxidizers, phenol oxidizers (Nelson *et al.* 1987; Ensley, 1991; Folsom and Chapman, 1991; Hopkins *et al.* 1993), and methane oxidizers (methanotrophs) (Little *et al.* 1988; Halden and Chase 1991; Park *et al.* 1991, Higgins *et al.* 1980). Methanotrophs have been suggested to be one of the more favorable groups of bacteria for *in situ* TCE bioremediation due to their ubiquity in nature, their ability to degrade chlorinated alkenes to non-toxic compounds that can be utilized by heterotrophic bacteria, and their ability to reduce TCE levels to below drinking water standards.

1.2. Trichloroethylene Biodegradation by Methanotrophs

Methanotrophs are Gram-negative bacteria that utilize methane as a sole source of carbon and energy. They oxidize methane to carbon dioxide by a route involving two-electron oxidation steps via methanol, formaldehyde and formate (Figure 1.1) (Higgins *et al.* 1980). Methane mono-oxygenase (MMO), the first enzyme in the pathway, is capable of inserting an oxygen atom into a variety of hydrocarbon substrates and chlorinated

compounds, including TCE, to produce alkene epoxides, which then break down in water to intermediates that are easily utilized by heterotrophic bacteria (Figure 1.2)(Little *et al.* 1988, Halden and Chase 1991).

The methanotrophs are divided into three groups (type I, type II and type X) based on their morphological, biochemical, and phylogenetic characteristics (Hanson *et al.* 1991). MMO is found in two forms in methanotrophs: soluble (sMMO) and membrane-bound, or particulate (pMMO). The pMMO is present in all known methanotrophs, whereas sMMO is found in only a few strains, mostly type II and type X (Hanson *et al.* 1991; King 1992; Peltola *et al.* 1993). In strains that contain both pMMO and sMMO, pMMO predominates in cultures grown under conditions of copper-sufficiency, while sMMO is found only under conditions of copper limitation (Halden and Chase 1991; Park *et al.* 1991; King 1992; Tsien and Hanson 1992; Chan *et al.* 1993; Peltola *et al.* 1993).

Both pMMO and sMMO can oxidize TCE, but the maximum TCE oxidation rates by cells containing sMMO are 100-1000 fold higher than cells containing pMMO (DiSpirito *et al.* 1992). However, a recent study (DiSpirito *et al.* 1992) has shown that type I methanotrophs expressing only pMMO are capable of TCE removal to the level required for drinking water (5ppb).

Little is known of the structure of pMMO since it is highly unstable *in vitro* and until very recently (Ngyuen and Chan, unpublished) has not been reproducibly purified. However, it appears to be a copper enzyme (Chan *et al.* 1993; Ngyuen *et al.* 1994). It was suggested that the bulk of the membrane-bound copper ions exist in the form of trinuclear copper clusters serving as catalytic sites of monooxygenase activity of the

pMMO system (Chan *et al.* 1993; Ngyuen *et al.* 1994). Addition of copper to growth medium in a concentration range that is neither growth-limiting nor toxic results in increased cell yield and MMO activity (Collins *et al.* 1991), as well as changes in pMMO kinetics (Semrau *et al.* 1993). This effect is even more dramatic on TCE oxidation, as cells containing pMMO that are grown at 2 μ M copper added to the medium show no detectable TCE degradation (Semrau 1995, Smith 1996). Therefore, these responses to copper could have a major influence on TCE bioremediation by natural populations of methanotrophs, especially the type I strains that lack sMMO. All available data suggest that natural populations of methanotrophs are not copper-limited (Lidstrom and Semrau 1995). It is important, therefore, to investigate copper bioavailability to a type I methanotroph under conditions of copper-sufficiency.

1.3. Copper Speciation in Various Environments and its Bioavailability

Copper is widely found in the environment. It is present as a component in such ores as chalcopyrite (CuFeS_2) and chalcocite (Cu_2S). Copper, released from minerals during weathering, forms soluble cupric and cuprous salts, as well as organic complexes. An extensive use of copper as an antimicrobial agent in agriculture causes its additional release into soils and groundwater (Brown *et al.* 1992a).

1.3.1. Copper in Seawater

Copper is a trace element in seawater. Total copper concentrations in seawater vary from 0.1-0.5 nM at the surface to 5 nM in bottom waters. Copper distribution in seawater was proposed to be controlled by its depletion at the surface and regeneration from the sediments, as well as by copper scavenging throughout the water column (Boyle and Edmond 1975; Bruland *et al.* 1980). It appears from numerous studies that greater than 99.7% of the total dissolved copper is present as organic complexes in seawater (Sunda and Ferguson 1983; Sunda and Hanson 1987; Coale and Bruland 1988; Coale and Bruland 1990; Moffett *et al.* 1990; Van den Berg *et al.* 1990, Bruland *et al.* 1991; Van den Berg and Donat 1992). At depths of 1000 m, about 50-70% of the total dissolved copper is organically bound. Two classes of copper-binding ligands were identified throughout the water column and were suggested to be of biological origin: a strong ligand class [$\log K_{\text{stab}}=11.5$] in the surface waters (low copper concentrations) and a weaker class of ligands at middepths (higher copper concentrations) [$\log K_{\text{stab}}=8.5$] (Coale and Bruland 1990). A pH, temperature and, possibly, pressure dependence of the ligand/copper association has been suggested by Coale and Bruland (1990).

Inorganic copper species contribute less than 0.3 % of the total copper with free cupric ion [$\text{Cu}^{2+}(\text{H}_2\text{O})_6$] comprising approximately 4% of the inorganic fraction (Bruland *et al.* 1991). Complexation with carbonate and hydroxide dominates the inorganic copper speciation in seawater; a significant effect of sulfide complexation on

inorganic copper speciation has been also reported in some areas (Coale and Bruland 1990). The free copper concentration varies from $10^{-13.1}$ M at the surface to $10^{-9.9}$ M at 300 m depth. It appears that only a small fraction of total copper is present as Cu(I) in sea water (Moffett and Zika 1988).

1.3.2. Copper in Soil

Copper is distributed between the liquid and solid phase in soils. The total concentration of Cu in pore water is estimated to be on the order of 10^{-7} - 10^{-9} M. Over 99% of the Cu is complexed by ligands, predominately humic substances (Hodgson *et al.* 1965; Berggren 1989). Concentrations of free copper depend on the type of the soil, and are in a range between 10^{-10} M and 10^{-12} M for uncontaminated soils (Hodgson *et al.*, 1965.).

1.3.3. Copper in Freshwater Environments

Copper in freshwater environments can be distributed between several phases including sediment, suspended particulates, true solution (porewater and water column) and it can be adsorbed onto hydrous oxide and humic colloids in water. Copper in true solution can exist as the free aqueous species $[\text{Cu}^{2+}(\text{H}_2\text{O})_6]$, inorganic complexes, and organic complexes (Guy and Kean 1980). On the basis of studies of oxidation kinetics of Cu(I) (Moffett and Zika 1983), it has been concluded that concentrations of Cu(I) in freshwater and low salinity environments should be exceedingly small. A significant fraction of the Cu(II) in freshwater is complexed by humic substances (Hering and Morel

1988), which results in cupric ion concentrations of 10^{-11} - 10^{-18} M (Apte *et al.* 1990a, Van Den Berg *et al.* 1990).

1.3.4. Copper Bioavailability

Copper exhibits complex chemical speciation in the environment, however, there is a general agreement that biological uptake of copper and its toxicity depend on the level of cupric ion, not the total copper concentration (Sunda and Guillard 1976; Anderson and Morel 1978; Zevenhuizen *et al.* 1979; Blust *et al.* 1986; Coale and Bruland 1990; Bruland *et al.* 1991; Langford and Guzman 1992). Inorganically complexed metal species equilibrate very rapidly with free metal ion. Thus, the total inorganic complex concentrations define an upper limit for the bioavailability of the metal (Morel *et al.* 1991).

The significant effects of hardness, temperature, and pH on copper bioavailability have been indicated in many studies (Gadd and Griffiths 1978; Sunda and Ferguson 1983; Coale and Bruland 1990; Meador 1991). The work of Bruland and coworkers (1991) has established the importance of Cu^{2+} : Mn^{2+} and Cu^{2+} : Zn^{2+} competition for cellular uptake sites in overall copper bioavailability.

Several experiments reported in the literature on metal- biota interactions have shown that speciation and, thus, bioavailability of copper ions may change during growth of microorganisms. A growing microorganism excretes compounds that can form complexes with metals and change the pH of the medium causing precipitation of metal ions as oxalates or phosphates (Bird *et al.* 1985; Hughes *et al.* 1991; Cabral, 1992). It has

been found, however, that EDTA and NTA added to normal culture media overwhelm such effects (Guy and Kean 1980).

1.4. Copper Ion Selective Electrode as a Method for Measuring Cupric Ion Concentration in Fresh Water Medium

Various techniques have been used to measure free copper concentration. These methods include:

- Anodic Stripping Voltammetry (ASV) and Differential Pulse Anodic Stripping Voltammetry (DPASV) (Coale and Bruland 1988; Powell and Town 1991);
- Adsorption on an ion-exchange resin;
- Liquid/liquid extraction (Berggren 1992; Hodgson *et al.* 1965; Moffett and Zika 1987; Moffett *et al.* 1990; Nair *et al.* 1991);
- Cathodic Stripping Voltammetry (CSV) (Van den Berg 1984; Apte *et al.* 1988; Jones and Hart 1989; Apte *et al.* 1990a; Apte *et al.* 1990b; Van den Berg *et al.* 1990; Gardner and Ravenscroft, 1991, Ravenscroft and Gardner, 1991, Van den Berg 1992);
- Chemiluminescence detection (Sunda and Huntsman 1991; Coale *et al.* 1992);
- Competitive equilibrium with acetyl acetone or EDTA and subsequent SEP-PAK adsorption (Sunda and Hanson 1987);
- Ion-selective electrode (ISE) measurements (Sunda and Guillard 1976, McKnight and Morel 1979; Zevenhuizen *et al.* 1979; Jardim and Pearson 1984; Shuttleworth and Unz 1991; Cabral 1992).

ISE presents a simple and inexpensive approach to copper speciation. It allows the direct detection of the free copper in fresh water or other media with low chloride ion activity. Chloride interference with cupric ion selective electrode measurements has been reported (Westall et al. 1979). The assay of metal uptake does not require separation of cells from the medium, thus limiting artifacts in experiments with cultures. At constant temperature and ionic strength, the potential of an ISE is directly proportional to the logarithm of the primary ion concentration. The copper selective electrode, when calibrated with an appropriate metal-buffer can be used to monitor free copper ion in bacterial medium with cupric ion concentrations as low as 10^{-19} M (Avdeef et al. 1983). To obtain the best performance of an ICE, the response of the electrode should be close to the Nernstian response over the widest possible pCu range, i.e. the electrode potential E should obey the equation: $E = E^{\circ'} + \frac{RT}{2F} \ln[\text{Cu}^{2+}]$,

where $[\text{Cu}^{2+}]$ is the concentration of copper(II) in the measured solutions.

Calibration of ion-selective electrodes in the range below $1\mu\text{M}$ - $10\mu\text{M}$ with solutions obtained from salts or by dilution of more concentrated standard solutions is undesirable for the following reasons:

- The preparation of very dilute solutions is inaccurate,
- Loss or contamination of dilute solutions may create serious positive or negative errors (Avdeef *et al.* 1983; Hulanicki *et al.* 1991).

The use of metal buffers helps to avoid these difficulties. Several copper buffers have been reported to be successfully used to obtain linear calibration curves up to

$pCu=12$ ($pCu=-\log[Cu^{2+}]$): Cu^{2+}/NH_3 ; $Cu^{2+}/EDTA$; Cu^{2+}/NTA ; Cu^{2+}/en

(ethylenediamine) (Avdeef *et al.* 1983). Since Cu^{2+} concentration depends on pH, a pH buffer should be added also. The following buffers have been often used: acetate, maleate, borax, TRIS [tris(hydroxymethyl)-methylamine], ACES [2-(2-amino-2-oxoethyl-amino)ethanesulfonic acid,2-(carbamoyl-methylamino)ethanesulfonic acid], HEPES [4-(2-hydroxyethyl] piperazine-1-ethanesulfonic acid)], PIPES [piperazine-1,4-bis(2-ethanesulfonic acid)], etc. (Hulanicki *et al.* 1991). In this study a $Cu^{2+}/EDTA$ /borax buffer system was used to calibrate a copper ion selective electrode in the low concentration range.

1.5. Mechanisms of Metal Uptake and Transport Across the Cell

Membrane Found in Microorganisms

Metal uptake by microorganisms, defined as transport of nutrient metals through membrane(s) into the cytoplasm for further assimilation, appears to occur mainly in the following ways: nonspecific binding of metal to cell surfaces, passive diffusion of lipid soluble inorganic metal complexes, and specific transport (Doyle *et al.* 1975; Gadd and Griffiths 1978; Blust *et al.* 1986).

The first method of uptake is important since most heavy metals are easily adsorbed onto the surface of microbial cells, both living and dead. Copper can be complexed by polygalacturonic acid, one of the components of the outer layers of

bacterial cells (Gadd and Griffiths 1978). The hydrophobic nature of the cell membrane prevents passive movement of polar solute molecules such as inorganic salts, and ions. However, despite careful regulation of heavy metal uptake in cells, liposoluble uncharged complexes may penetrate cell membranes by becoming dissolved in the lipid phase of the membrane and so the second mechanism of metal uptake also occurs (Doyle *et al.* 1975).

The third mechanism of specific transport is widespread in microorganisms, and involves various transport systems. They can be classified on the basis of the mechanism and the protein components of a given system into the following groups: active transport, secondary active transport, binding protein dependent transport, and group translocation (Neidhardt *et al.* 1990) (Figures 1.3 and 1.4). Active transport (Figure 1.3A) is a process involving an energy-dependent pump in which the substance being transported combines with a stereospecific, transmembrane protein which then releases the chemically unchanged substance inside the cell (Brock and Madigan 1991).

A movement of a substrate across the cytoplasmic membrane due to a previously established ion gradient is called secondary active transport. It employs three types of proteins: symports (Figure 1.4A), antiports (Figure 1.4B) and uniports (Figure 1.4C). Uniports transport a substance from one side of the membrane to another. Antiports and symports move the substrate across the membrane along with a second substrate required for transport of the first. With antiports, the first and second substrate move in opposite

directions across the membrane, whereas with symports both substrates move in the same direction (Neidhardt *et al.* 1990; Brock and Madigan 1991).

Binding protein-dependent transport systems (Figure 1.3B) include a periplasmic substrate-binding protein and three or four additional inner membrane-associated proteins. The former serves as the primary recognition site for uptake, the latter are involved in substrate translocation and energy coupling. This mechanism has been proven to be ATP dependent (Higgins *et al.* 1990). Sensitivity to osmotic shock and differential sensitivity to metabolic inhibitors distinguish this transport system from others (Higgins *et al.* 1990). Group translocation (Figure 1.3C) is a mechanism in which the substrate is chemically altered as it crosses the cytoplasmic membrane, usually via phosphorylation (Neidhardt *et al.* 1990; Brock and Madigan 1991).

A special uptake system has been identified in microorganisms grown under iron limitation. Iron(III)-specific chelating compounds (siderophores) are responsible for solubilization of iron(III) hydroxide aggregates and their further uptake by some bacterial, yeast, and fungal species (Simpson and Neilands 1976; Trick *et al.* 1983). Siderophores are released into the medium for subsequent transmembrane transfer of the metal-ligand complex via specialized receptor proteins (Morel *et al.* 1991). Once ferrisiderophore (siderophore with bound iron) has been linked to the receptor, iron uptake may occur by two different mechanisms. In the first, only iron enters the membrane while the ligand remains outside. In the alternative mechanism the ferrisiderophore complex enters the cell and the chelate is either hydrolyzed or reused after iron release (Martinez *et al.* 1990).

1.6. Copper Resistance and Metabolism in Bacteria

Copper plays a dual biological role as an essential micronutrient which is required for the synthesis of metalloproteins and as a growth inhibitor at high concentrations. Copper toxicity is associated with its ability to modify the active sites of metalloproteins and to catalyze membrane disrupting redox reactions in the cells. Therefore, the microorganisms must possess delicate mechanisms for maintaining such a restricted level of free copper within a cell that is neither limiting nor toxic (Sunda and Huntsman 1985; Lee *et al.* 1990; Silver and Walderhaug 1992; Brown *et al.* 1992b). A number of bacteria have been shown to be copper resistant due to nonspecifically produced high levels of extracellular polysaccharides (Bitton 1978), iron-binding siderophores (McKnight and Morel 1979) and other organic products (Mittelman and Geesey 1985; Hardstedt-Romeo and Guassia-Barelli 1980). However, some examples of a specific copper-inducible resistance have been identified.

Copper concentrations in bacterial cells can be regulated at two levels: metal sequestration and metal uptake. Metallothioneins, low molecular weight cysteine-rich metalloproteins are involved in sequestering intracellular copper in eukaryotes (Ecker *et al.* 1986; Butt *et al.* 1984). The marine bacterium *Vibrio alginolyticus* produces extracellular copper-binding proteins for copper detoxification (Harwood-Sears and Gordon 1990), while sulfate-reducing *Desulfovibrio* spp. tolerate high copper levels by producing sulfide that complexes copper and reduces copper toxicity (Cervantes and Gutierrez-Corona 1994). Sequestration of copper by a set of four periplasmic and outer

membrane proteins has been suggested as a resistance mechanism in *Pseudomonas syringae* (Mellano 1988; Cha and Cooksey 1991; Cooksey and Azad 1992; Cha and Cooksey 1993) (Figure 1.5). This mechanism has been well-studied. Four genes have been shown to encode these proteins, *copA*, *copB*, *copC* and *copD*. These genes have been sequenced and several copper binding motifs have been identified. Two additional genes *pcoR* and *pcoS* follow the *pcoABCD* operon and seem to be members of a two-component regulatory system involved in copper regulation (Cervantes and Gutierrez-Corona 1994). The proteins produced by *cop* genes are copper-inducible. It has been found that the periplasmic proteins CopA and CopC are able to bind 11 and 1 copper atoms per polypeptide, respectively (Figure 1.5). CopB is an outer membrane protein and CopD is a probable inner membrane protein. (Brown *et al.* 1992b; Silver 1992; Mellano 1988; Cha and Cooksey 1991; Cooksey and Azad 1992; Cha and Cooksey 1993, Cooksey 1994). It is thought that in addition to the copper sequestering function of CopC, it can also function in copper uptake, together with CopD (Cooksey 1994).

An alternative strategy for maintaining internal cupric ion concentrations is adopted by *Escherichia coli*. Four plasmid-encoded genes (*pcoARBC*) are required for copper resistance and seven chromosomal genes (*cutA-cutF*, *cutR*) are involved in copper metabolism in *E. coli* (Figure 1.6). Under non-toxic copper concentrations, copper enters the cell via two uptake proteins: CutA and CutB. CutA is a specific copper uptake protein, whereas CutB is also involved in Zn uptake. There are two intracellular copper-binding storage/carrier proteins (CutE and CutF) that may be responsible for preventing Cu(I) from damaging intracellular components. Export of copper that exceeds

physiological requirements is mediated by two structural proteins: CutC and CutD, which are probably copper efflux ATPases (Cervantes and Gutierrez-Corona 1994). Under conditions of high copper concentrations plasmid-encoded *pco* genes are expressed. It appears that *pcoA* and *pcoB* genes interact with *cutC* and *cutD* to export extra copper from the cell, whereas *pcoC* is involved in cytoplasmic copper storage/transport. *CutR* and *pcoR* genes have been suggested to be involved in regulation of copper metabolism and resistance in *E. coli* and they seem to belong to the large family of bacterial two-component regulatory systems involved in sensing environmental signals (Silver and Walderhaug 1992; Brown *et al.* 1992b; Lee *et al.* 1990; Rogers *et al.* 1991; Cooksey, 1993; Gupta *et al.* 1995).

Recent work has correlated rearrangements in the gene encoding a copper-transporting P-type ATPase with Menkens syndrome, a lethal disease that involves reduced activity of numerous copper-containing proteins (Vulpe 1993). There are, as well, several examples of bacterial copper transport P-type ATPases. Two copper efflux ATPases have been identified in *Enterococcus hirae* (Oddermatt *et al.* 1993), the above-mentioned proteins CutC and CutD of *Escherichia coli* have been suggested to be copper efflux ATPases (Cervantes and Gutierrez-Corona 1994), and a *Helicobacter pylori* gene encoding a putative copper ATPase has been cloned and sequenced recently (Ge and Taylor 1995). Examples of other cation P-type ATPases, both eukaryotic and bacterial, include Na^+ , K^+ -ATPase isolated from sheep kidney (Shull *et al.* 1985), K^+ -ATPase of *Escherichia coli* (Hesse *et al.* 1984), Ca^{2+} -ATPase of rabbit sarcoplasmic reticulum (Hesse *et al.* 1984; Brandl *et al.* 1986), a putative cation ATPase of *Synechococcus* sp.

(Kashiwagi *et al.* 1995), Cd²⁺-efflux ATPase of *Staphylococcus aureus* (Nucifora *et al.* 1989), K⁺ATPase of *Streptococcus faecalis* (Soloiz *et al.* 1987), and many others.

These enzymes belong to a family of membrane-bound cation translocation pumps consisting of a main polypeptide chain of about 110,000 MW that perform both catalytic and transport functions. In some cases there are additional subunits or dimerization (Cervantes and Gutierrez-Corona 1994; Inesi and Kirtley 1992). There are several common structural features in all P-type ATPases despite the variety of ions they transport. The polypeptide chain includes a relatively large extramembranous domain and eight to ten transmembrane helical structures that span the membrane bilayer, forming four to five hairpins (Figure 1.7). All ion transporting ATPases contain a phosphorylation domain with the conserved amino acid sequence DKTGT(I/L)T and an aspartyl residue that is involved in the formation of a covalent intermediate (E-P) during the reaction cycle (Figure 1.8). Another common feature is two conformational forms of the phosphorylated intermediate, referred to as E1 and E2, covalently identical but differing in their affinity to substrates (Epstein 1990).

Despite the importance of copper to the physiology of methanotrophs, nothing is presently understood about the molecular mechanisms of copper acquisition from the environment. The research presented in this thesis investigates this area.

1.7. References

- Anderson, D. M. and F. M. M. Morel.** 1978. Copper sensitivity of *Gonyaulax tamarensis*. *Limnol. Oceanogr.* **23(2)**:283-295.
- Apte, S. C., M. J. Gardner, and J. E. Ravenscroft.** 1988. An evaluation of voltammetric titration procedures for the determination of trace metal complexation in natural waters by use of computer simulation. *Anal. Chim. Acta* **212**:1-21.
- Apte, S. C., M. J. Gardner, and J. E. Ravenscroft.** 1990a. An investigation of copper complexation in the severn estuary using differential pulse cathodic stripping voltammetry. *Mar. Chem.* **29**:63-75.
- Apte, S. C., M. J. Gardner, J. E. Ravenscroft, and J. A. Turrell.** 1990b. Examination of the range of copper complexing ligands in natural waters using a combination of cathodic stripping voltammetry and computer simulation. *Anal. Chim. Acta* **235**:287-297.
- Arciero, D., T. Vannelli, M. Logan, and A.B. Hooper.** 1989. Degradation of trichloroethylene by the ammonia-oxidizing bacterium *Nitrosomonas europaea*. *Biochem. Biophys. Res. Commun.* **159**:640-643.
- Avdeef, A., J. Zabronsky, and H. H. Stuting.** 1983. Calibration of copper ion selective electrode response to pCu 19. *Anal. Chem.* **55**:298-304.
- Berggren, D.** 1989. Speciation of aluminum, cadmium, copper, and lead in humic soil solutions - a comparison of the ion-exchange column procedure and equilibrium dialysis. *Intern. J. Environ. Anal. Chem.* **35**:1-15.
- Berggren, D.** 1992. Speciation of copper in soil solutions from podzols and cambisols of S. Sweden. *Water Air And Soil Pollution* **62**:111-123.
- Bird, N. P., J. G. Chambers, R. W. Leech, and D. Cummins.** 1985. A note on the use of metal species in microbiological tests involving growth media. *J. Appl. Bacteriol.* **59**:353-355.
- Bitton, G. and V. Freihofner.** 1978. Influence of extracellular polysaccharides on the toxicity of copper and cadmium toward *Klebsiella aerogenes*. *Microb. Ecol.* **4**:119-125.
- Blust, R., E. Verheyen, C. Doumen, and W. Declair.** 1986. Effect of complexation by organic ligands on the bioavailability of copper to the Brine Shrimp, *Artemia* sp. *Aquatic Toxicol.* **8**:211-221.

- Bouwer, E. J., and P.L. McCarty.** 1983. Transformation of 1- and 2-carbon halogenated aliphatic organic compounds under methanogenic conditions. *Appl. Environ. Microbiol.* **45**:1286-1294.
- Boyle, E. A. and J. M. Edmond.** 1975. Copper in surface waters south of New Zealand. *Nature* **253**:107-109.
- Brandl, C. J., N. M. Green, B. Korczak, and D. H. MacLennan.** 1986. Two Ca²⁺ ATPase genes: homology and mechanistic implications of deduced amino acid sequences. *Cell* **44**:597-607.
- Brock, T. D. and M. T. Madigan.** 1991. p. 50-55. In *Biology of Microorganisms*. Prentice Hall, Englewood Cliffs.
- Brown, C. M. and C. G. Trick.** 1992a. Response of the cyanobacterium, *Oscillatoria tenuis*, to low iron environments - the effect on growth-rate and evidence for siderophore production. *Arch. Microbiol.* **157**:349-354.
- Brown, N. L., D. A. Rouch, and B. T. O. Lee.** 1992b. Copper resistance determinants in bacteria. *Plasmid* **27**:41-51.
- Bruland, K. W.** 1980. Oceanographic distributions of cadmium, zinc, nickel, and copper in the North Pacific. *Earth and Planet. Sci. Lett.* **47**:176-198.
- Bruland, K. W., J. R. Donat, and D. A. Hutchins.** 1991. Interactive influences of bioactive trace metals on biological production in oceanic waters. *Limnol. Oceanogr.* **36**:1555-1577.
- Butt, T. R., E. J. Sternberg, J. A. Gorman, P. Clark, D. Hamer, M. Rosenberg, and S. Crooke.** 1984. Copper metallothionein of yeast, structure of the gene, and regulation of expression. *Proc. Natl. Acad. Sci. USA* **81**:3332-3336.
- Cabral, J. P. S.** 1992. Limitations of the use of an ion-selective electrode in the study of the uptake of Cu²⁺ by *Pseudomonas syringae*. *J. Microbiol. Methods* **16**:149-156.
- Cervantes, C. and F. Gutierrez-Corona.** 1994. Copper resistance mechanisms in bacteria and fungi. *FEMS microbiol. rev.* **14**:121-138.
- Cha, J. S. and D. A. Cooksey.** 1991. Copper resistance in *Pseudomonas syringae* mediated by periplasmic and outer-membrane proteins. *Proc. Natl. Acad. Sci. USA* **88**:8915-8919.

- Cha, J. S. and D. A. Cooksey.** 1993. Copper hypersensitivity and uptake in *Pseudomonas syringae* containing cloned components of the copper resistance operon. *Appl. Environ. Microbiol.* **59**:1671-1674.
- Chan, S. I., H. H. T. Nguyen, A. K. Shiemke, and M. E. Lidstrom.** 1993. Biochemical and biophysical studies toward characterization of the membrane-associated methane monooxygenase, p. 93-107. In J. C. Murrell and D. P. Kelly (eds.), *Microbial Growth on C1 Compounds*. Intercept, Andover.
- Coale, K. H. and K. W. Bruland.** 1988. Copper complexation in the Northeast Pacific. *Limnol. Oceanogr.* **33**:1084-1101.
- Coale, K. H. and K. W. Bruland.** 1990. Spatial and temporal variability in copper complexation in the north pacific. *Deep-Sea Res.* **37**:317-336.
- Coale, K. H., K. S. Johnson, P. M. Stout, and C. M. Sakamoto.** 1992. Determination of copper in sea water using a flow-injection method with chemiluminescence detection. *Anal. Chim. Acta* **266**:345-351.
- Collins, M. L. P., L. A. Buchholz, and C. C. Remsen.** 1991. Effect of copper on *Methylomonas albus* BG8. *Appl. Environ. Microbiol.* **57**:1261-1264.
- Cooksey, D. A. and H. R. Azad.** 1992. Accumulation of copper and other metals by copper-resistant plant- pathogenic and saprophytic pseudomonads. *Appl. Environ. Microbiol.* **58**:274-278.
- Cooksey, D. A.** 1993. Copper uptake and resistance in bacteria. *Mol. microbiol.* **7(1)**:1-5.
- Cooksey, D. A.** 1994. Molecular mechanisms of copper resistance and accumulation in bacteria. *FEMS microbiol. rev.* **14**:381-386.
- Cronan, J. E., R. B. Gennis, and S. R. Maloy.** 1989. p. 31-55. In F. C. Neidhardt, J. L. Ingraham, B. Magasanik, K. B. Low, M. Schaechter, and H. E. Umbarger (eds.), *Escherichia coli* and *Salmonella typhimurium*. Cellular and Molecular biology. American Society for Microbiology, Washington, D.C.
- Dancis, A., D. S. Yuan, D. Haile, C. Askwith, D. Eide, C. Moehle, J. Kaplan, and R. D. Klausner.** 1994. Molecular characterization of a copper transport protein in *S.cerevisiae*: An unexpected role for copper in iron transport. *Cell* **76**:393-402.
- Dispirito, A. A., J. Gullede, J. C. Murrell, A. K. Shiemke, M. E. Lidstrom, and C. L. Krema.** 1992. Trichloroethylene oxidation by the membrane associated methane monooxygenase in type I, type II and type X methanotrophs. *Biodegr.* **2**:151-164.

- Doyle, J. J., R. T. Marshall, and W. H. Pfander.** 1975. Effects of cadmium on the growth and uptake of cadmium by microorganisms. *Appl. Microbiol.* **29**:562-564.
- Ecker, D. J., T. R. Butt, E. J. Sternberg, M. P. Neeper, C. Debouck, J. A. Gorman, and S. T. Crooke.** 1986. Yeast metallothionein function in metal ion detoxification. *The J. Biol. Chem.* **261**:16895-16900.
- Ensley, B.D.** 1991. Biochemical diversity of trichloroethylene metabolism. *Ann. Rev. Microbiol.* **45**:283-299.
- Epstein, W.** 1990. Bacterial transport ATPases. p. 87-110. In I. C. Gunsalus, J. R. Sokatch, and L. N. Ornston (eds.), *The bacteria: A treatise on structure and function*. Academic Press, San Diego.
- Folsom, B. R. and P. J. Chapman.** 1991. Performance characterization of a model bioreactor for the biodegradation of trichloroethylene by *Pseudomonas cepacia* G4. *Appl. Environ. Microbiol.* **57**:1602-1608.
- Gadd, G. M. and A. J. Griffiths.** 1978. Microorganisms and heavy metal toxicity. *Microb. Ecol.* **4**:303-317.
- Gardner, M. and J. Ravenscroft.** 1991. The behavior of copper complexation in rivers and estuaries: 2 studies in North East England. *Chemosphere Limnol. Oceanogr.* **23**:695-713.
- Ge, Z., K. Hiratsuka, and D. E. Taylor.** 1995. Nucleotide sequence and mutational analysis indicate that two *Helicobacter pylori* genes encode a P-type ATPase and a cation-binding protein associated with copper transport. *Mol. microbiol.* **15**:97-106.
- Gupta, S. D., B. T. O. Lee, J. Camakaris, and H. C. Wu.** 1995. Identification of *cutC* and *cutF (nlpE)* genes involved in copper tolerance in *Escherichia coli*. *J. Bact.* **177**:4207-4215.
- Guy, R. D. and A. R. Kean.** 1980. Algae as a chemical speciation monitor - a comparison of algal growth and computer calculated speciation. *Wat. Res.* **14**:891-899.
- Halden, K. and H. A. Chase.** 1991. Methanotrophs for cleanup of polluted aquifers. *Wat. Sci. Tech.* **24**:9-17.
- Hanson, R. S., A. I. Netrusov, and K. Tsuji.** 1991. p. 2350-2364. In A. Balows, H. G. Truper, M. Dworkin, W. Harder, and K. H. Schleifer (eds.), *The Prokaryotes*. Springer-Verlag, New York.

Hardstedt-Romeo, M. and M. Gnassia-Barelli. 1980. Effect of complexation by natural phytoplankton exudates on the accumulation of cadmium and copper by the Haptophyceae *Cricosphaera elongata*. Mar. Biol. **59**:79-84.

Harwood-Sears, V. and A. S. Gordon. 1990. Copper-induced production of copper-binding supernatant proteins by the marine bacterium *Vibrio alginolyticus*. Appl. Environ. Microbiol. **56**:1327-1332.

Hering, J. G. and F. M. M. Morel. 1988. Humic-acid complexation of calcium and copper. Environ. Sci. Technol. **22**:1234-1237.

Hesse, J. E., L. Wiczorek, K. Altendorf, A. S. Reicin, D. Elizabeth, and W. Epstein. 1984. Sequence homology between two membrane transport ATPases, the Kdp-ATPase of *Escherichia coli* and the Ca²⁺-ATPase of sarcoplasmic reticulum. Proc. Natl. Acad. Sci. USA **81**:4746-4750.

Higgins, I. J., D. J. Best, and R. C. Hammond. 1980. New findings in methaneutilizing bacteria highlight their importance in the biosphere and their commercial potential. Nature **286**:561-564.

Higgins, C. F., S. C. Hyde, M. M. Mimmack, U. Gileadi, D. R. Gill, and M. P. Gallagher. 1990. Binding protein-dependent transport-systems. J. Bioenerg. Biomembr. **22**:571-592.

Hodgson, J. F., H. R. Geering, and W. A. Norvell. 1965. Micronutrient cation complexes in soil solution: partition between complexed and uncomplexed forms by solvent extraction. Soil Sci. Soc. Proc. 665-669.

Hopkins, G. D., L. Sempriani, and P.L. McCarty. 1993. Microcosm and in situ field studies of enhanced biotransformation of trichloroethylene by phenol-utilizing microorganisms. Appl. Environ. Microbiol. **59**(7):2277-2285.

Hughes, M. N. and R. K. Poole. 1991. Metal speciation and microbial growth - the hard (and soft) facts. J. Gen. Microbiol. **137**:725-734.

Hulanicki, A., F. Ingman, and E. Wanninen. 1991. Metal buffers in chemical-analysis. Part II: Practical considerations. Pure Appl. Chem. **63**:639-642.

Inesi, G. and M. R. Kirtley. 1992. Structural features of cation transporting ATPases. J. bioenerg. biomembr. **24**:271-283.

Jardim, W. F. and H. W. Pearson. 1984. A study of the copper-complexing compounds released by some species of cyanobacteria. Wat. Res. **18**:985-989.

- Jones, M. J. and B. T. Hart.** 1989. Copper complexing capacity in fresh-waters using the catechol-cathodic stripping voltametric method. *Sci. Technol. Lett.* **1**:59-63.
- Kashiwagi, S., K. Kanamaru, and T. Mizuno.** 1995. A *Synechococcus* gene encoding a putative pore-forming intrinsic membrane protein. *Biochim. Biophys. Acta* **1237**:189-192.
- King, G. M.** 1992. Ecological aspects of methane oxidation, a key determinant of global methane dynamics. *Adv. Microb. Ecol.* **12**:431-46
- Langford, C. H. and D. W. Gutzman.** 1992. Kinetic studies of metal ion speciation. *Anal. Chim. Acta* **256**:183-201.
- Lee, B. T. O., N. L. Brown, S. Rogers, A. Bergemann, J. Camakaris, and D. A. Rouch.** 1990. Bacterial response to copper in the environment: copper resistance in *Escherichia coli* as a model system. *NATO ASI Series G* **23**:625-632.
- Little, C. D., A. V. Palumbo, S. E. Herbes, M. E. Lidstrom, R. L. Tyndall, and P. J. Gilmer.** 1988. Trichloroethylene biodegradation by a methane-oxidizing bacterium. *Appl. Environ. Microbiol.* **54**:951-956.
- Lidstrom, M.E. and J.D. Semrau.** 1995. Metals and microbiology--the influence of copper on methane oxidation. *Adv. Chem. Ser.* **244**: 195-201.
- Martinez, J. L., A. Delgadoiribarren, and F. Baquero.** 1990. Mechanisms of iron acquisition and bacterial virulence. *FEMS Microbio. Rev.* **75**:45-56.
- McKnight, D. M. and F. M. M. Morel.** 1979. Release of weak and strong copper-complexing agents by algae. *Limnol. Oceanogr.* **24(5)**:823-837.
- Meador, J. P.** 1991. The interaction of pH, dissolved organic carbon, and total copper in the determination of ionic copper and toxicity. *Aqua.Toxicol.* **19**:13-31.
- Mellano, M. A.** 1988. Nucleotide sequence and organization of copper resistance genes from *Pseudomonas syringae* pv. *tomato*. *J. Bact.* **170**:2879-2883.
- Mittelman, M. W. and G. G. Geesey.** 1985. Copper-binding characteristics of exopolymers from a freshwater-sediment bacterium. *Appl. Environ. Microbiol.* **49**:846-851.
- Moffett, J. W. and R. G. Zika.** 1983. Oxidation-kinetics of Cu(I) in seawater: implications for its existence in the marine environment. *Mar. Chem.* **13**:239-251.
- Moffett, J. W. and R. G. Zika.** 1987. Solvent-extraction of copper acetylacetonate in studies of copper(II) speciation in seawater. *Mar. Chem.* **21**:301-313.

- Moffett, J. W. and R. G. Zika.** 1988. Measurement of copper(I) in surface waters of the sub-tropical atlantic and Gulf of Mexico. *Geochim. Cosmochim. Acta* **52**:1849-1857.
- Moffett, J. W., R. G. Zika, and L. E. Brand.** 1990. Distribution and potential sources and sinks of copper chelators in the Sargasso Sea. *Deep-Sea Res.* **37**:27-36.
- Morel, F. M. M., R. J. M. Hudson, and N. M. Price.** 1991. Limitation of productivity by trace metals in the sea. *Limnol. Oceanogr.* **36**:1742-1755.
- Murray, W. D. and M. Richardson.** 1993. Progress toward the biological treatment of C₁ and C₂ halogenated hydrocarbons. *Crit. Rev. Environ. Sci. Technol.* **23(3)**:195-217.
- Nair, C. K., A. N. Balchand, and P. N. K. Nambisan.** 1991. Heavy metal speciation in sediments of cochin estuary determined using chemical extraction techniques. *Sci. Total Environ.* **102**:113-128.
- Neidhardt, F. C., J. L. Ingraham, and M. Schaechter.** 1990. Physiology of the Bacterial Cell: a Molecular Approach. p.174-183. Sinauer Associates, Sunderland.
- Newman L.M. and L. P. Wackett.** 1991. Fate of 2,2,2-trichloroacetaldehyde (chloral hydrate) produced during trichloroethylene oxidation by methanotrophs. *Appl. Environ. Microbiol.* **57**:2399-2402.
- Nelson, M. J. K., S. O. Montgomery, W. R. Mahaffey, and P. H. Pritchard.** 1987. Biodegradation of trichloroethylene and involvement of an aromatic biodegradative pathway. *Appl. Environ. Microbiol.* **53**:949-954.
- Nguyen, H. H. T., A. K. Shiemke, S. J. Jacobs, B. J. Hales, M. E. Lidstrom, and S. I. Chan.** 1994. The nature of the copper ions in the membranes containing the particulate methane monooxygenase from *Methylococcus capsulatus* (Bath). *J. Biol. Chem.* **269(21)**:14995-15005.
- Nucifora, G., L. Chu, and S. Silver.** 1989. Cadmium resistance from *Staphylococcus aureus* plasmid p1258 *cadA* gene results from a cadmium-efflux ATPase. *Proc. Natl. Acad. Sci. USA* **86**:3544-3548.
- Oddermatt, A., H. Suter, R. Krapf, and M. Solioz.** 1993. Primary structure of two P-type ATPases involved in copper homeostasis in *Enterococcus hirae*. *J. Biol. Chem.* **268**:12775-12779.

- Park, S., M. L. Hanna, R. T. Taylor, and M. W. Droege.** 1991. Batch cultivation of *Methylosinus trichosporium* OB3b. I: production of soluble methane monooxygenase. *Biotech. Bioeng.* **38**:423-433.
- Peltola, P., P. Priha, S. Laakso.** 1993 Effect of copper on membrane lipids and on methane monooxygenase activity of *Methylococcus capsulatus* (Bath). *Arch. Microbiol.* **159**:521-525.
- Phelps, T. J., J. J. Niedzielski, R. M. Schram, S. E. Herbes, and D. C. White.** 1990. Biodegradation of trichloroethylene in continuous-recycle expanded-bed bioreactors. *Appl. Environ. Microbiol.* **56**:1702-1709.
- Powell, H. K. J. and R. M. Town.** 1991. Interaction of humic substances with hydrophobic metal complexes: a study by anodic stripping voltammetry and spectrophotometry. *Anal. Chim. Acta* **248**:95-102.
- Ravenscroft, J. and M. J. Gardner.** 1991. Performance of metal-ligand titration techniques. *Analyt. Proc.* **28**:61-63.
- Semrau, J. D., K. S. Smith, and M. E. Lidstrom.** 1993. Parameters affecting the ability of methanotrophs to oxidize methane and trichloroethylene. *J. Cell. Biochem.* 198-198.
- Semrau, J.D.** 1995. Kinetic, biochemical, and genetic analysis of the particulate methane monooxygenase. Ph.D. dissertation, Caltech, Pasadena.
- Semrau, J. D., D. Zolanz, M. E. Lidstrom, and S. I. Chan.** 1995. The role for copper in the pMMO of *Methylococcus capsulatus* Bath: A structural vs. catalytic function. *J. Inorg. Bio.* **58(4)**: 235-244.
- Shull, G. E., A. Schwartz, and J. B. Lingrel.** 1985. Amino-acid sequence of the catalytic subunit of the (Na⁺ + K⁺)ATPase deduced from a complementary DNA. *Nature* **316**:691-695.
- Shuttleworth, K. L. and R. F. Unz.** 1991. Influence of metals and metal speciation on the growth of filamentous bacteria. *Wat. Res.* **25**:1177-1186.
- Silver, S. and M. Walderhaug.** 1992. Gene regulation of plasmid- and chromosome-determined inorganic ion transport in bacteria. *Microbiol. Rev.* **56(1)**:195-228.
- Simpson, F. B. and J. B. Neilands.** 1976. Siderochromes in cyanophyceae: isolation and characterization of schizokinen from *Anabaena* Sp. *J. Physiol.* **12**:44-48.
- Smith, K. S.** 1996. Enrichment dynamics of a marine methanotrophic population and its kinetics of methane and TCE oxidation. Ph.D. dissertation, Caltech, Pasadena.

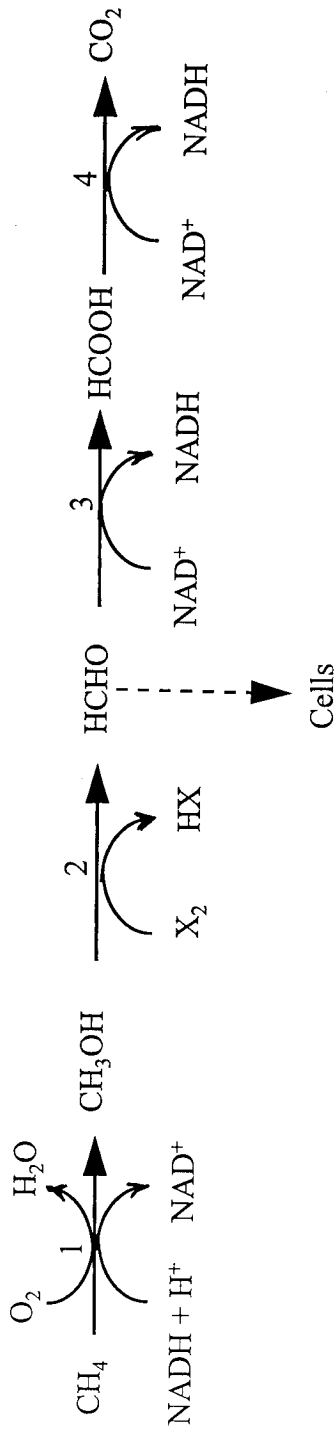
- Smith, R. L., L. J. Thompson, and M. E. Maguire.** 1995. Cloning and characterization of MgtE, a putative new class of Mg²⁺ transporter from *Bacillus firmus* OF4. *J. Bact.* **177**:1233-1238.
- Solioz, M., M. Mathew, and P. Furst.** 1987. Cloning of K⁺-ATPase of *Streptococcus faecalis*. *J. Biol. Chem.* **262**:7358-7362.
- Sunda, W. and R. R. L. Guillard.** 1976. The relationship between cupric ion activity and the toxicity of copper to phytoplankton. *J. Mar. Res.* **34**:511-529.
- Sunda, W. G. and R. L. Ferguson.** 1983. Sensitivity of natural bacterial communities to addition of copper and cupric ion activity: a bioassay of complexation in seawater. *Mar. Sci.* **4**:871-891.
- Sunda, W. G. and A. K. Hanson.** 1987. Measurement of free cupric ion concentration in seawater by a ligand competition technique involving copper sorption onto C₁₈ SEP-PAK cartridges. *Limnol. Oceanogr.* **32**:537-551.
- Sunda, W. G. and S. A. Huntsman.** 1991. The use of chemiluminescence and ligand competition with EDTA to measure copper concentration and speciation in seawater. *Mar. Chem.* **36**:137-163.
- Trick, C. G., R. J. Andersen, A. Gillam, and P. J. Harrison.** 1983. Procoentrin: an extracellular siderophore produced by the marine dinoflagellate *Prorocentrum minimum*. *Science* **219**:306-308.
- Tsien, H. C. and R. S. Hanson.** 1992. Soluble methane monooxygenase component B gene probe for identification of methanotrophs that rapidly degrade trichloroethylene. *Appl. Environ. Microbiol.* **58**:953-960.
- U.S. Environmental Protection Agency.** 1985. Document NPL-U3-6-3. Anonymous Washington, D.C.
- Vandenberg, C. M. G.** 1984. Determination of the complexing capacity and conditional stability constants of complexes of copper(II) with natural organic ligands in seawater by cathodic stripping voltametry of copper-catechol complex ions. *Mar. Chem.* **15**:1-18.
- Vandenberg, C. M. G., M. Nimmo, P. Daily, and D. R. Turner.** 1990. Effects of the detection window on the determination of organic copper speciation in estuarine waters. *Anal. Chim. Acta* **232**:149-159.
- Vandenberg, C. M. G. and J. R. Donat.** 1992. Determination and data evaluation of copper complexation by organic ligands in sea water using cathodic stripping voltammetry at varying detection windows. *Anal. Chim. Acta* **257**:281-291.

Vogel, T.M. and P.L. McCarty. 1991. Biotransformation of tetrachloroethylene to trichloroethylene, dichloroethylene, vinyl chloride, and carbon dioxide under methanogenic conditions. *Appl. Environ. Microbiol.* **49**:1080-1083.

Vulpe, C., B. Levinson, S. Whitney, S. Packman, and J. Gitschier. 1993. Isolation of a candidate gene for Menkens disease and evidence that it encodes a copper-transporting ATPase. *Nature genetics* **3**:7-13.

Westall, J. C., F. M. M. Morel, and D. N. Hume. 1979. Chloride interference in cupric ion selective electrode measurements. *Anal. Chem.* **51(11)**:1792-1798.

Zevenhuizen, L. P. T. M., J. Dolfing, E. J. Eshuis, and I. J. Scholten-Koerselman. 1979. Inhibitory effects of copper on bacteria related to the free ion concentration. *Microbiol. Ecol.* **5**:139-146.



1. Methane monooxygenase
2. Methanol dehydrogenase
3. Formaldehyde dehydrogenase
4. Formate dehydrogenase

Figure 1.1 The oxidation of methane to carbon dioxide by methanotrophs (from Murray and Richardson 1993).

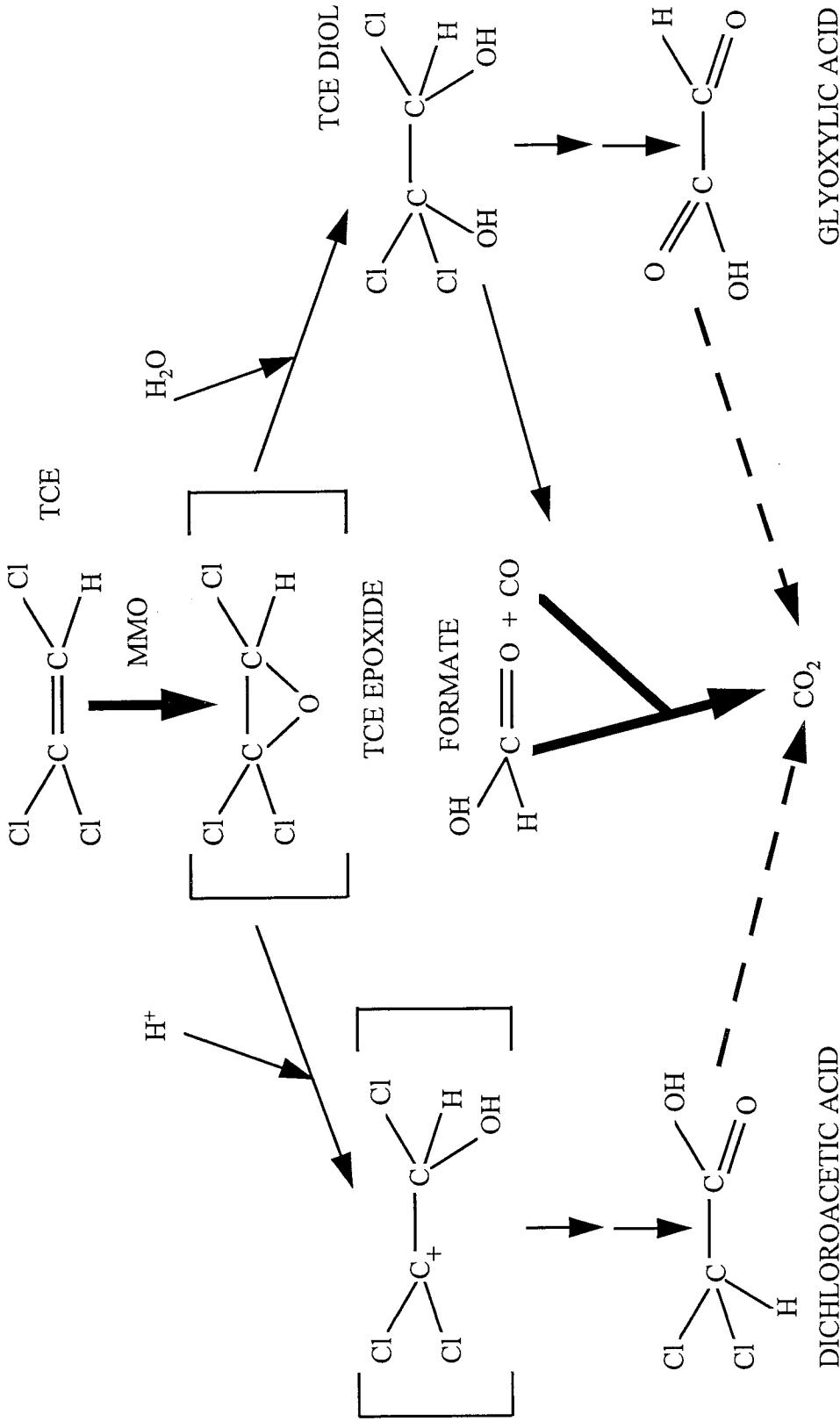


Figure 1.2 Major products of TCE degradation by methanotrophic bacteria. Methanotrophs mediate steps indicated by the thick arrows, the thin arrows indicate spontaneous breakdown of TCE epoxide in water; the dashed arrows reflect processes that are stimulated by heterotrophic bacteria (from Little *et al.* 1988). Chloral is produced at a low level (1-5% of total products), but it does not accumulate in whole cells (Newman and Wackett 1991).

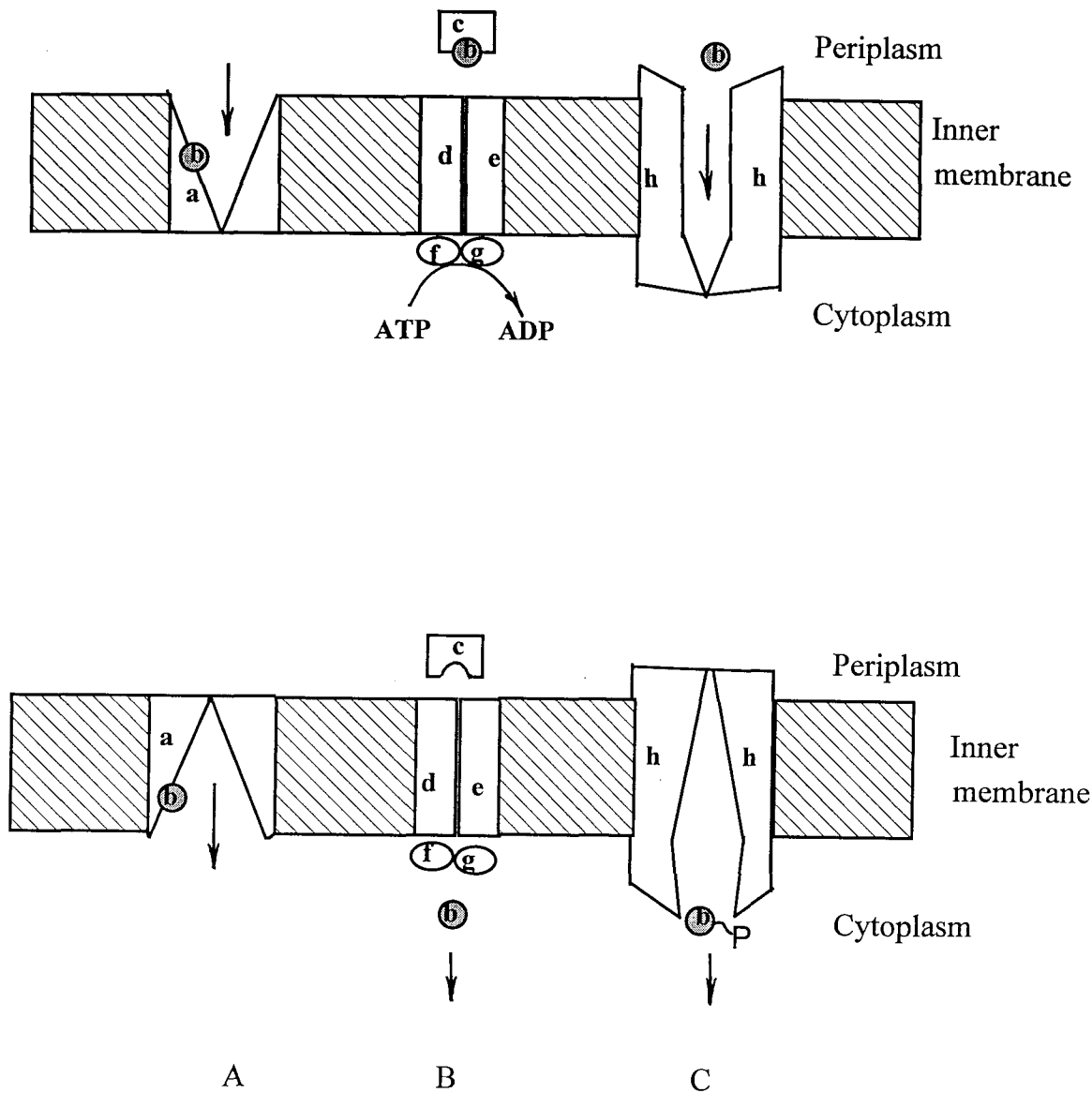


Figure 1.3 Examples of microbial nutrient transport systems (modified from Cronan *et al.* 1989).

Upper panel shows initial step, lower panel shows conformation after transport.

A. Active transport of a nutrient (b) involves conformational change of the stereospecific, transmembrane protein (a).

B. Binding protein-dependent transport system. b, periplasmic nutrient; c, binding protein; d-g, inner-membrane-associated proteins. f and g proteins couple ATP hydrolysis to the transport.

C. Group translocation is a mechanism in which the substrate (b) is chemically altered, usually phosphorylated, as it is transported by a protein h.

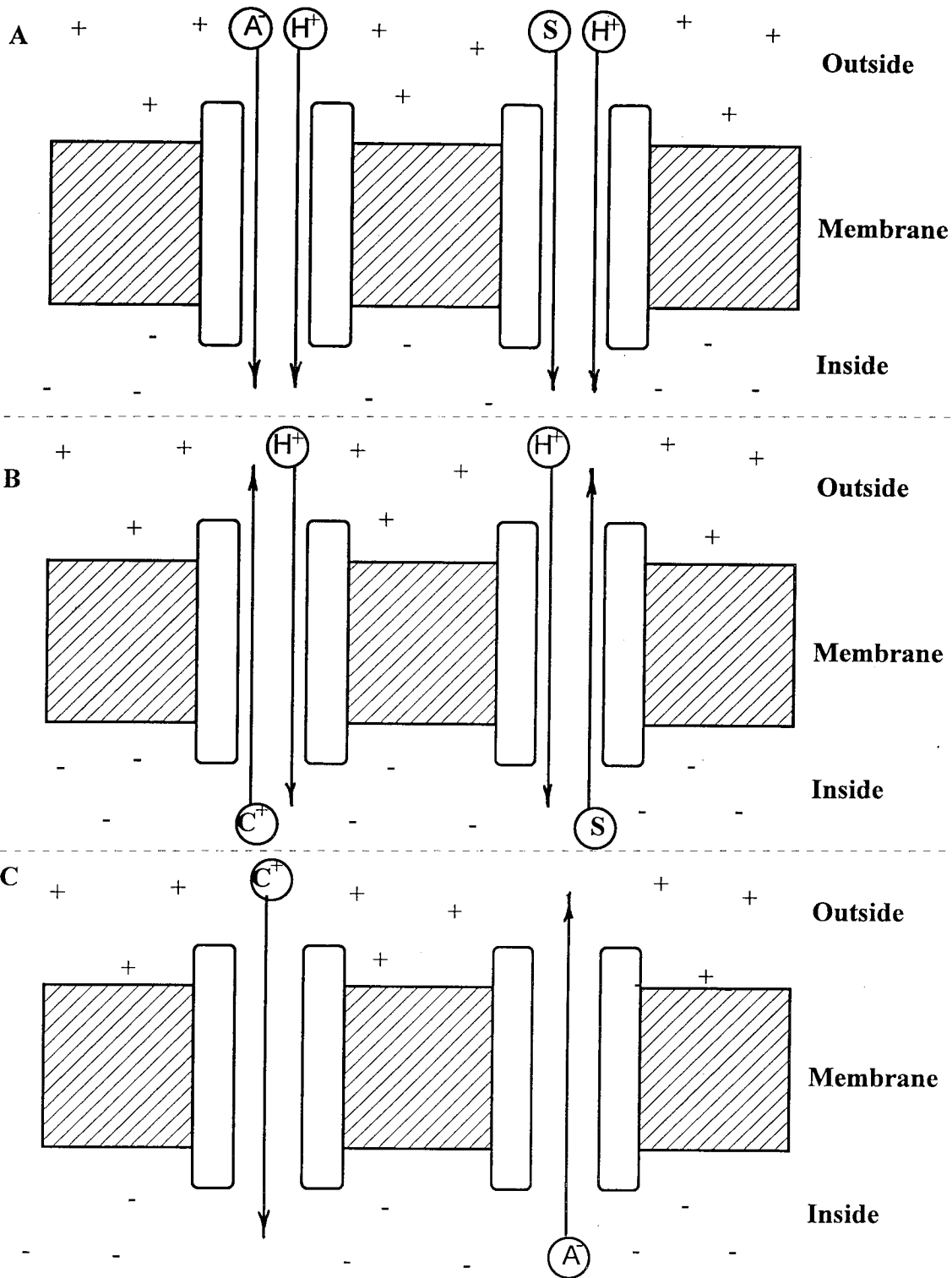


Figure 1.4 Secondary active transport through symports, antiports and uniports: schematic presentation (from Neidhardt *et al.* 1990).

Panel A shows a symport; panel B displays an antiport; panel C exhibits a uniport.

A^- , anion; C^+ , cation; S, uncharged substrate, H^+ , proton.

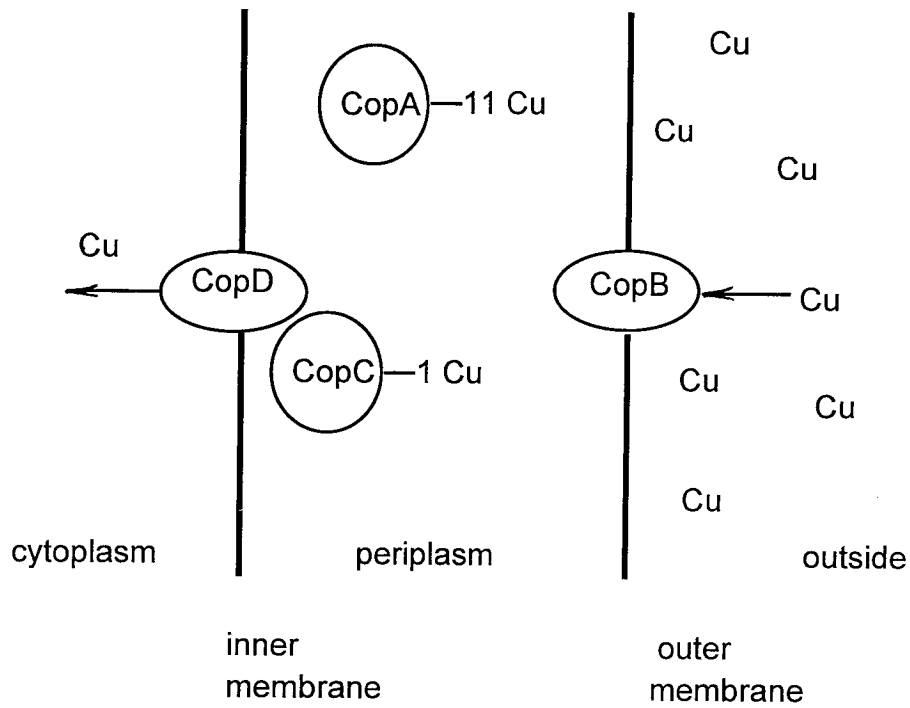


Figure 1.5 Model for the mechanism of copper resistance in *P. syringae* (from Cooksey 1993).

The periplasmic proteins CopA and CopC, and the outer membrane protein CopB are involved in sequestering copper. CopC and CopD (inner membrane protein) are thought to be involved in copper transport into the cytoplasm.

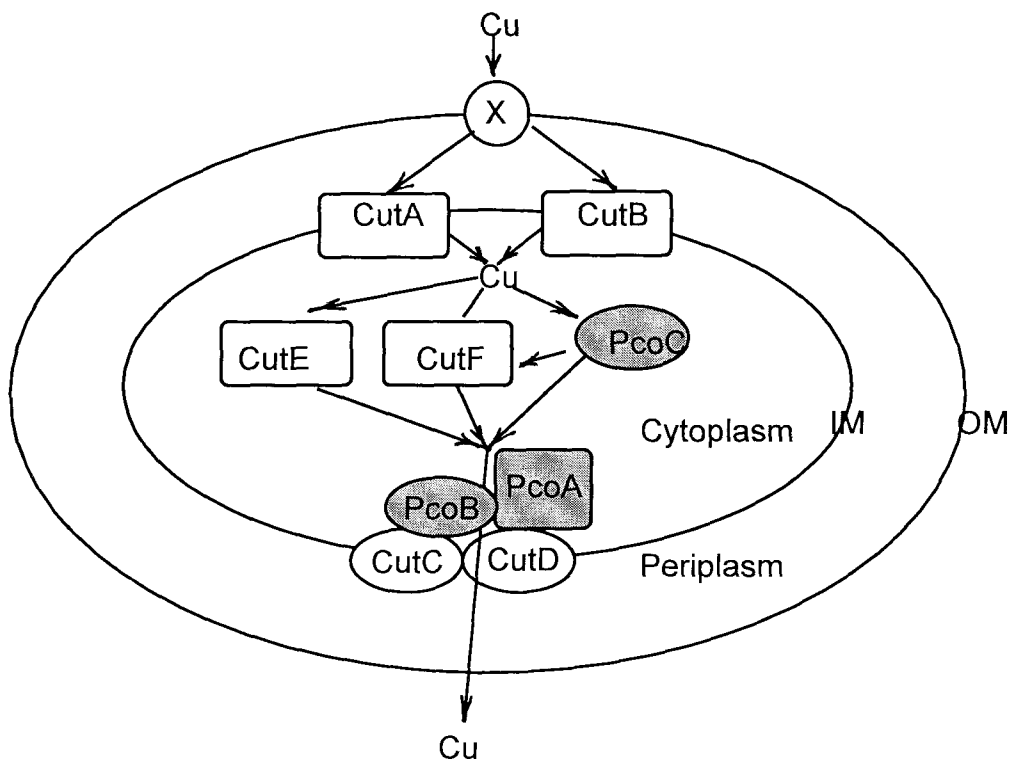


Figure 1.6 A model of copper resistance and metabolism in *E. coli*.

Copper enters the periplasm through a porin X. CutA and CutB are copper uptake proteins; CutE and CutF are storage/intracellular transport proteins; CutC and CutD are copper efflux ATPases. The copper resistance proteins increase intracellular copper storage (PcoC) and increase the export of copper (PcoA and PcoB). CutR, involved in regulation of copper metabolism, is not shown on the diagram. IM, inner membrane; OM, outer membrane.

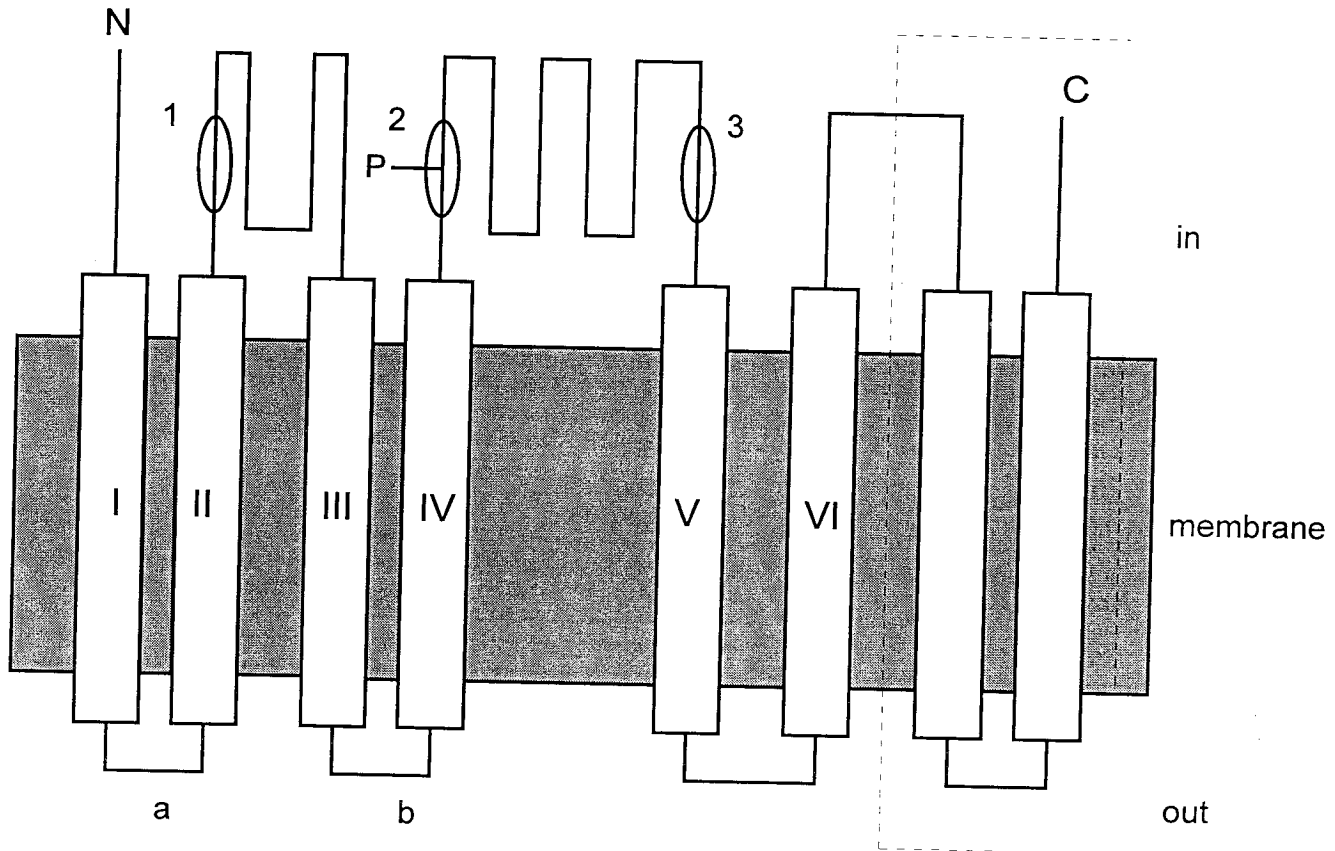


Figure 1.7 A diagram of the general structure of P-type ATPases (from Epstein, 1990).

The conserved feature is a cation channel formed by the six membrane-spanning regions I-VI. The dashed line indicates the C-terminus region where variation in the number of membrane-spanning domains is possible. The regions of highly conserved protein sequence are circled. Region 1 is the phosphatase domain, which removes the phosphate from an aspartic acid residue as part of the reaction cycle. Region 2 is the phosphorylation domain (shown phosphorylated). Region 3 is the ATP-binding domain. The external loops labeled a and b are hydrophilic in most P-type ATPases.

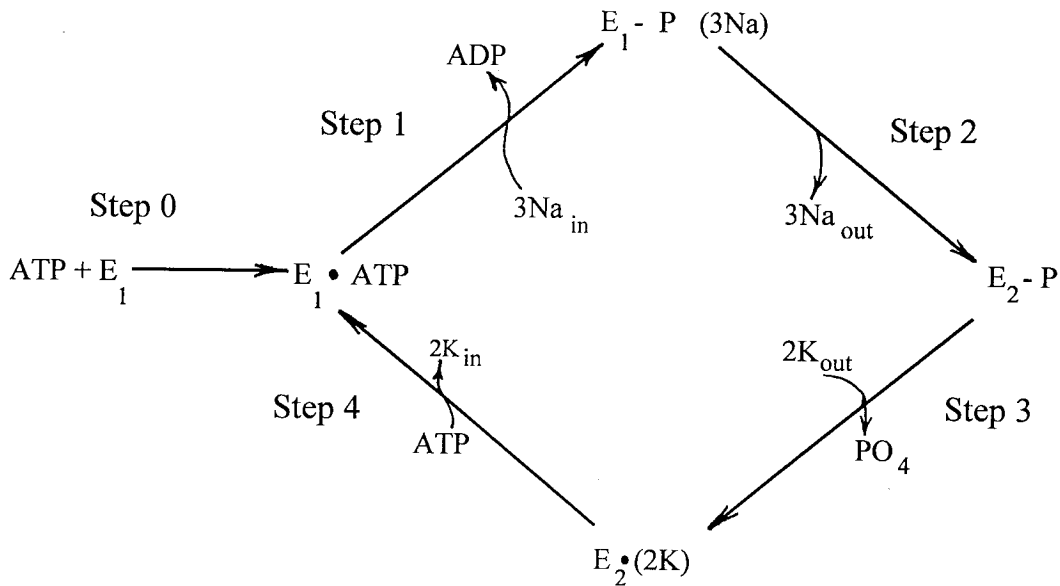


Figure 1.8 A schematic diagram of the reaction cycle of the Na⁺,K⁺-ATPase (from Epstein, 1990).

Covalent binding of enzyme (E) and phosphate (P) is indicated by a line (-), tight but noncovalent binding is shown by a dot (•).

Step 1. E₁ with bound ATP is phosphorylated and binds three Na⁺ ions from the inside of the cell.

Step 2. Conformational change of P-E₁ to P-E₂ with release of Na⁺ outside of the cell.

Step 3. E₂ occludes two K⁺ ions from the outside and releases phosphate.

Step 4. E₂ releases K⁺ inside the cell, while binding ATP.

Chapter Two

Study of Copper Accumulation by the Type I Methanotroph Methylomicrobium albus BG8^a

2.1. Introduction

Copper plays a significant role in the physiology of methanotrophs, Gram-negative bacteria that grow aerobically on methane as a sole source of carbon (1), by activating and stabilizing a key enzyme, particulate methane monooxygenase (pMMO). The addition of copper to the growth medium in the range that is neither growth-limiting nor toxic results in increased cell yield and pMMO activity, as well as a pronounced change in pMMO kinetics (2).

There has been considerable interest in these bacteria in recent years because of the possibility of using methanotrophs for the removal of trichloroethylene (TCE) from contaminated aquifers (3, 4). These microorganisms can degrade TCE through MMO to non-toxic compounds that can be utilized by heterotrophic bacteria (5-7). A variation in copper concentrations in the growth medium produces a significant change in the kinetics of TCE oxidation (2). Such a response to copper could have a major influence on TCE bioremediation by natural populations of methanotrophs. However, very little is presently known about the mechanism of copper uptake or the bioavailability of different copper

^a reprinted with permission from Olga Berson and Mary E. Lidstrom, *Environ. Sci. Technol.*, 30, 1996, 802-809. Copyright 1996 American Chemical Society.

species in these bacteria. One study of mutants in the type II methanotroph, *M. trichosporium* OB3b, has suggested that a specific uptake system exists in this strain (8).

Several copper species can be present simultaneously in natural waters as well as in a culture medium. These include aqueous cupric ion $[\text{Cu}^{2+}(\text{H}_2\text{O})_6]$, which we will refer to as cupric ion, inorganic complexes (e.g., hydroxide and carbonate complexes), and organic complexes (9). However, studies of copper toxicity in microorganisms have demonstrated that cupric ion is the most bioavailable chemical species and that chelators affect total copper availability by altering cupric ion concentrations or activities (10-16). Three mechanisms of trace element uptake by microorganisms have been proposed: nonspecific sorption on cell surfaces, metabolism-dependent intracellular uptake, and passive diffusion of lipid-soluble inorganic metal complexes (12, 17, 18). It is not known in methanotrophs whether the uptake of copper is mediated by an active or passive transport mechanism.

In our work, we considered three pools of copper, as depicted in Figure 2.1: copper in the growth medium (“bulk copper”), copper sorbed on the cellular surface (“surface-associated copper”), and copper inside the cells (“internal copper”). We refer to the sum of surface-associated and internal copper as “accumulated copper.” “Total copper” refers to the amount of copper that was added to the medium as copper nitrate, and includes various copper species present in all three pools.

The objectives of the work presented here were two-fold. The first objective was to study the effect of a range of total copper and chelator (EDTA) concentrations on copper accumulation by *M. albus* cells and to determine the relationship between cupric

ion concentrations in the external medium and cellular copper concentrations. The second objective was to establish the existence of an active transport system for copper in *M. albus* BG8. An EDTA wash was used to remove surface-bound copper and to separate copper uptake from copper sorption. These experiments were carried out under conditions in which copper was neither growth-limiting nor toxic, since the physiological effects of copper on methanotrophs that have been observed occur under these conditions (2, 19).

2.2. Experimental Section

2.2.1. Bacterial Strain and Growth Conditions.

M. albus BG8 (20), a type I methanotroph, was used. The bacteria were grown on nitrate mineral salts (NMS) medium (1), under an atmosphere of 1:1 methane/air mixture at 30°C. Liquid cultures were inoculated from agar plate cultures and grown with shaking at 200 rpm. Total copper in the medium used for agar plates was 10 μ M unless stated otherwise. Concentration of copper in the stock solution was verified with mass spectrometer measurements.

All chemicals used for medium preparation were of reagent grade. All solutions were made with double distilled water (dd H₂O). All glass flasks, jars, and polypropylene beakers used were presoaked in 1N HCl overnight, and then rinsed with dd H₂O three times to minimize trace metal contamination.

Copper nitrate was filter sterilized and was added aseptically to autoclaved medium to give the desired total copper concentration.

NMS medium (1) contains 11.7 μ M EDTA including 11 μ M Fe-EDTA complex and 0.7 μ M EDTA, which is added to the medium from a preequilibrated stock of trace elements and is mostly present in the form of metal-EDTA complexes. A medium containing metal-EDTA complexes, Fe-EDTA in particular, equilibrates with cupric ion relatively slowly (9, 16). We found that in NMS medium, 24 h is needed to achieve a pseudoequilibrium, after which there is no further significant decrease in cupric ion concentration (Figure A2.1). We use the term pseudoequilibrium to refer to a state of the system in which all fast exchange reactions are completed, but true equilibrium has not been established due to the slow kinetics of exchange for Fe-EDTA against cupric ion. Therefore, in all experiments performed we allowed at least 24 h of medium incubation before inoculation with *M.albus* BG8 to avoid short-term high cupric ion concentration toxic effects on cells and to bring the system to pseudoequilibrium.

2.2.2. Ion Selective Electrode (ISE) Pretreatment and Calibration.

The Orion (Boston, MA) 942900 solid-state Copper ISE (CuISE) and the Orion 900200 double junction, half-cell electrode were used to measure cupric ion concentrations in the medium. The electrodes were connected to an Orion 710A pH/mV meter. Ionic strength adjuster (0.1M sodium nitrate, final concentration) was added to all standards and samples to swamp small variations in sample ionic strength and to keep the activity coefficient constant. The electrodes were stored and cleaned as described by Avdeef (21).

All readings were taken when the rate of change of potential had fallen below 0.2 mV/min, as was recommended by Simpson (22). All measurements were performed at 25 °C.

In the range 10^{-3} - 10^{-5} M cupric ion, successive dilutions of a 0.1 M standard solution of CuNO_3 in dd H_2O were used as calibrating solutions. Lower cupric ion concentrations for CuISE calibration were obtained with cupric ion buffers [$\text{Cu}^{2+}(\text{H}_2\text{O})_6/\text{EDTA}$ with borax buffer for pH control], prepared as described by Hansen (23). The calibrations were always performed at the beginning of the series of solutions and checked every 3 h thereafter.

The response of the electrodes was tested and has been found to be linear in the range of pCu 3-10, as expected (23) (Figure A2.2). In 42 calibrations performed during the experiments, the mean slope was 27.8 mV per decade of cupric ion concentration change. The calculated ideal theoretical Nernstian slope is 29.5 mV/pCu at 25°C.

2.2.3. Mass Spectrometry.

A Perkin-Elmer (Norwalk, CT) 5000 inductively coupled plasma/mass spectrometer (ICP/MS) was used to analyze solutions for total copper concentrations. The additions calibration technique was used to compensate for sample matrix effects (24). Copper was measured as ^{63}Cu since it is more abundant than ^{65}Cu . Diluted solutions of 1000 ppm copper nitrate standard were used for ICP/MS calibration (Figure A2.3). A diluted yttrium nitrate standard solution served as an internal standard. Both standards were obtained from Perkin-Elmer.

The nebulizer flow was optimized before each series of measurements to minimize oxide interferences. All samples were diluted 10-fold before analysis to meet ICP/MS requirements on total dissolved solids (maximum of 2%) (24).

Parameters were set as follows: dwell time of 30 ms; 7 sweeps per reading ; 7 readings per replicate; 1 point per pick. Measurements were performed on high-resolution mode.

2.2.4. Optical Density Measurement and Calibration.

Optical density was measured with a Klett - Summerson (Long Island City, NY) photoelectric colorimeter and was reported as Klett units. Optical density was calibrated to viable cell numbers by dilution plating of cell suspensions at several Klett unit values. One Klett unit was considered equal to $(6.7 \pm 0.3) \times 10^5$ viable cells.

2.2.5. Copper Accumulation.

The accumulation of cupric ion by *M. albus* BG8 cells was determined by growing cells in NMS medium containing eight total copper concentrations: 3, 4.2, 8.4, 12.3, 17.3, 19.1, 28.1, and 37.0 μM as measured by ICP/MS (Table 2.1). In all experiments the pH of the medium before inoculation was 6.5, and did not change during growth of *M. albus* BG8. Cell-free NMS medium was used as an adsorption control (Figure A2.4). The medium in control and experimental flasks for each experiment was prepared exactly the same way.

After preequilibration of the medium (250 mL in each flask) for at least 24 h, the experimental flasks were inoculated with *M. albus* BG8. Just prior to BG8 addition and at

different times afterwards, 5-mL samples were collected for cupric ion concentration, pH, and ICP/MS measurements. At the same time optical density of the growing cells was measured with a Klett colorimeter. Duplicate 1-mL cell-containing subsamples were prepared from 5-mL samples by centrifugation at 16000g for 10 min, at room temperature. The supernatant phases were collected, diluted and measured for copper by ICP/MS. The pelleted cells were washed with 1 mL of dd H₂O, and centrifuged again. The washing solution was retained for ICP/MS analysis in several experiments and was found to contain a negligible amount of copper (less than 1% of the added amount). Cells then were harvested, resuspended and lysed. The obtained subsamples with cell digests and cell-free samples (controls) were diluted and measured with ICP/MS.

The average moles of copper per cell was calculated by dividing the quantity of moles of copper in 1 mL of cell pellet by the number of cells in 1 mL of pellet, assuming no cell loss during centrifugation.

The SURFEQL computer model (25) was used to predict copper speciation in NMS medium prior to inoculation (after 24-hour preequilibration). The program was run at fixed hydrogen ion concentration (pH= 6.5), corresponding to the pH of NMS medium. The equilibrium constants were from the SURFEQL database. Case-specific input included total concentrations of metals and ligands present in the medium. We considered two limiting cases. For the equilibrium case we assumed that all EDTA, including EDTA added as an iron complex, was available for complexation. In the second, nonequilibrium case, the Fe-EDTA complex was presumed to have a low chemical reactivity with respect to change in complexation (9), thus being kinetically

unavailable. A negligible amount of copper (less than 2% of the added amount) was measured to partition as solid precipitates with the cells during centrifugation.

2.2.6. Copper Accumulation in *M. albus* BG8 under Different Complexation Conditions.

Four complexation experiments were performed with different total EDTA concentrations (11.7, 15.7, 21.7, 31.7 μM). It was not possible to use EDTA concentrations outside of this range because of poor growth of the culture, presumably due to altered bioavailability of required trace elements under these conditions. In each experiment the cells were exposed to eight total copper concentrations in the range from 1 to 100 μM . Cellular copper concentrations for these experiments were measured at the end of logarithmic growth, but no later than 30 h. after inoculation. Ionic copper concentrations were measured with ISE before *M. albus* BG8 inoculation in all experiments (Table 2.1). The samples were prepared and analyzed as described in the previous section, except that three replicates instead of two were prepared for ICP/MS measurements.

2.2.7. Sorption Estimates.

Cells were grown on agar plates containing either 10 μM or 2 μM copper. The cells from plates containing 10 μM copper were exposed to a range of total copper concentrations from 1.2 to 54 μM as measured by ICP/MS. The cells from plates containing 2 μM copper were inoculated into liquid NMS medium containing total copper in the range from 0 to 7 μM . The total EDTA concentration in the medium was

11.7 μM except for one experiment where it was increased to 15.7 μM and 31.7 μM , while copper concentrations ranged from 0 to 2.8 μM . Ionic copper concentrations were measured with ISE prior to *M.albus* BG8 inoculation in all experiments. All samples were prepared in duplicate.

Sorption experiments were started by inoculation of *M. albus* BG8 into pre-equilibrated NMS medium. At time intervals, the optical density of the growing cells was measured with a Klett colorimeter, and 1-mL samples were removed for either further ICP/MS analysis (untreated samples), to assess copper accumulated by the cells (sorbed plus internal) or for an EDTA wash (washed samples) to remove sorbed copper. The untreated samples were prepared and analyzed as described above. The samples intended for EDTA wash were centrifuged at 16000g for 10 min, at room temperature. The pelleted cells were washed with 1 mL dd H₂O, and centrifuged again. The collected cells then were resuspended in dd H₂O containing 0.1M EDTA (final concentration) for 24 h. The cells were then harvested by centrifugation, washed with 1 mL dd H₂O, and prepared for ICP/MS measurements as described above.

2.2.8. Study of Uptake of Cell-Surface Associated Copper.

M. albus BG8 was exposed to five total copper concentrations: 2.3, 3.5, 7.5, 39.0 and 55 μM as measured by ICP/MS. The total EDTA concentration in the medium was 11.7 μM . Within 1 h after inoculation, 1-mL samples were withheld for ICP/MS analysis with or without EDTA wash to determine the amount of sorbed copper. After 1.5 or 3.5 h of incubation (at 30°C, with shaking at 200 rpm) the remaining cells were harvested by

centrifugation of the flask contents (150 mL) at 16000g for 10 min, at room temperature. The pelleted cells were washed with 10 mL of 1mM PIPES buffer (pH=6.5) to remove loosely-bound copper, and centrifuged again. The collected cells then were transferred into modified NMS medium, which differed from the regular NMS by the absence of copper, Fe-EDTA, and EDTA. Otherwise growth conditions were normal.

At time intervals, the optical density of the growing cells was measured with a Klett colorimeter, and 1-mL untreated and washed samples were prepared as described above. Two replicates were made on each sample.

2.3. Results And Discussion

2.3.1. Copper Accumulation.

Because of the importance of cupric ion to copper bioavailability in other systems, the relationship between copper accumulation and cupric ion concentration in the medium was studied in actively growing cultures of *M. albus* BG8. The cells were grown in medium containing eight different total copper concentrations. No significant change in the growth rate of *M. albus* BG8 was observed within the total copper concentration range from 3 to 37 μM (Figure 2.2), showing that copper was both sufficient and non-toxic to *M. albus* BG8 in these experiments.

Cupric ion concentration in NMS medium was determined during growth of *M. albus* BG8 for all eight initial copper concentrations tested. Since the same general trends were observed in all eight experiments, the results for only the lowest (3 μM) and highest

(37 μM) total copper concentrations tested are presented in Figure 2.3A (all the other results are shown in Figures A2.4-A2.6). The cupric ion concentration decreased with time, while cell-free controls showed no significant cupric ion (Figure 2.3A) or total copper loss (Figure A2.7) within the time of the experiments. This allowed us to attribute the change in cupric ion concentration to the presence of *M. albus* BG8, and to assume that the effect was not due to further copper complexation by EDTA present in the medium or to copper adsorption to the walls of the flasks.

In all eight experiments, the same pattern of cupric ion concentration in the medium was observed: an initial rapid depletion within 10 h after inoculation, which was followed by a slow but detectable decrease. A different pattern was seen for the cellular copper accumulation. In this case, there was rapid accumulation within the first hour after inoculation, and only a small further accumulation occurred (Figure 2.3B). The difference in the patterns could be explained if the rapid initial cellular accumulation of copper disturbs the equilibrium between cupric ion and other copper species in the medium. SURFEQL predictions indicate that the two main contributors to the pool of bulk copper are Cu-EDTA complexes and $\text{Cu}_3(\text{PO}_4)_2$ precipitates, and establishment of equilibria of cupric ion with these pools is expected to be slower than the rapid cellular accumulation rates observed (9, 16) (Figure 2.1). It is possible that the two phases of cupric ion decrease in the medium reflect two different processes in which equilibria are being reestablished, perhaps in combination with ongoing accumulation in the first phase. In order to examine the dependence in *M. albus* BG8 of the cellular copper content on

cupric ion concentration in the medium, accumulation experiments under different complexation conditions were carried out.

2.3.2. Copper Accumulation in *M. albus* BG8 under Different Complexation Conditions.

M. albus BG8 cells were grown in media containing different total copper concentrations and different EDTA concentrations. Before inoculation, initial cupric ion concentrations were determined (Table 2.1). At the end of growth the copper content per cell and the copper in the medium were determined as described in the Experimental Procedures. Metal recovery (sum of cell digests and filtrates) based on the measured total copper added was 101% (average). All replicates showed very good reproducibility: most of the error bars on Figures 2.4 and 2.5 are within the symbols that represent the averaged data. However, cupric ion concentration measurements showed more variability (Table 2.1).

When the copper per cell from these experiments and from the experiments shown in Figure 2.3 was plotted against the negative logarithm of the total copper concentration (Figure 2.4), a decrease in copper content per cell was seen as the EDTA concentration increased. The results of experiments with the two highest EDTA concentrations (21.7 and 31.7 μM) are similar, presumably because in these cases copper complexation by EDTA produced almost the same initial cupric ion concentrations, as measured with ISE (Table 2.1).

In contrast to Figure 2.4, the copper content of *M. albus* BG8 cells plotted as a function of pCu for all experiments falls on one curve (Figure 2.5), suggesting that cellular accumulation of copper depends on the cupric ion concentration. A hyperbolic relationship between cell copper content and cupric ion activity was observed in a similar study with an alga (10). We found that the cellular copper content of *M. albus* BG8 also demonstrates a hyperbolic dependence with cupric ion concentration (Figure 2.5). The following model was used, based on that presented by Sunda and Guillard (10):

$$\text{Cu/cell} = \frac{1.54 \times 10^{-15} [\text{Cu}^{2+}]}{[\text{Cu}^{2+}] + 1.43 \times 10^{-7}}, \text{ where } [\text{Cu}^{2+}] \text{ is the cupric ion concentration,}$$

$(1.54 \pm 0.06) \times 10^{-15}$ mol/cell is an estimation of a mean maximum binding capacity, and $(1.43 \pm 0.05) \times 10^{-7}$ mol/L reflects an apparent half-saturation constant.

The observed hyperbolic dependence is consistent with two main hypotheses. The first assumes reversible binding of copper to several similar cellular ligand sites with their eventual saturation (10). The second involves carrier-mediated transport with saturation of transport molecules (26).

2.3.3. Sorption versus Uptake (Surface-Associated versus Internal Copper).

In order to determine what portion of the copper accumulated by *M. albus* BG8 cells was due to nonspecific sorption, experiments were carried out in which cells were washed with EDTA. It is assumed that most of the copper removable by EDTA is nonspecifically sorbed to external sites. Cells were grown first on agar plates containing 2 μM or 10 μM copper and then in a medium containing different total copper

concentrations. Samples were withdrawn at different time points during growth, and the copper content in cells that were untreated and cells incubated with 0.1 M EDTA for 24 h and then washed was analyzed and reported as moles of copper per cell. Figure 2.6 shows the results of three experiments with NMS medium containing 1.2, 12, and 43 μM total copper. The other experiments demonstrated the same pattern of copper incorporation (Figure A2.8).

In all cases the amount of copper per cell increased significantly after exposure of the cells to the copper-containing medium, and then as cells increased in number, the average amount of copper per cell decreased and leveled out for both untreated and washed samples (Figure 2.6). The pattern of total copper accumulation by the biomass in these cultures was similar to that shown in Figure 2.3B (Figure A2.9). These data suggest that in both untreated and washed cells no significant copper accumulation occurs after the initial accumulation on a per cell basis.

A significant difference in the total copper per cell was observed between the treated and untreated samples, with as much as a 40-fold decrease after EDTA treatment at the higher copper concentrations. These data suggest that most of the copper accumulated by the cells in these experiments was sorbed to the cellular surface at all copper concentrations tested. The pattern of copper accumulation seen in untreated samples suggests that cells inoculated from agar plates rapidly sorb copper, but as they grow exponentially in liquid medium, new copper sorption does not occur at a significant level. This may be due to changes in cellular surface characteristics, for instance amounts

of extracellular polysaccharide synthesized, under these two different physiological conditions.

In all of these experiments, rapid saturation of cellular accumulation of copper in both EDTA-treated and non-treated samples occurred (Figure 2.6). However, while the amount of copper measured in untreated cells showed the expected dependence on the pCu of the medium, the amount of copper found in the cell digests after EDTA wash was essentially constant, at about 3×10^{-17} mol of copper per cell for experiments that had been inoculated from plates containing 10 μM copper, and at about 1×10^{-17} mol of copper per cell for inoculation from plates containing 2 μM copper, despite a 100-fold change in both cupric ion and total copper concentrations (Figure 2.7). This constancy was seen both for samples collected within 1 h of inoculation of cells into copper-containing medium (Figure 2.7) and for samples prepared at the end of growth, 25-30 h after inoculation (Figure A2.10).

Copper that is not removable by a strong chelating agent like EDTA during a 24-h exposure and wash treatment may be either inside the cells or complexed on the outside of the cell at sites with higher affinity for copper than EDTA. However, the literature indicates that microorganisms are not normally capable of copper uptake from metal-EDTA complexes present in the medium (9, 12, 27, 28) and, therefore, the existence of copper-binding sites with such high affinity seems unlikely, suggesting that the copper not removable by EDTA may be inside the cells (28). If this copper does represent copper inside the cell, then an analysis of Figure 2.7 shows that the saturation of copper

uptake into the cells could be achieved at approximately $1\text{-}3 \times 10^{-17}$ moles of copper per cell.

In phytoplankton, the uptake of essential trace metals is believed to occur via binding to a surface ligand and subsequent transfer across the cell membrane (29). This process usually follows Michaelis-Menten kinetics. Our results are also consistent with such a mechanism (Figure 2.1). However, we were unable to estimate Michaelis-Menten parameters from our data, because the rapid uptake precluded measuring the initial uptake rates in these experiments by our protocol.

Since copper uptake into the cells was saturated in our experiments and because most of the copper accumulated by the cells was sorbed to the cellular surface, the hyperbolic model presented above reflects mainly the reversible binding of copper to cellular sites with a mean binding capacity of 1.54×10^{-15} moles/cell, and an apparent half saturation constant of 1.43×10^{-7} moles/l. The rapid adsorption saturation seen in our experiments (untreated samples) probably reflects saturation of two types of sites: a relatively small number of specific, possibly membrane-bound, sites associated with a putative copper transport system, and a relatively large number of nonspecific sites, possibly reflecting various functional groups such as amino acid, carboxylic, hydroxy groups, etc. (Figure 2.1). Since in all cases the amount of copper removable by EDTA was greater than that which was not EDTA removable, the kinetics of sorption observed would be expected to be dominated by the nonspecific sites.

2.3.4. Desorption of Cell-Surface Associated Copper and Uptake into the Cells.

To study the fate of the cell surface-bound copper (presumably on non-specific sites), a series of experiments was conducted in which *M. albus* BG8 cells were incubated in copper-containing NMS medium for a short period of time (1.5 or 3.5 h) to allow accumulation of copper and then were transferred to copper-free medium. Samples were then taken at various times and copper was measured in four pools: total cellular copper accumulated by the cells, cellular copper not removable by EDTA, copper removed with the EDTA treatment, and copper in the filtrate (medium from which cells had been removed). Since the results were the same in both sets of experiments (1.5 or 3.5 h of incubation), data from only the experiments with 1.5 h. incubation are shown.

In all experiments, cells grew slower than usual after transfer to copper-free medium. Doubling time increased on the average by a factor of 2 as compared to growth in regular NMS medium. This is probably due to the absence of EDTA in the copper-free medium, which is important in providing solubility and availability of trace elements essential for growth. EDTA was excluded from the copper-free NMS medium in these experiments to prevent stripping of copper from the cellular surface.

A comparison of the data for the untreated and EDTA-treated cells shows that the protocol gave good recovery and good reproducibility. The measured copper accumulated by the cells was approximately equal to the sum of the EDTA-removable and nonremovable copper (Figure 2.8). An insignificant amount of copper was found in the filtrate in the experiments with 2.3, 3.5, or 7.5 μM total copper concentration (Figures

2.8A and 2.8B) suggesting that little copper was desorbed from the cell surface during this time period. The total amount of copper accumulated by the cells and the copper not removable by EDTA both remained approximately constant in these experiments. When cells were grown initially with higher copper (39 μM), the amount of copper lost to the medium was substantial (Figure 2.8C), and was correlated with the loss of copper from the cells. However, in this case, the copper not removable by EDTA was approximately constant (Figures 2.8A-C). This implies that under these conditions, the copper species sorbed on non-specific sites was not further internalized by *M. albus* BG8 cells either directly, or indirectly after re-entering the medium. This lack of availability of desorbed species for further uptake during the tested time period may be due to kinetic factors: an imbalance between rates of desorption, reequilibration in the medium, and copper uptake (Figure 2.1).

The combined results of our experiments suggest the scenario shown in Figure 2.1, in which the cupric ion is directly available for accumulation including both sorption and internalization by *M. albus* BG8, and suggest that the rates of copper accumulation are greater than the dissociation and medium reequilibration rates. Therefore, cupric ion concentration in the medium is probably kinetically controlled by a balance between all sources and sinks (Figure 2.1) and this determines overall copper availability to *M. albus* BG8. Moreover, the results of sorption versus uptake experiments demonstrated saturable kinetics of copper uptake and independence of cellular uptake from a 100-fold extracellular copper concentration variation. This suggests that cupric ion is probably taken up by *M. albus* BG8 via a specific transport system (Figure 2.1).

The data presented here suggest that the growth of *M. albus* BG8 will not be copper-limited in most natural environments due to their efficient copper uptake system(s), which are yet to be studied in detail. This is supported by previous reports suggesting that natural populations of methanotrophs are not copper-limited (2, 8). If we wish to employ a type I methanotroph in TCE removal from a contaminated site, it may not be necessary to fertilize soil with copper to encourage high TCE degradation rates.

2.4. References

- (1) Whittenbury, R.; Dalton, H. In *The Prokaryotes*; Starr, M., Stolp, H., Truper, H., Balows, A., Schlegel, H., Eds.; Springer-Verlag: Berlin, **1981**; pp 894-902.
- (2) Semrau, J. D.; Smith, K. S.; Lidstrom, M. E. *J.Cell.Bioc.* **1993**, 198.
- (3) Park, S.; Hanna, M. L.; Taylor, R. T.; Droege, M. W. *Biotechnol. Bioeng.* **1991**, 38, 423-433.
- (4) Halden, K.; Chase, H. A. *Water Sci. Technol.* **1991**, 24(11), 9-17.
- (5) DiSpirito, A. A.; Gullede, J.; Murrell, J. C.; Shiemke, A. K.; Lidstrom, M.E.; Krema, C. L. *Biodegradation* **1992**, 2, 151-164.
- (6) Brusseau, G. A.; Tsien, H.-C.; Hanson, R. S.; Wackett, L. P. *Biodegradation* **1990**, 1, 19-29.
- (7) Tsien, H.-C.; Brusseau, G. A.; Hanson, R. S.; Wackett, L. P. *Appl. Environ. Microbiol.* **1989**, 55, 3155-3161.
- (8) Fitch, M. W.; Graham, D. W.; Arnold, R. G.; Agarwal, S. K. *Appl. Environ. Microbiol.* **1993**, 59(9), 2771-2776.
- (9) Jackson, G. A.; Morgan, J. J. *Limnol. Oceanogr.* **1978**, 23(2), 268-282.
- (10) Sunda, W.; Guillard, R. R. L. *J. Mar. Res.* **1976**, 34, 511-529.
- (11) Zevenhuizen, L. P. T. M.; Dolfing, J.; Eshuis, E. J.; Scholten-Koerselman, I. J. *Microb. Ecol.* **1979**, 5, 139-146.
- (12) Blust, R.; Verheyen, E.; Doumen, C.; Decler, W. *Aquat. Toxicol.* **1986**, 8, 211-221.
- (13) Coale, K. H.; Bruland, K. W. *Deep-Sea Res.* **1990**, 37(2), 317-336.
- (14) Bruland, K. W.; Donat, J. R.; Hutchins, D. A. *Limnol. Oceanogr.* **1991**, 36(8), 1555-1577.
- (15) Langford, C. H.; Gutzman, D. W. *Anal. Chim. Acta* **1992**, 256, 183-201.

- (16) Anderson, D. M.; Morel, F. M. M. *Limnol. Oceanogr.* **1978**, *23*(2), 283-295.
- (17) Gadd, G. M.; Griffiths., A. J. *Microb. Ecol.* **1978**, *4*, 303-317.
- (18) Doyle, J. J.; Marshall, R. T.; Pfander, W. H. *Appl. Microbiol.* **1975**, *29*, 562-564.
- (19) Chan, S. I.; Nguyen, H. H. T.; Shiemke, A. K.; Lidstrom, M. E. In *Microbial Growth on Cl Compounds*; Murrell, J. C., Kelly, D. P., Eds., Intercept: Andover, 1993, pp93-107.
- (20) Whittenbury, R.; Phillips, K. C.; Wilkinson, J. F. *J.Gen.Microbiol.* **1970**, *61*, 205-218.
- (21) Avdeef, A.; Zabronsky, J.; Stuting, H. H. *Anal.Chem.* **1983**, *55*, 298-304.
- (22) Simpson, R.J. In: *Ion-selective electrode methodology*. 1979 Boca Raton, Fla.: CRC Press, 1979; *1*; pp43-66.
- (23) Hansen, E. H.; Lamm, C. G.; Ruzicka, J. *Anal.Chim.Acta* **1972**, *59*, 403-426.
- (24) *Inductively Coupled Plasma - Mass Spectrometry. User Course.* 1993 Perkin Elmer Sciex.
- (25) Scott, M. J. *SURFEQL User's Manual*, Environmental Engineering Science, California Institute of Technology, 1989.
- (26) Sunda, W. G.; Huntsman, S. A. *Mar.Chem.* **1991**, *36*, 137-163.
- (27) Guy, R. D.; Kean, A. R. *Water Res.* **1980**, *14*, 891-899.
- (28) Shuttleworth, K. L.; Unz, R. F. *Appl. Environ. Microbiol.* **1993**, *59*(5), 1274-1282.
- (29) Morel, F. M. M.; Hudson, R. J. M.; Price, N. M. *Limnol. Oceanogr.* **1991**, *36*(8), 1742-1755.

Table 2.1 Results of ICP/MS and ISE Measurements of the Initial Concentrations of Total Copper and Cupric Ion.

Experiment series	EDTA added (μM)	Copper added (μM)	Copper measured by ICP/MS (μM)	Cupric ion measured by ISE (10^{-9} M)
1 Copper accumulation experiments	11.7	1	3.0	2.6
	11.7	2	4.2	2.8
	11.7	5	8.4	3.4
	11.7	10	12.3	4.6
	11.7	15	17.3	7.3
	11.7	20	19.1	11.0
	11.7	30	28.1	32.0
	11.7	40	37.0	60.0
2a Copper accumulation under various complexation conditions	11.7	1	4.4	3.4
	11.7	5	7.6	4.8
	11.7	10	13.4	6.9
	11.7	20	20.9	11.0
	11.7	30	33.2	41.0
	11.7	40	43.2	180.0
	11.7	60	64.4	320.0
	11.7	70	67.0	430.0
b	15.7	1	3.6	2.6
	15.7	10	10.6	2.7
	15.7	20	19.9	3.7
	15.7	30	34.4	11.0
	15.7	40	42.9	33.0
	15.7	50	52.0	80.0
	15.7	70	79.0	370.0
	15.7	100	97.0	460.0
c	21.7	1	2.5	2.4
	21.7	5	8.4	2.5
	21.7	20	19.4	2.7
	21.7	30	34.8	4.2
	21.7	50	48.9	7.6
	21.7	60	55.9	20.0
	21.7	80	77.6	100.0
	31.1	100	101.7	300.0
d	31.7	1	2.4	2.3
	31.7	5	8.8	2.5
	31.7	10	13.9	2.8
	31.7	30	29.4	3.2
	31.7	40	39.9	3.7
	31.7	50	45.3	8.0
	31.7	70	67.9	150.0
	31.7	90	87.4	280.0

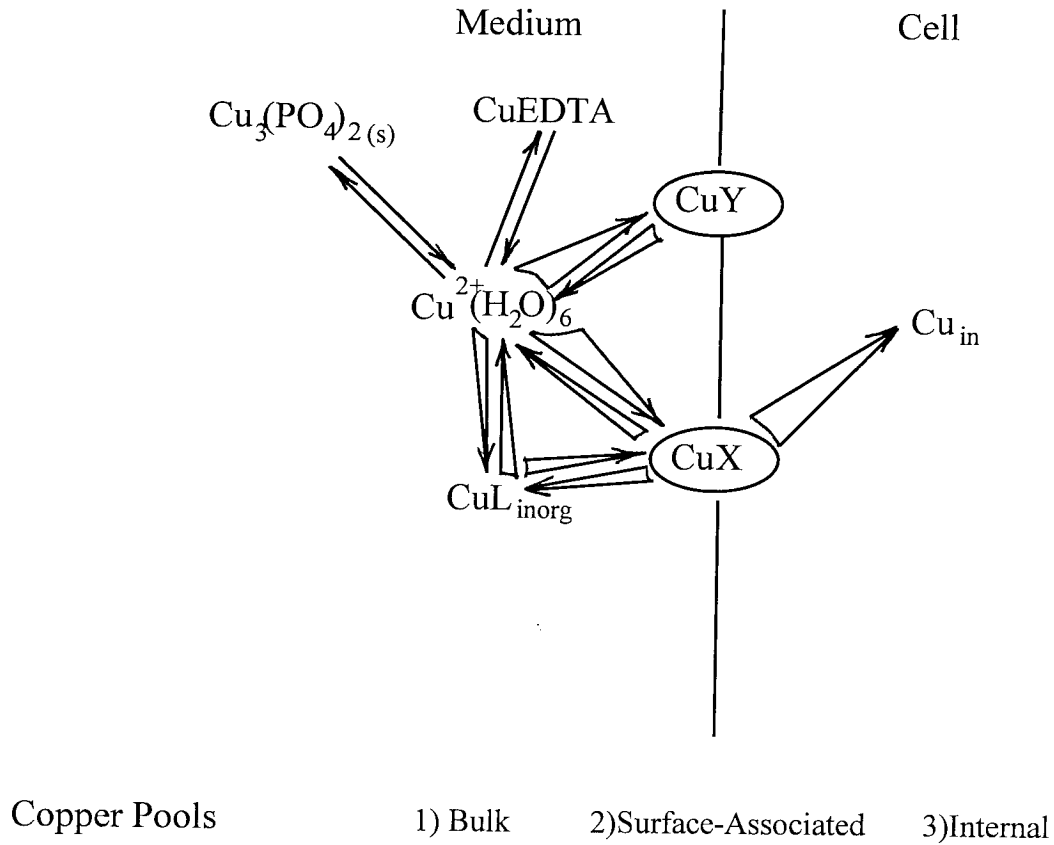


Figure 2.1 Model for copper accumulation by *M. albus* BG8 .

Three pools of copper are assumed: (1) copper in the growth medium (bulk copper), including $\text{CuL}_{\text{inorg}}$ (soluble copper complexes with inorganic ligands, such as CuCO_3 , CuHPO_4 , CuSO_4 , $(\text{CuOH})^+$, etc.), $\text{Cu}_3(\text{PO}_4)_2$ precipitate, CuEDTA and $\text{Cu}^{2+}(\text{H}_2\text{O})_6$; (2) surface-associated copper including transport site complexes (CuX) and copper sorbed on non-specific surface sites removable by EDTA (CuY); and (3) internal copper (Cu_{in}). Arrow widths show the probable relative rates of each reaction when transport system is not saturated.

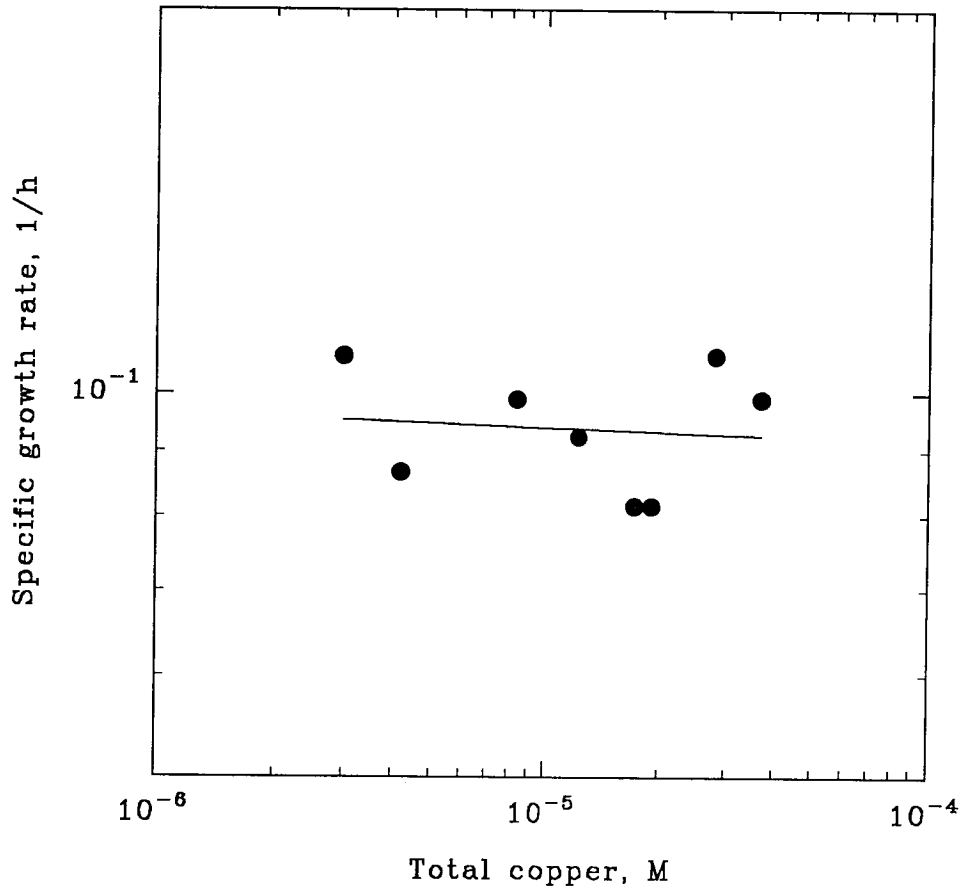


Figure 2.2 Specific growth rate observed within a total copper concentration range from 3 to 37 μM .

Total copper is the amount of copper nitrate added to the growth medium.

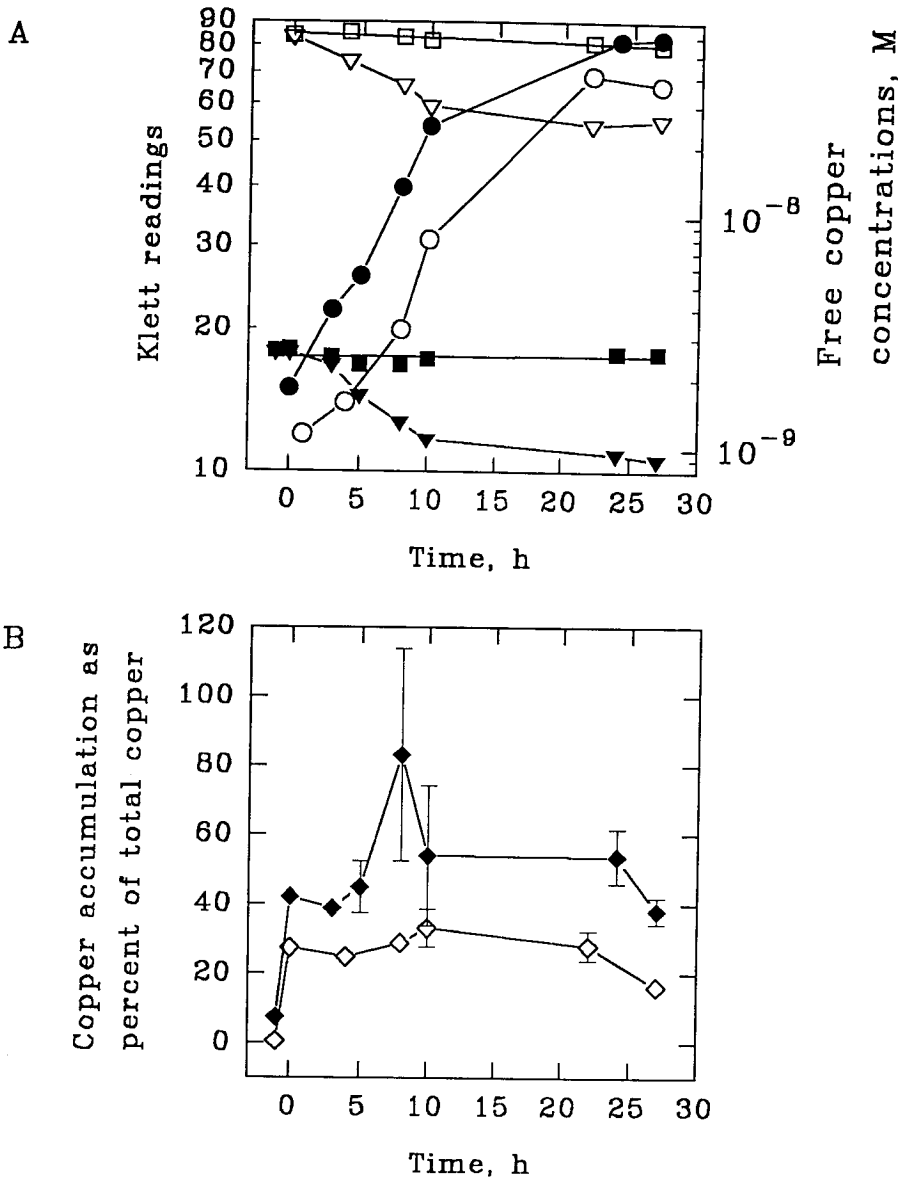


Figure 2.3 Cupric ion concentration and copper accumulation by *Methylobacterium albus* BG8 during growth.

Cells were inoculated into the medium at time 0.

A. Cupric ion concentration in the medium. Filled symbols denote 3 μ M, open ones denote 37 μ M total copper added to NMS. Circles show optical densities as measured by the Klett colorimeter. Squares indicate cupric ion concentration measured by CuISE in the control flasks (no *M. albus* BG8). Triangles show the time course of cupric ion disappearance from the medium in the flasks inoculated with *M. albus* BG8 as measured with CuISE.

B. Change in relative amount of cell-associated copper during the time course of the experiment. Filled diamonds indicate 3 μ M and open ones indicate 37 μ M total copper added to NMS.

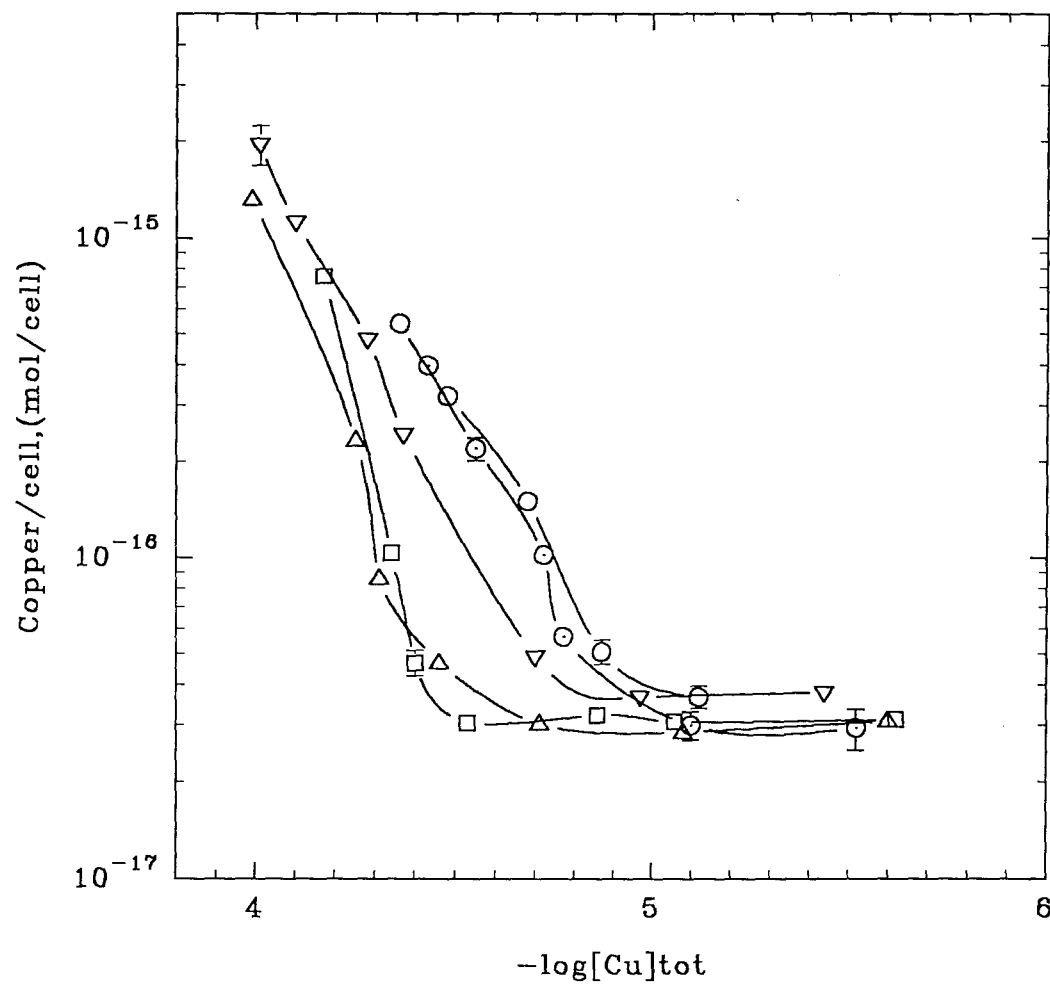


Figure 2.4 Cellular copper content of *M. albus* BG8 versus negative logarithm of total copper added to the medium.

- , [EDTA]=11.7 μM; ▽, [EDTA]= 15.7 μM; □, [EDTA]=21.7 μM;
 △, [EDTA]=31.7 μM;
 ⊙, data from Figure 2.3 ([EDTA]=11.7 μM).

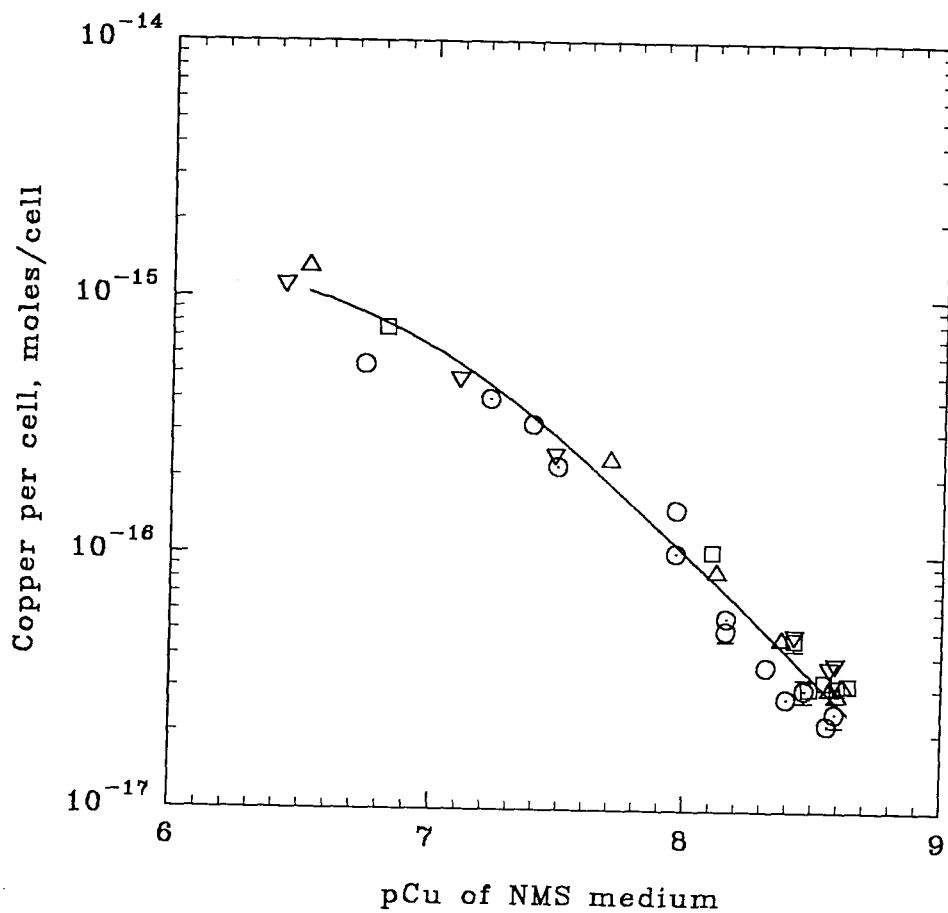


Figure 2.5 Cellular copper content of *M. albus* BG8 versus negative logarithm of the cupric ion concentration (pCu) in the medium at different EDTA concentrations.

Symbols are as in Figure 2.4.

The curve is a plot of the hyperbolic model.

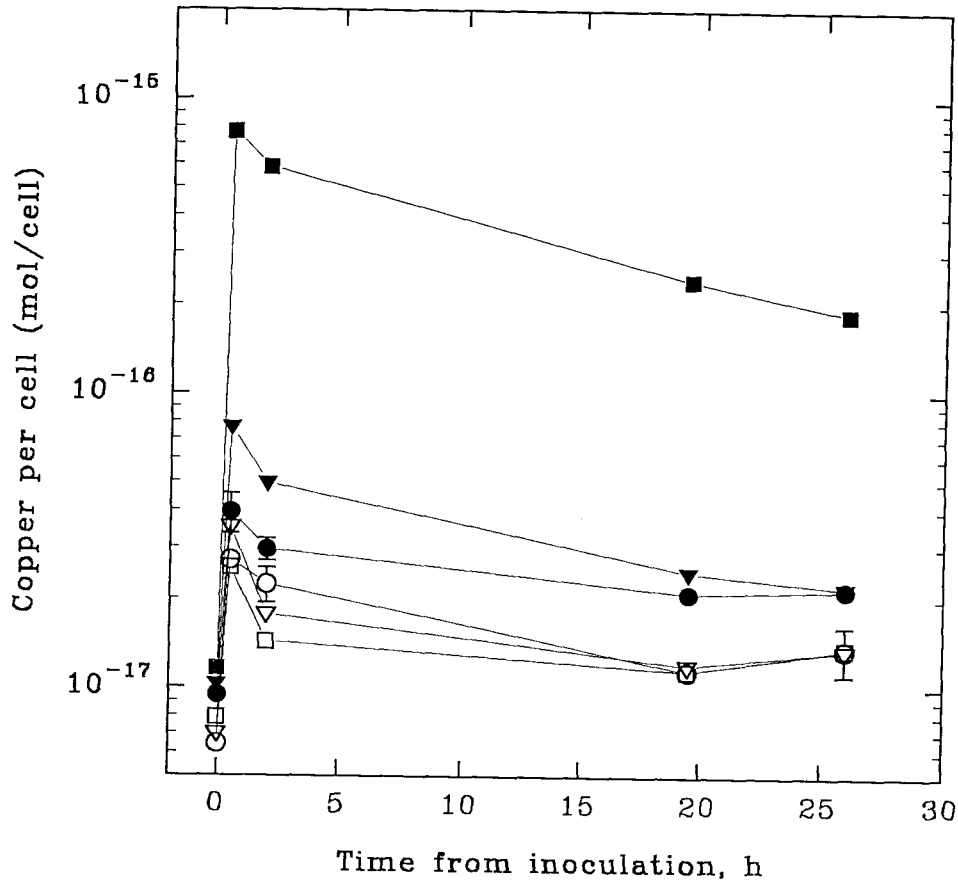


Figure 2.6 Copper accumulation in cells either untreated or incubated with EDTA and then washed.

Filled symbols represent untreated samples; open ones indicate washed samples (incubated in 0.1M EDTA for 24 h and then washed).

Total copper concentrations in the medium:

circles - 1.2 μ M, triangles - 12 μ M, squares - 43 μ M.

Growth curves were similar to these shown in Figure 2.3A.

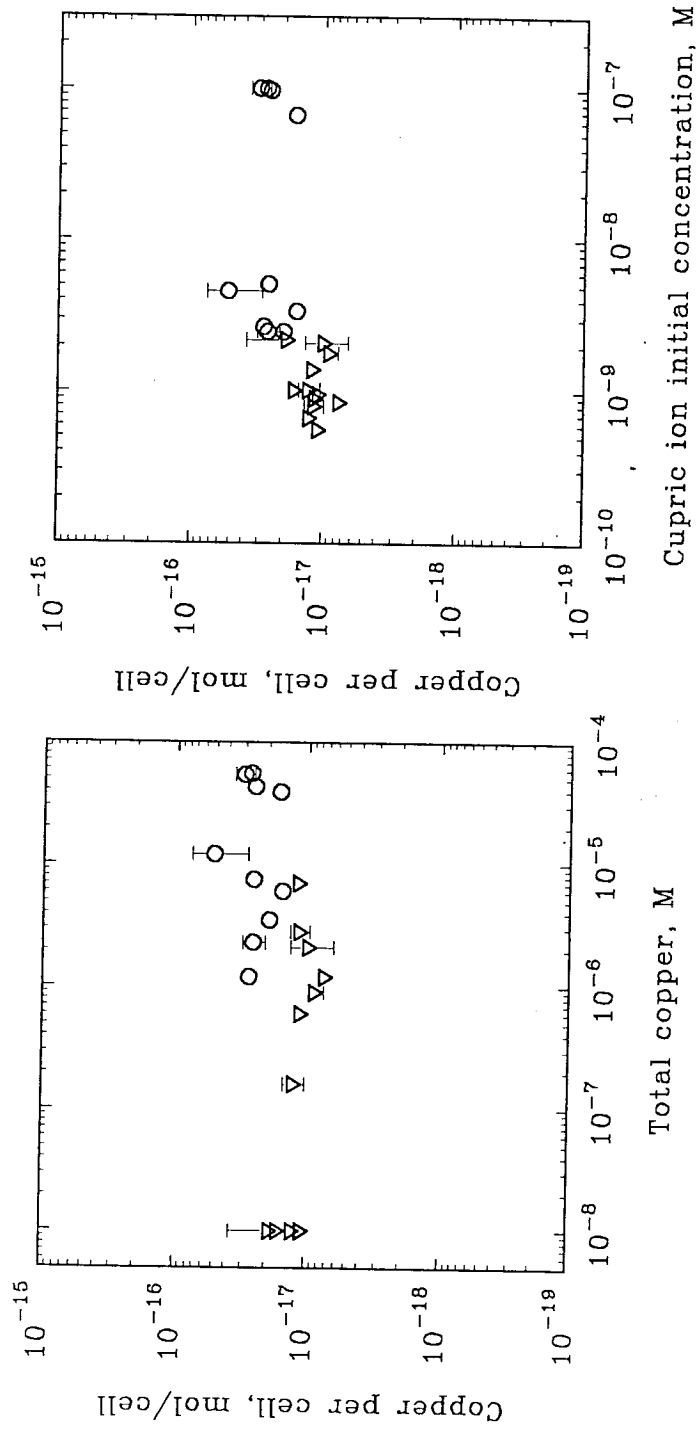


Figure 2.7 Copper accumulated in cells within 1h of inoculation during sorption experiments versus total copper concentration and cupric ion concentration.

Circles, experiments were inoculated from agar plates containing $10 \mu\text{M}$ copper; triangles, experiments were inoculated from agar plates with $2 \mu\text{M}$ copper.

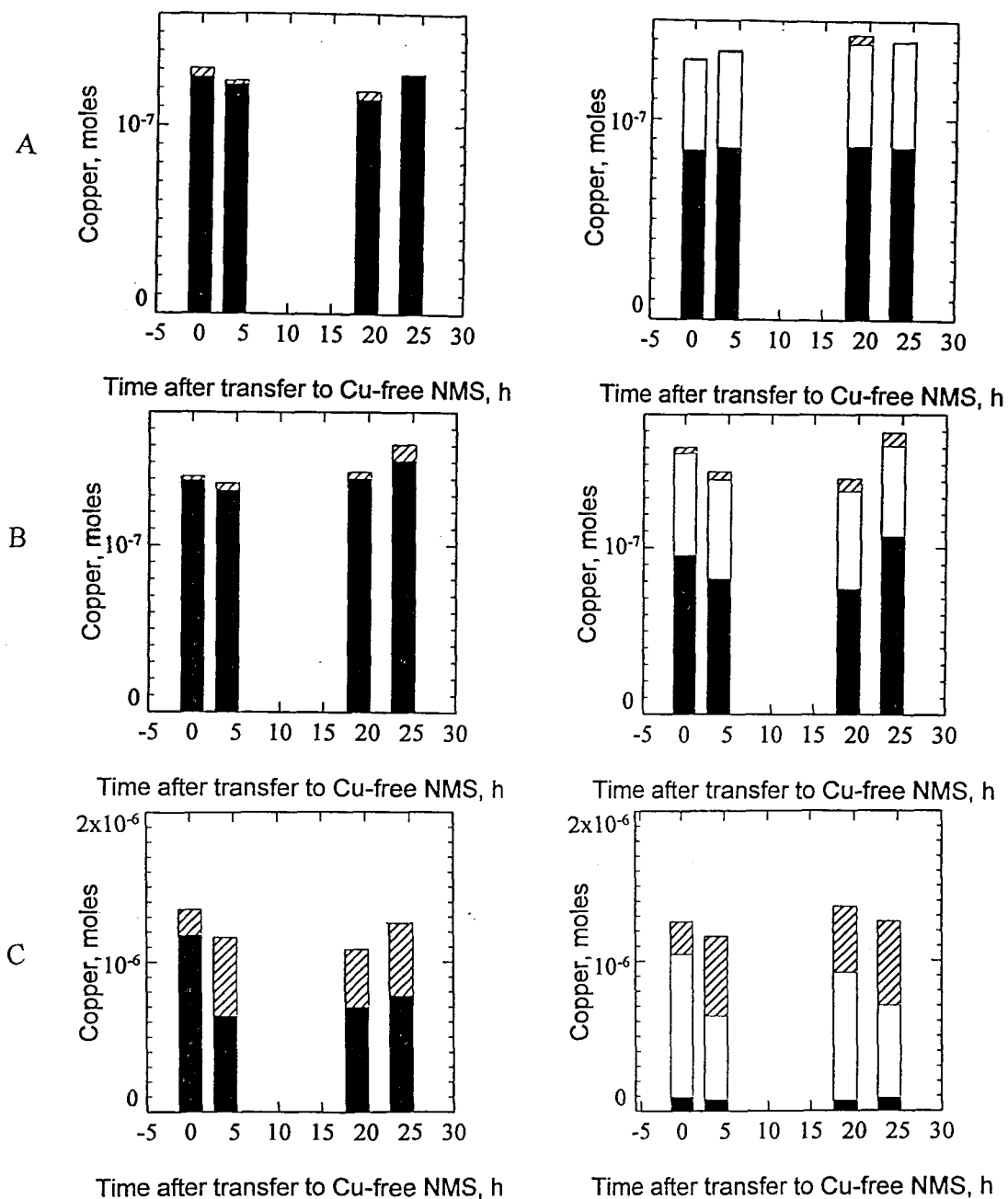


Figure 2.8 Fate of cell-surface associated copper.

Averaged data (from two replicates) are shown in all figures.

Filled bars, copper measured in the cell digests (mol); hatched bars, copper measured in the filtrates (mol); open bars, copper measured in EDTA-treated fractions (mol).

Plots on the left represent measurements in untreated samples; plots on the right reflect measurements in washed samples. Panels A-C show data for three experiments with the following total copper concentrations used for growth before transfer to copper-free medium: 2.3 μM , 7.5 μM , and 39 μM .

Appendix

In this appendix, figures that are relevant to Chapter Two but were not included in the original paper (Berson and Lidstrom 1996) are presented.

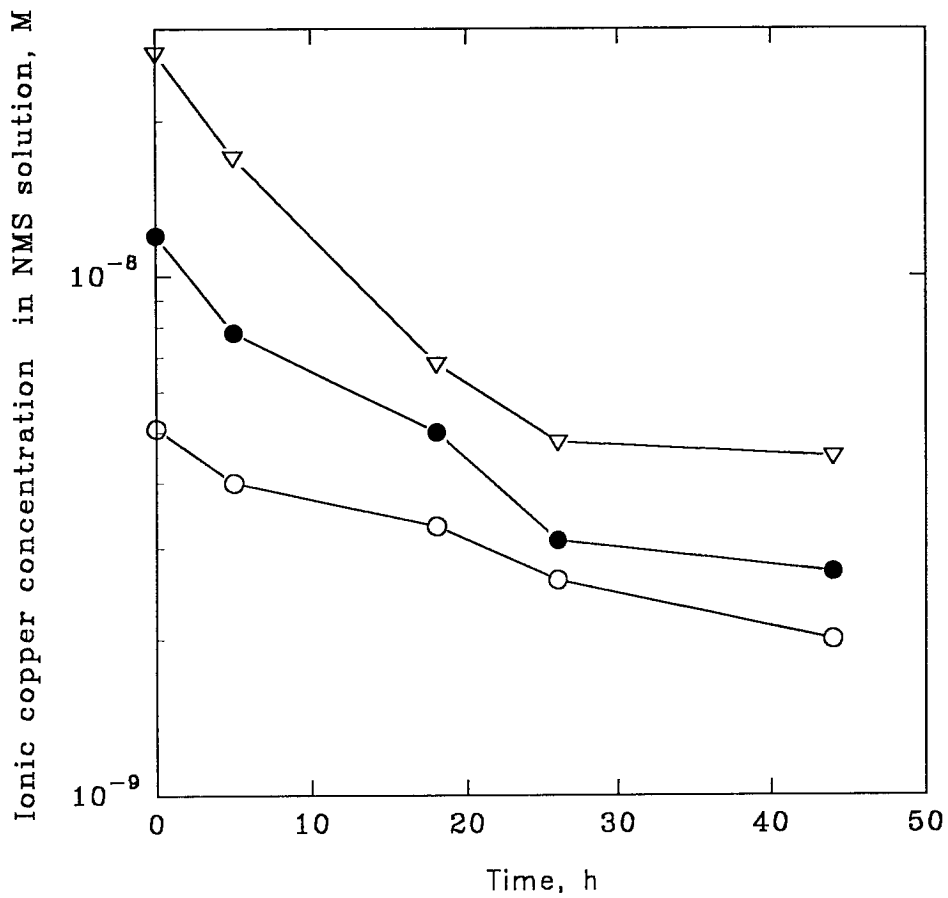


Figure A2.1 The decrease in free copper concentration during media preequilibration.

The time required to achieve a pseudoequilibrium in NMS media at various total copper concentrations was studied. Open circles, 3 μM total copper; solid circles, 7 μM total copper; triangles, 12 μM total copper in NMS media.

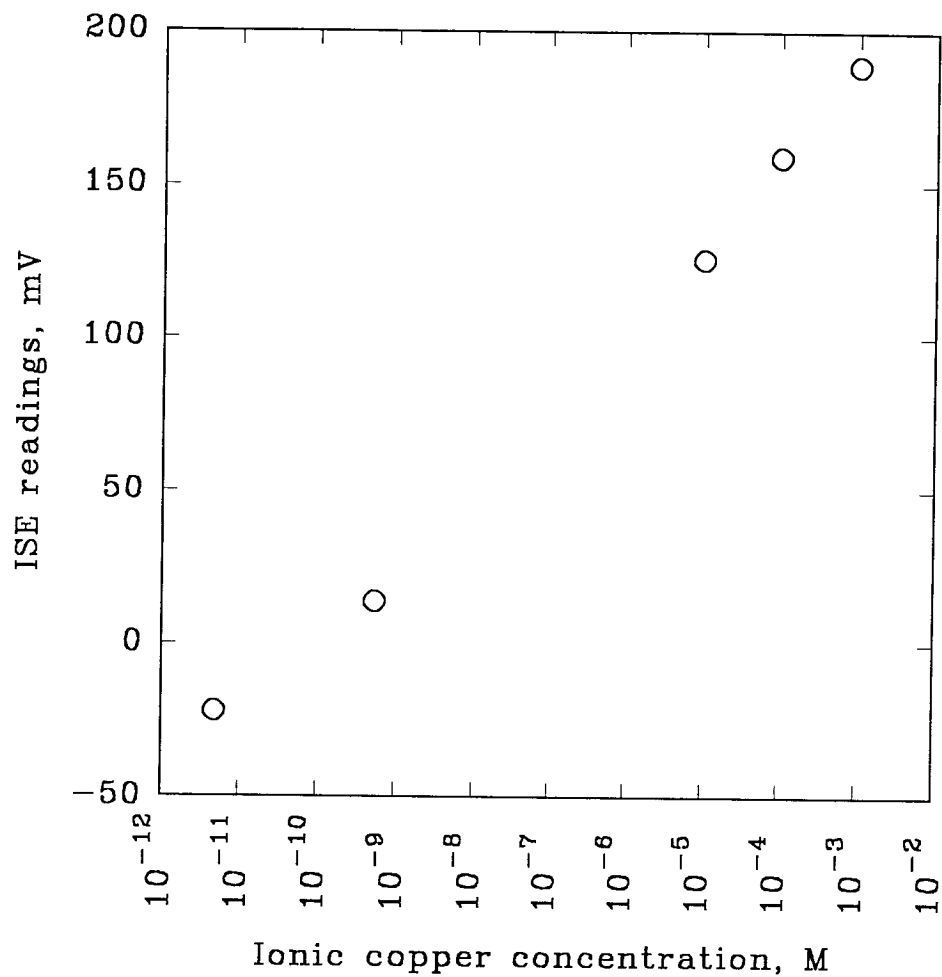


Figure A2.2 One of the cupric ion selective electrode calibrations obtained with cupric ion buffers [$\text{CuNO}_3/\text{EDTA}/\text{borax}$].

This particular calibration gave a slope of 28 mV/pCu in the range from 10^{-10} to 10^{-3} M . The calculated ideal theoretical Nernstein slope is 29.5 mV/pCu at 25 °C.

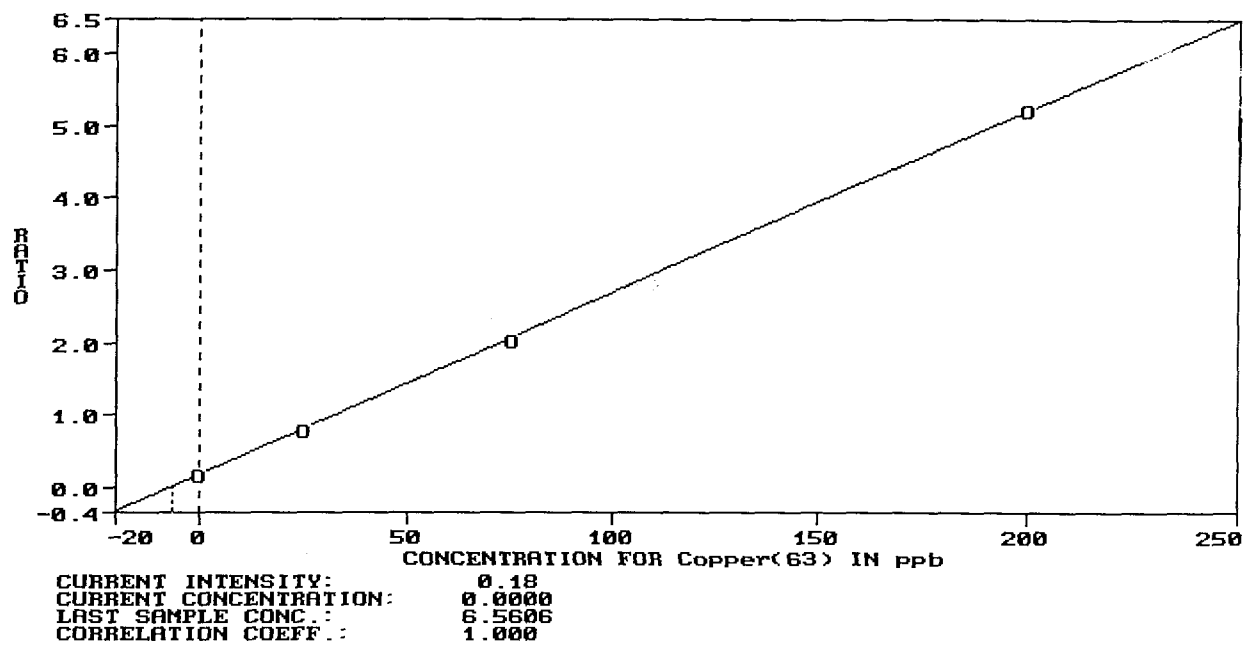


Figure A2.3 An example of ICP/MS addition calibration with copper nitrate standards.

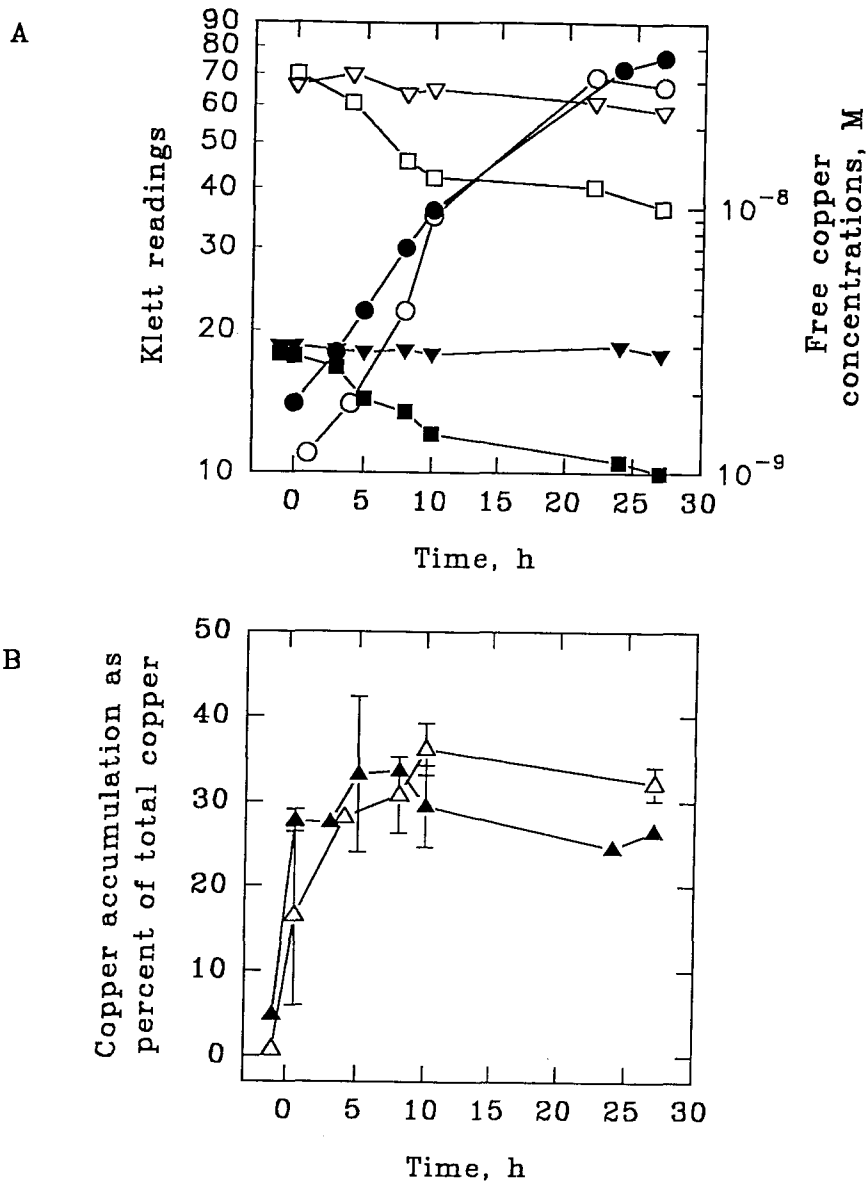


Figure A2.4 Cupric ion concentration and copper accumulation by *Methylobacterium albus* BG8 during growth; 4 μM (filled symbols) and 28 μM (open symbols) total copper added to NMS.

Cells were inoculated into the medium at time 0.

A. Cupric ion concentration in the medium. Circles show optical densities as measured by the Klett colorimeter. Triangles indicate cupric ion concentration measured by CuISE in the control flasks (no *M. albus* BG8). Squares show the time course of cupric ion disappearance from the medium in the flasks inoculated with *M. albus* BG8 as measured with CuISE.

B. Change in relative amount of cell-associated copper during the time course of the experiment.

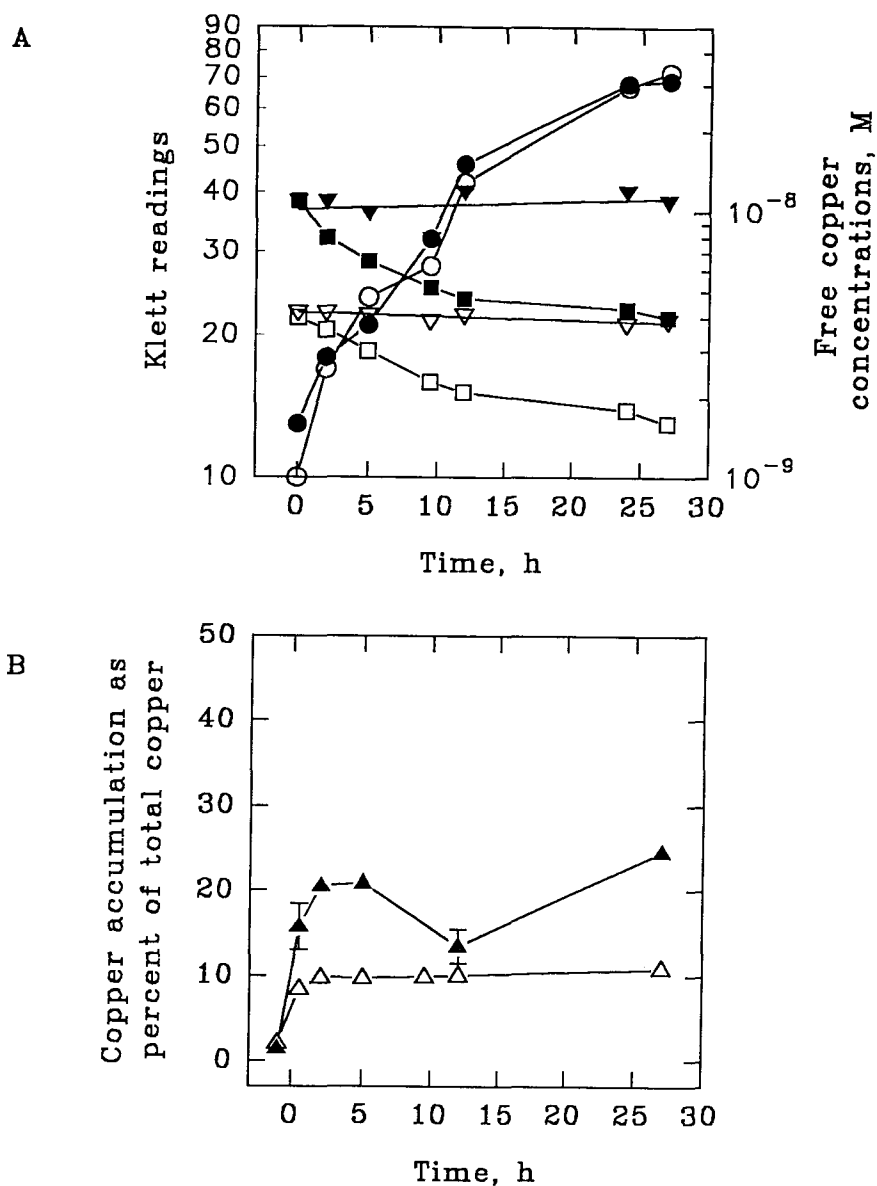


Figure A2.5 Cupric ion concentration and copper accumulation by *Methylomicrobium albus* BG8 during growth; 12 μM (open symbols) and 19 μM (filled symbols) total copper added to NMS.

Cells were inoculated into the medium at time 0.

A. *Cupric ion concentration in the medium.* Circles show optical densities as measured by the Klett colorimeter. Triangles indicate cupric ion concentration measured by CuISE in the control flasks (no *M. albus* BG8). Squares show the time course of cupric ion disappearance from the medium in the flasks inoculated with *M. albus* BG8 as measured with CuISE.

B. *Change in relative amount of cell-associated copper during the time course of the experiment.*

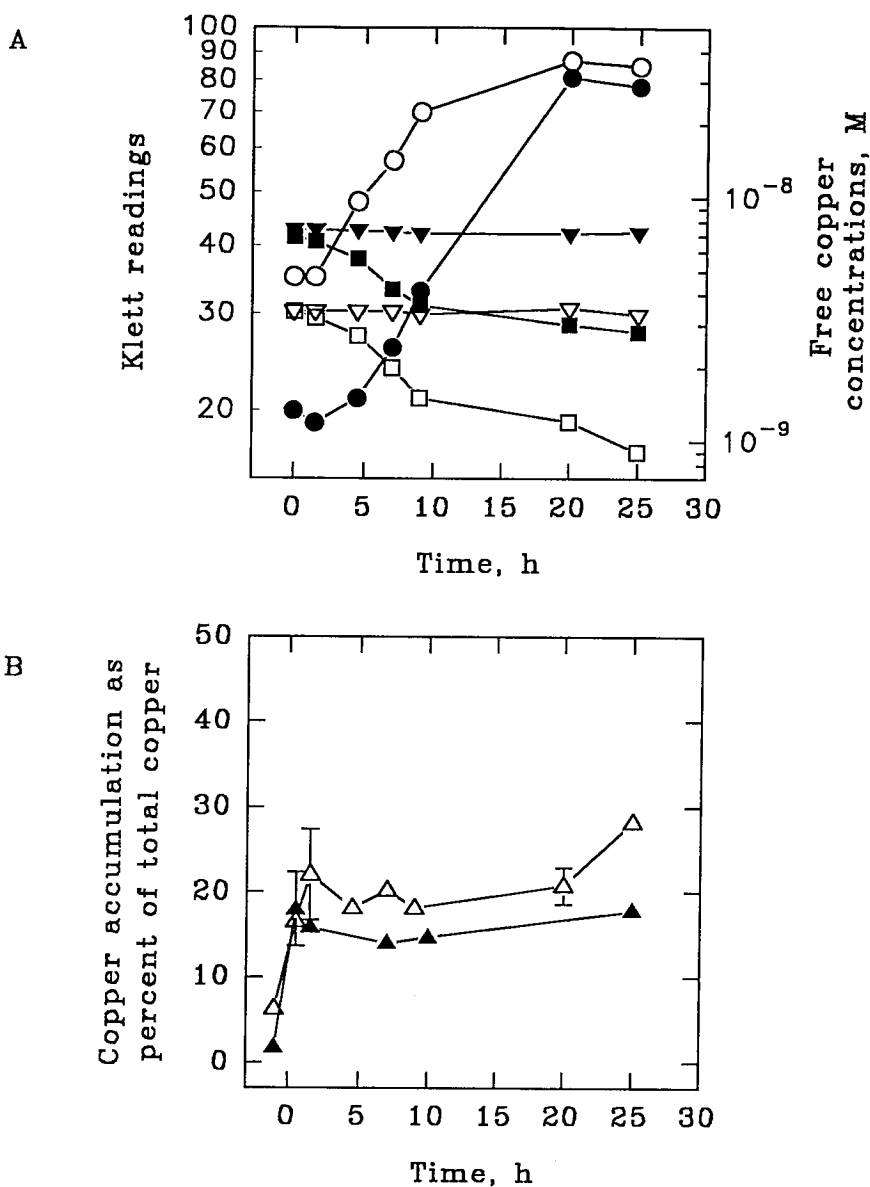


Figure A2.6 Cupric ion concentration and copper accumulation by *Methylomicrobium albus* BG8 during growth; 8 μ M (open symbols) and 17 μ M (filled symbols) total copper added to NMS.

Cells were inoculated into the medium at time 0.

A. *Cupric ion concentration in the medium.* Circles show optical densities as measured by the Klett colorimeter. Triangles indicate cupric ion concentration measured by CuISE in the control flasks (no *M. albus* BG8). Squares show the time course of cupric ion disappearance from the medium in the flasks inoculated with *M. albus* BG8 as measured with CuISE.

B. *Change in relative amount of cell-associated copper during the time course of the experiment.*

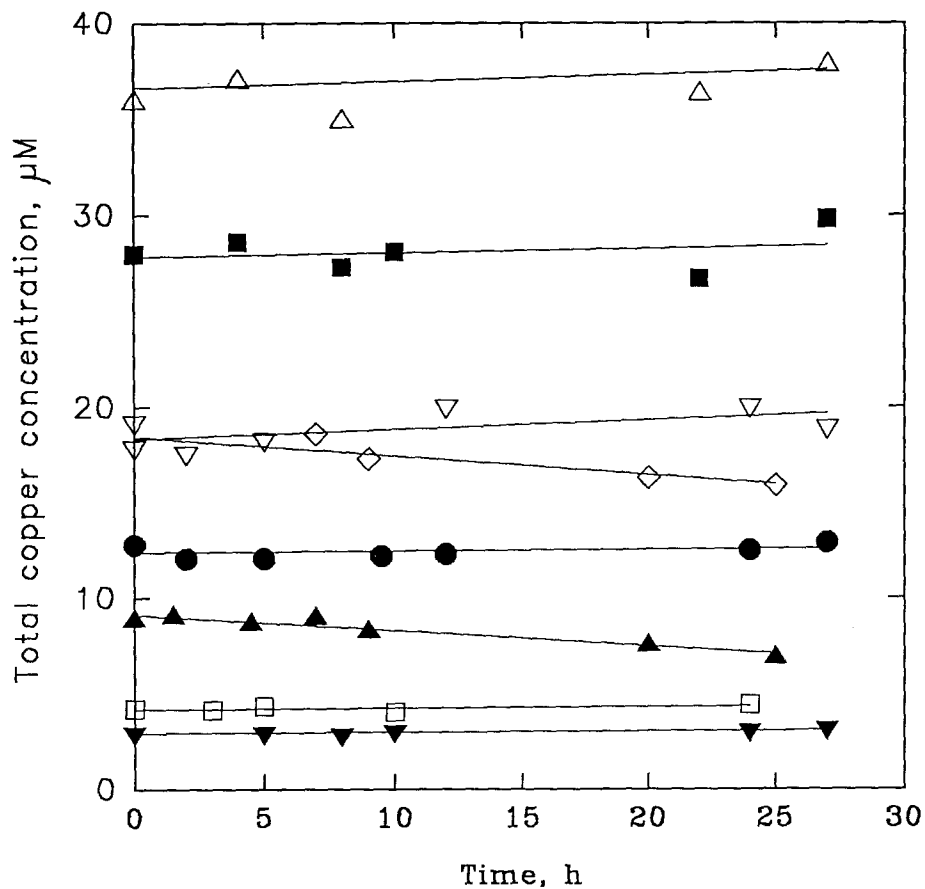


Figure A2.7 Total copper concentration in adsorption controls (cell-free NMS medium) versus time.

The following total copper concentrations were studied:

- ▼ , 3.0 μM ; □ , 4.2 μM ; ▲ , 8.4 μM ; ● , 12.3 μM ;
- ◇ , 17.3 μM ; ▽ , 19.1 μM ; ■ , 28.1 μM ; △ , 37.0 μM .

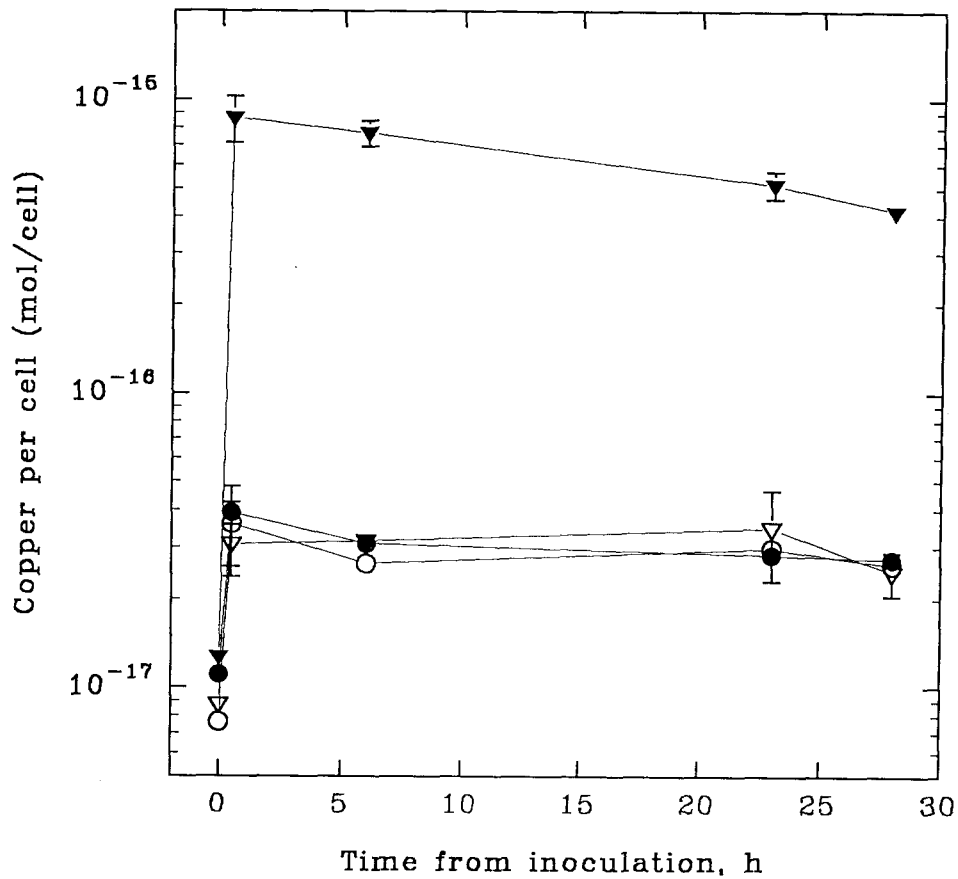


Figure A2.8 Copper accumulation in cells either untreated or incubated with EDTA and then washed; 6 μ M (circles) and 54 μ M (triangles) total copper concentration in the medium.

Filled symbols represent untreated samples; open ones indicate washed samples (incubated in 0.1M EDTA for 24 h and then washed). Growth curves were similar to those shown in Figure 2.3A.

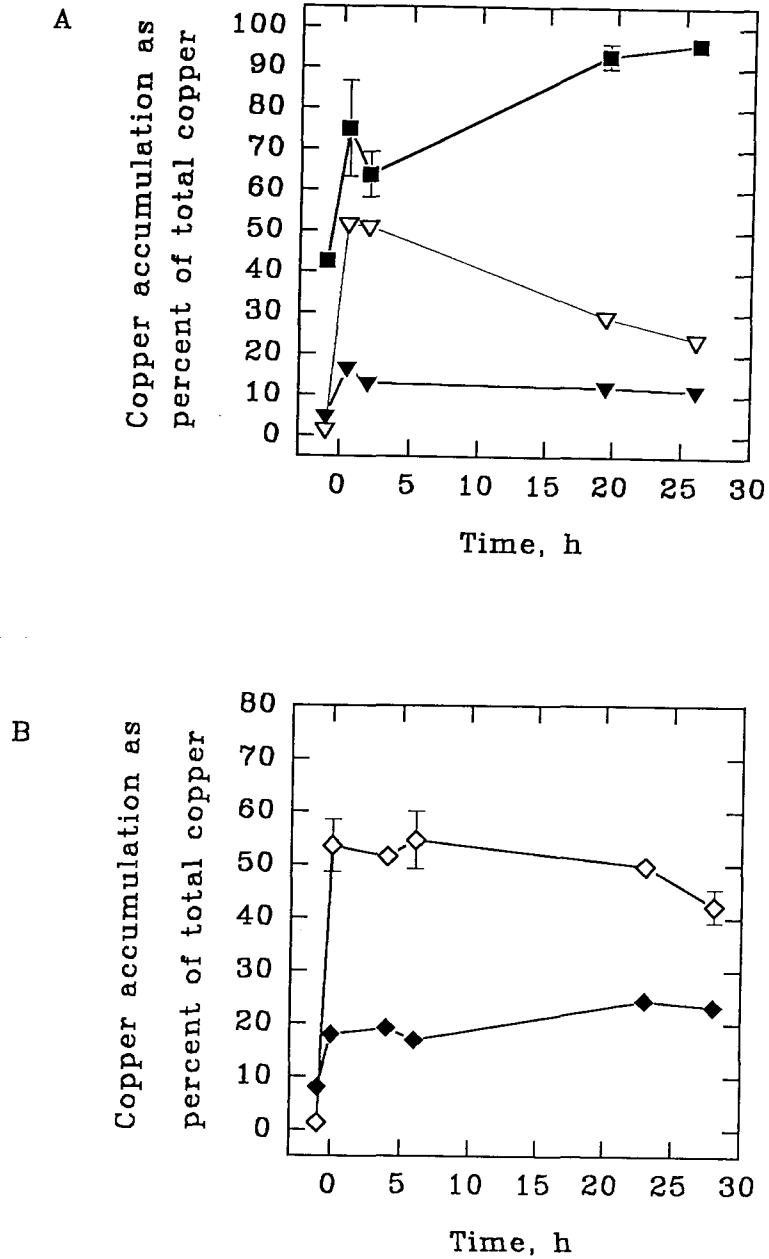


Figure A2.9 Copper accumulation by *Methylobacterium albus* BG8 during sorption experiments.

Cells were inoculated into the medium at time 0.

A. Filled squares, 1.2 μM total copper in the medium; filled triangles, 12 μM total copper in the medium; open triangles, 43 μM total copper in the medium

B. Filled diamonds, 6 μM total copper in the medium; open diamonds, 54 μM total copper in the medium.

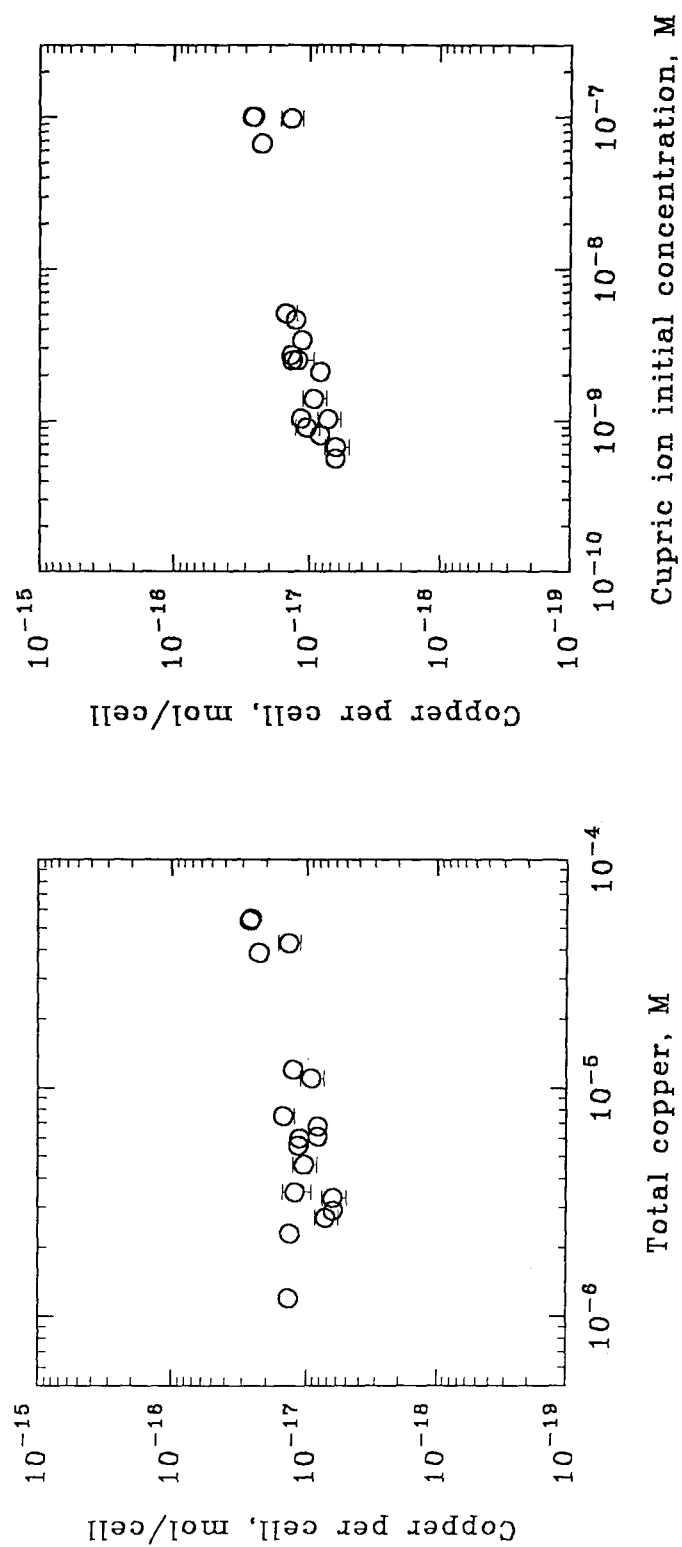


Figure A2.10 Copper accumulated in cells by the end of growth (25-30 h) during sorption experiments versus total copper concentration and cupric ion concentration.

Growth media were inoculated from agar plates containing $10 \mu\text{M}$ copper.

Chapter Three

Cloning and Characterization of corA, a Gene Encoding a Copper-repressible Polypeptide Presumably Involved in Copper Uptake by Methylobacterium albus BG8.

3.1. Introduction

The initial step in the oxidation of methane by methanotrophic bacteria involves methane monooxygenase (MMO). It has been found that the membrane-associated (particulate) form of MMO (pMMO) is a copper-containing enzyme with copper arranged in trinuclear clusters serving as the sites of the enzymatic activity (Chan *et al.* 1993). Copper is found widely in the environment (see Chapter One: 1.3.1.-1.3.3.). The total concentration of Cu in various environments is estimated to be on the order of 10^{-7} - 10^{-9} M (Hodgson *et al.* 1965; Boyle and Edmond 1975; Bruland *et al.* 1980). However, a significant fraction of copper is associated with various organic ligands present in sea water (Sunda and Hanson 1987; Coale and Bruland 1988; Coale and Bruland 1990; Moffett *et al.* 1990; Van den Berg *et al.* 1990, Bruland *et al.* 1991; Van den Berg and Donat 1992), fresh water (Hering and Morel 1988) and soils (Hodgson *et al.* 1965; Berggren 1989). Consequently, the reported concentrations of free copper are very low: $10^{-9.9}$ - $10^{-13.1}$ M for sea water (Coale and Bruland 1990), 10^{-11} - 10^{-18} M in fresh water (Apte *et al.* 1990, Van Den Berg *et al.* 1990), and 10^{-13} - 10^{-16} M for soils (Hodgson *et al.* 1965). As described in Chapter Two, our copper accumulation experiments with the type

I methanotroph *Methylomicrobium albus* BG8 have shown that copper availability to the cells is related to the cupric ion concentrations, not simply its total concentration (Berson and Lidstrom, 1996). Copper uptake by methanotrophs, therefore, is expected to involve a high-affinity copper transport system capable of overcoming low cupric ion concentrations in the environment.

Very little is presently known about the mechanisms by which copper enters cells in methanotrophs. Fitch and co-authors (1993) have indicated the existence of specific copper uptake and metabolism in the type II methanotroph, *M. trichosporium* OB3b. Our recent work (Berson and Lidstrom 1996) has established that a rapid saturation of copper uptake occurs in *M. albus* BG8 cells at $1-3 \times 10^{-17}$ moles of copper per cell despite a 100-fold variation in medium total copper and cupric ion concentrations. This suggests that cupric ion is taken up via a specific transport system.

Many transport mechanisms for uptake of trace metals are presently known (Hughes and Poole 1989; Silver and Walderhaug 1992; Brown *et al.* 1992b; Lee *et al.* 1990; Rogers *et al.* 1991; Cooksey, 1993). In some, multiple transporters for a single ion are found, in others, one transporter is able to transfer several different ions across the membrane (Silver and Walderhaug, 1992). Since copper uptake is central to methane oxidation by the pMMO, it is expected that methanotrophs might employ multiple systems. However, it is possible to obtain some understanding of a specific transport process by identifying and studying putative copper uptake proteins. Such proteins are expected to be copper-repressible, as at high levels of copper they would be needed in lower amounts, and under copper-limitation they should be overexpressed. However,

proteins involved in copper efflux might be copper inducible. In this chapter a screen for copper-regulated polypeptides was undertaken, and the cloning and characterization of *corA*, a gene encoding a copper-repressible protein are presented.

3.2. Materials and Methods

3.2.1. Growth of *M. albus* BG8.

Methylomicrobium albus BG8 (Whittenbury *et al.* 1970), a type I methanotroph, was grown on nitrate mineral salts (NMS) medium (Whittenbury *et al.* 1981) in batch culture with shaking at 200 rpm. Filter sterilized copper nitrate and separately autoclaved phosphate buffer (Whittenbury *et al.* 1981) were added aseptically to autoclaved medium to avoid formation of precipitates. The media then was incubated for 24h with shaking before inoculation to avoid short-term toxic effects of the copper (Berson and Lidstrom 1996). The cells were grown to the late exponential phase at 30°C under a methane/air atmosphere (approximately 1:3 vol/vol) and harvested. Cells were grown at three total copper levels: under conditions of copper limitation (no copper added to the medium), in medium with optimal physiological levels of copper (10 µM and 20 µM), or in medium with high copper concentration, but still not toxic to *M. albus* BG8 under these growth conditions (40 µM). Mutants grew poorly in liquid cultures and, therefore, they were maintained on NMS plates. For chromosomal DNA isolation from mutants, they were grown on the plates for 2 to 3 weeks and harvested by resuspension in a small volume of NMS medium.

3.2.2. Isolation of a Copper-repressible Protein and Sequence

Determination.

Membrane and cytoplasmic/periplasmic fractions of *M.albus* BG8 were prepared as follows. Cells were harvested by centrifugation at 5000g for 10 min. and then washed three times with 20 mM PIPES [piperazine-*N,N'*-bis(2-ethanesulfonic acid)] buffer (pH 7.0). Cells were then resuspended in the same buffer (approximately 3g (wet weight) of bacteria was resuspended in 5 ml of PIPES). The cell suspension was passed three times through a French pressure cell at 137 Mpa. Remaining whole-cell debris was removed by centrifugation at 10,000g for 20 min. The supernatant from this centrifugation was recentrifuged at 150,000g for 1h. The resulting supernatant consisted of periplasm plus cytoplasm (soluble fraction); the pellet contained outer and inner membranes (membrane fraction). The membrane fraction was resuspended 1:2 [wt/vol] in 20 mM PIPES buffer and homogenized. This suspension was diluted in a dissociation buffer 1:4 vol/vol, and incubated for 2 h at room temperature. The soluble fraction was boiled for 10 min. in a dissociation buffer solution added as 1:1 [vol/vol]. The dissociation buffer was prepared as follows: 250mM Tris-HCl, 5% [wt/vol] SDS, 3.3% [vol/vol] β -mercaptoethanol, 20% [vol/vol] glycerol, 0.2% [wt/vol] bromophenol blue.

The SDS-PAGE screening of copper-repressible proteins was performed with an Hoefer Mighty Small™ Gel Electrophoresis Unit (Hoefer Scientific Instruments, San Francisco, Ca). Various concentrations of acrylamide/bis-acrylamide in base and stacker gels were tested, but the best resolution was obtained on the 14% (membranes) and 10% (soluble fraction) gels. The gels were cast as follows. The base gel contained 14 % (10%)

[wt/vol] acrylamide, 0.37% (0.27%) [wt/vol] bis-acrylamide, 2M Tris-Base, pH 8.6, 20% [wt/vol] SDS, 10% [wt/vol] ammonium persulfate, 5 μ l of TEMED per 10 ml of the solution. The stacker gel consisted of 7.2% (5.1%) [wt/vol] acrylamide, 0.19% (0.14%) [wt/vol] bis-acrylamide, 0.5M Tris-Base, pH 6.2, 20% [wt/vol] SDS, 10% [wt/vol] ammonium persulfate, 5 μ l of TEMED per 5ml of the solution. The running buffer contained 200mM glycine, 0.1% [wt/vol] SDS, and 20 mM Tris-Base. The gels were run at a constant current of 20mA per gel until the tracking dye reached the bottom of the gel (approximately 1h). Depending on sample concentration, 10 to 20 μ L of membrane or soluble fraction was loaded. The gels were stained with FastStain™ (Zoion Biotech, Newton, Ma) to visualize polypeptide bands.

After the polypeptide bands of interest were identified in the course of the initial screening, SDS-PAGE was carried out with the Xcell II gel system (Novex, Inc., San Diego, Ca). Precast 1-mm-thick 8-16% polyacrylamide gradient Tris-glycine gels were used for protein separation. The gels were prerun with the dissociation buffer to remove any residual free radicals that commonly cause blocked amino termini of polypeptides. Then, the gel was run again with samples prepared from cultures grown without copper added to the medium and a control sample prepared from the cultures grown with 10 μ M copper added. The electrophoresis was performed at 4°C to minimize any heat damage to proteins and under a constant current of 40 mA. The running buffer contained 250 mM glycine, 0.1% [wt/vol] SDS, 25 mM Tris, and 0.1 mM thioglycolate (added fresh just before use). Polypeptide bands were blotted from the SDS-polyacrylamide gel onto an Immobilon P membrane (Millipore Corp., Bedford, Ma) at 4°C. A Bio-Rad Trans-Blot

cell was used to transfer polypeptide bands overnight at 100 V in a transfer buffer. The transfer buffer consisted of 12mM Tris, 96mM glycine, 10% [vol/vol] methanol, and 0.5 mM dithiothreitol. The membranes were stained in Coomassie blue (0.2 [wt/vol] Coomassie blue R-250 in 45% [vol/vol], 10% [vol/vol] acetic acid). The membranes were destained in 45% [vol/vol] and 10% [vol/vol] acetic acid. The membranes were rinsed several times in water to decrease the glycine and Tris concentrations. Appropriate bands were excised and sequenced by Edman degradation on ABI 476 pulsed liquid protein sequencer (Applied Biosystems, Inc., Foster City, Ca) by the Protein/Peptide Micro Analytical Facility at California Institute of Technology. One of these sequences was used to design an oligonucleotide probe using an eight-amino acid sequence fragment, Gly-Thr-Phe-Phe-Asp-Lys-Asn-Asn. The oligonucleotide probe OB1, 5'-GG(A, G, C, or T)-AC(A, G, C, or T)-TT(C or T)-TT-(C or T)-GA-(C or T)-AA(A or G)-AA(C or T)-AA-3', with 512-fold redundancy, was synthesized at the Microchemical Facility at the California Institute of Technology.

3.2.3. DNA Purification.

Chromosomal DNA was isolated from *M.albus* BG8 by a slightly modified procedure of Satio and Miura (1963). The cells were grown to the late exponential phase, harvested by centrifugation at 7,500g for 10 min., washed once with saline-EDTA (0.15 M NaCl and 1 M EDTA, pH 8.0), and resuspended in 10 ml of saline-EDTA to which 4 mg per ml of lysozyme was added. The suspensions were placed in a -70°C freezer for 1h. 10 ml of Tris-SDS buffer (0.1 M Tris, 1% SDS, 0.1 M NaCl, pH 9.0) was

added to the frozen samples, and the tubes with the suspensions were swirled in a 50°C water bath until the solution became clear or nearly clear. The DNA was extracted with neutral phenol-saline-EDTA solution (phenol was saturated with 2 volumes of 0.1 M Tris [pH 9.0], 1 volume TE buffer [10 mM Tris-HCl, pH 7.4, 1 mM EDTA, pH 8.0] and then saturated with the saline-EDTA solution until pH 7.0). The extracted DNA was precipitated with isopropanol and washed in ethanol until no phenol smell could be detected. This DNA was resuspended in TE buffer.

Plasmid DNA isolation was carried out as follows. 3 ml of Luria-Bertani (LB) medium (1% [wt/vol] bacto-tryptone, 0.5% [wt/vol] bacto-yeast extract, 1% [wt/vol] NaCl) containing an appropriate antibiotic was incubated with a single colony clone overnight at 37°C with shaking. Cells were harvested and resuspended in 250 µl of TE buffer to which 4 mg per ml lysozyme was added. The cell suspension then were diluted with 50 µl of 10% [wt/vol] SDS solution and boiled at 100°C for 2 min. To precipitate proteins, 150 µl of 7.5 M ammonium acetate solution was added to the suspensions, they were incubated on ice for 10 min. and then centrifuged at 16000g for 10 min. The supernatant containing DNA was collected, and DNA was precipitated with isopropanol, pelleted, and washed with ethanol. This plasmid DNA was resuspended in TE buffer.

All enzymes used were purchased from New England Biolabs, Inc. (Beverly, Ma). Restriction enzyme digestions were performed as described by Maniatis (*et al.*, 1982). DNA fragments obtained from restriction enzyme digestions were separated by electrophoresis (150 V, approximately 1h) through 1% agarose gels in a Tris-borate buffer (0.089 M Tris-borate; 0.089M boric acid; 0.002M EDTA). A 1Kb DNA Ladder

(Boehringer, Mannheim, Germany) was used for sizing both chromosomal and plasmid DNA fragments. The gels were stained by adding the fluorescent dye ethidium bromide (0.5 µg/ml) to the buffer. The gels intended for hybridizations with a nucleotide probe were denatured in a solution of 150 mM NaCl and 0.5 N NaOH for 30 min. on a shaker at room temperature. The denaturing solution was then replaced with a neutralizing solution, 0.5M Tris-HCl (pH 8.0), and the gel was shaken for 30 min. at room temperature. Finally, the gel was dried at 80°C in a vacuum gel dryer (Bio-Rad, Hercules, CA).

3.2.4. Cloning and Sequencing of *corA*.

The oligonucleotide probe OB1 was end labeled with 5'-[$\gamma^{32}\text{P}$]ATP as described below. 20 pmoles (1µl) of the synthesized oligo was resuspended in 38 µl ddH₂O and put into a boiling water bath for 10 min. 10x phosphorylation buffer (5 µl), 20 units of T4 polynucleotide kinase (1µl), and 150 µCi of 5'-[$\gamma^{32}\text{P}$]ATP were mixed with the denatured oligo and incubated at 37°C for 45 min. To stop the reaction, 50 µl of 0.1 M EDTA was added to the mix after the incubation. 10x phosphorylation buffer is composed of 0.5M Tris-HCl, 0.1M MgCl₂, 50mM dithiothreitol, 1mM spermidine, 1mM EDTA.

The labeled oligo OB1 was denatured and hybridized to the dried gels overnight at 39°C with shaking. The temperature of the hybridization with OB1 was chosen based on the following formula (Maniatis *et al.* 1982): $T_{\text{hybr}} = T_m - 10^\circ\text{C} = [69.3 + 0.441(\text{GC}\%) - 650/L] - 10^\circ\text{C}$, where T_{hybr} , temperature of hybridization; T_m , oligo melting temperature; GC%, the percent of G and C in the oligo; L, number of base pairs in the oligo. The

hybridization solution consisted of 1M sodium chloride, 0.1M sodium citrate, 0.56 % [wt/vol] SDS, 200 μ l 0.5M EDTA (pH 8); 0.5% [wt/vol] dry powdered milk. After hybridization the gels were washed 3 times with 75 mM sodium chloride, 7.5 mM sodium citrate, and 0.1% SDS to remove any residual non-specifically bound radioactivity. Air dried gels were then exposed to X-ray film. To increase the sensitivity of the film, intensifying screens were always used, and the exposure was carried out at -75°C (Maniatis *et al.* 1982).

DNA fragments excised from agarose gels were purified using GeneClean II[®] kit (Bio 101 Inc., La Jolla, Ca). Transformations into competent *Escherichia coli* DH5 α [™] (Life Technologies, Gaithersburg, MD) were carried out following the protocol provided by the manufacturer. The transformants were grown on LB agar plates to which 2.5% [wt/vol] X-gal (5-bromo-4-chloro-3-indolyl- β -D-galactoside), 2.5% [wt/vol] IPTG (Isopropyl- β -D-thiogalactopyranoside), and 100 mg/ml [wt/vol] ampicillin (Amp) were added (Maniatis *et al.* 1982). White colonies (carrying recombinant plasmids) were transferred onto ME25 82 mm nitrocellulose filters (Schleicher & Schuell, Los Angeles, CA) placed on LB agar plates with Amp and onto master agar plates with Amp. All plates were grown overnight at 37°C . The next day DNA from the colonies grown on filters was liberated, bound onto the filters and hybridized at 39°C with OB1 probe using the procedures described by Maniatis (*et al.* 1982).

Plasmid DNA for sequencing was isolated using a Qiagen-tip 20 kit (Qiagen, Los Angeles, CA). DNA sequencing was performed with an Applied Biosystems automated sequencer at the California Institute of Technology, Pasadena, Sequencing Facility, for

both strands. Initial sequencing was performed with M13 Forward and M13 Reverse sequencing primers (New England Biolabs, Inc., Beverly, Ma). Synthetic oligodeoxynucleotide primers complementary or identical to previously sequenced DNA fragments were synthesized at the Microchemical Facility at the California Institute of Technology, and they were used for later sequencing. The DNA sequence translation and analyses of DNA and polypeptide sequences were performed by using Genetic Computer Group (GCG), University of Wisconsin programs.

3.2.5. Construction of an Insertion Mutation in *corA*

An insertion mutant in *corA* was constructed by homologous recombination as described elsewhere (Ruvkun and Ausubel 1981; Chistoserdova and Lidstrom 1994). A 1.4-kb DNA fragment containing a kanamycin resistance gene (Km^r) was excised from plasmid pUC4K (Pharmacia, Uppsala, Sweden) using *HincII* sites to produce blunt ends and purified. The plasmid containing the targeted *corA* gene was digested with *BstEII*. *BstEII* can not be inactivated by heat, and, therefore, the plasmid DNA was precipitated from the restriction reaction by adding 10 mM EDTA, 0.4 volumes of 5M ammonium acetate, and 2 volumes of isopropanol as recommended by Maniatis (*et al.* 1982). The *BstEII* 5'-protruding ends were made flush with Klenow fragment and deoxynucleoside triphosphates (dNTPs). The Kan^r gene was ligated into *BstEII* sites of the plasmid, and the construction was used to transform competent *E.coli* DH5 α TM cells as described by Maniatis (*et al.* 1982). The resulting construction (pOB17) was transformed into *E.coli* S17-1 (Simon *et al.* 1983) and the transformants were plated on LB plates with Amp,

Km, and tetracyclin (Tc). The disrupted *corA* was introduced into the *M. albus* BG8 chromosome by conjugation with an *E. coli* strain containing pOB17 and selection on NMS agar plates containing Km. The biparental matings were carried out as follows. Two full loops of *M. albus* BG8 cells, freshly grown on plates, and one full loop of *E. coli* containing pOB17 were resuspended into 1 ml of NMS each, and 600 μ l of *M. albus* suspension was mixed with 60 μ l of *E. coli* suspension. The mixture was centrifuged, resuspended in 50 μ l of NMS, and placed on a NMS agar plate (10 μ M total copper concentration) as a thin spot about 1 inch in diameter. The plates were incubated either under methane/air atmosphere, or with 0.1% [vol/vol] methanol for 2 days at 30°C. The biomass was washed off each plate with 2 ml of NMS. The volume of the suspensions was brought down to 100 μ l by centrifugation and resuspending in 100 μ l of NMS, and they were spread on NMS plates to which Km was added. The plates then were grown either with methane or methanol at 30°C for one to three weeks.

3.2.6. Analysis of Insertion Mutation in *corA*.

The *corA* insertion mutants were streaked on NMS plates containing Amp to determine their phenotype and to distinguish between single and double crossover events. One mutant (OB12.7), that seemed to be a result of a double crossover, was grown on an NMS plate with Km (it was not possible to grow the mutant in liquid culture), characterized by PCR amplification with primers PR12-F6 (5'-ATG-TAT-CCC-TGC-ATG-GCA-CTG-3') and PR12-R1 (5'-TTA-CGG-GAT-ACT-GAC-TTC-TAC-3'). The primer PR12-F6 was chosen from a region located 110 bp downstream from the start of

corA; the primer PR12-R1 was selected from the sequence located at the very end of *corA*. The PCR products obtained from OB12.7 and from wild-type *M. albus* (w.t.) with the above primers were compared. The PCR reactions were carried out in 100 μ l volumes under the following conditions: approximately 20ng template DNA, PCR buffer (10 mM Tris-HCl, 50 mM KCl), 1 mM MgCl₂, 0.2 mM of each dNTP, 1U of *Taq* polymerase (Boehringer, Germany), 100 pmol of each primer, and 5% [vol/vol] DMSO. A Hybaid thermal cycler (Combi TR-2) was used for 30-cycle amplification with following reaction conditions: denaturation, 94°C for 1 min.; annealing, 55°C or 50°C for 1 min.; polymerization, 72°C for 2 min.

To analyze the growth response of the OB12.7 mutant to copper concentration in the medium, the mutant and the w.t. were grown at three levels of total copper concentration in NMS medium: copper-limited conditions (no copper added to NMS), physiological level of copper (10 μ M copper added to NMS), and high, but still allowing the growth of w.t. copper concentration (50 μ M of copper added). Each experiment was performed in triplicate. After 24-h preequilibration of the medium (10 ml in each flask), the flasks were inoculated with w.t. or the mutant strain. At different times, the optical density of the growing cells was measured with a Klett - Summerson (Long Island City, NY) photoelectric colorimeter and was reported as Klett units. Optical density was calibrated to viable cell numbers as was described in 2.2.4.

3.3. Results and Discussion

3.3.1. Purification and Sequencing of the 29-kDa Polypeptide.

M. albus BG8 cells were screened for the presence of copper-regulated polypeptides, under the assumption that these should be involved in copper metabolism and/or transport. The screening was carried out as follows. Cells were grown at 4 copper levels, copper limitation (no copper added to NMS medium), 10 μM , 20 μM , and 40 μM total copper added. These cultures were harvested during the late exponential phase of growth and fractionated to produce soluble (cytoplasm and periplasm) and membrane (outer and inner membranes) fractions. These samples were screened by SDS gel electrophoresis for the presence of polypeptides found at different relative levels in the cells grown under copper limitation than in those grown with copper added to the medium. Three copper repressible (Cu_1^{rep} , Cu_2^{rep} , Cu_3^{rep} found at higher levels in copper-limited cells), and one copper inducible (Cu_1^{ind} ; found at lower levels in copper-limited cells) polypeptides were identified in both membrane (Figures 3.1a, A3.1a-A3.3a) and soluble (Figures 3.1b, A3.1b-A3.3b) fractions. Cu_1^{rep} was a strong band, while the others were minor. An attempt was made to transfer all of these polypeptides onto Immobilon P membranes for sequencing, by optimizing conditions of blotting for each protein band. To increase protein elution efficiency, gel composition was varied (both gradient and single gel concentrations were used), as well as several transfer buffers, transfer times and power settings. However, only the Cu_1^{rep} (membranes) and Cu_3^{rep} band (soluble fraction), found in samples prepared from cells grown under copper-limitation, were successfully

blotted onto membrane and sequenced. It is possible that the other polypeptides did not elute well onto membranes because they are present at lower levels. In some cases poor growth was obtained with cells grown with added copper (Figure 3.1a), but overexpression of CorA always correlated with lack of copper, not with poor growth, which implied that it is copper-repressible rather than a general starvation polypeptide. Therefore, Cu₁^{rep} was termed CorA, for Copper-rerepressible polypeptide A. The following N-terminal sequence was obtained for CorA: Ala-Thr-Ala-Ile-Ser-Gly-Thr-Phe-Phe-Asp-Lys-Asn-Asn-Thr-Ser-Ala-Asp-Met-Thr-Val-Arg-Ala-Tyr-Ser-(Ser)-Tyr-Asn-Leu-Ser-(Ser). The sequence was not significantly homologous to any protein sequences in SwissProt data base.

Cu₃^{rep} was not consistently expressed under copper limitation and, therefore, copper effect on the expression of this polypeptide was questioned. Indeed, its N-terminal sequence, Met-Lys-Lys-Ile-Leu-Asp-Val-Val-Lys-Pro-Gly-Val-Val-Thr-Gly-Glu-Asp-Val-Gln, showed high homology (76.5% to 84.2% in 19 aa overlap) to N-termini of fructose biphosphate aldolases (Figure 3.2). Fructose biphosphate aldolases are not involved directly or indirectly in metal uptake, consequently, the cloning of the gene, corresponding to polypeptide Cu₃^{rep}, was not undertaken.

3.3.2. Cloning and Sequencing of *corA*

Chromosomal DNA was isolated from *M. albus* BG8, digested with *SacI*, *PstI*, *SphI*, *Sall*, *XbaI*, and *BamHI*, separated on 1% agarose-Tris-borate gel and hybridized with the oligonucleotide probe OB1 (Figure 3.3). Bands of 6, 4, 6, 4.2, 0.5, and 8 kb,

respectively were identified. The probe was based on the Gly-Thr-Phe-Phe-Asp-Lys-Asn-Asn fragment of the N-terminal sequence (see 3.2.2.). A 4.2-kb *SalI* fragment was chosen for cloning. A fraction of *SalI*-digested *M. albus* BG8 chromosomal DNA containing DNA fragments sized from 3.5 to 5 kb was excised from an agarose gel and purified. The purified DNA was then ligated with *SalI*-digested pUC19 (New England Biolabs, Inc., Beverly, MA) and used to transform *E. coli*.

Plasmid DNA was isolated from the colonies that hybridized with the OB1 probe and screened for insert size. All of these clones appeared to have the same *SalI* insert of approximately 4.2 kb in either the forward or reverse orientation. Plasmid DNA from one of the clones with the forward insert (pOB10a) and one with the reverse insert (pOB10b) was isolated for further subcloning (Figure 3.4). Six clones per each insert, randomly chosen, were examined for the size and the orientation of the inserts. Three clones containing the 0.9-kb *SalI-SphI* fragment (pOB11) and three clones containing the 3.3-kb *SalI-SphI* fragment (pOB12) were identified (Figure 3.4). One of each of these clones was used for sequencing. The subclones pOB11 and pOB12 were then sequenced on both strands and the combined sequence is presented in Figure 3.5.

3.3.3. Analysis of the Sequence Data.

The sequence (Figure 3.5) was analyzed by identifying start and stop codons and by using Testcode program from the GCG Package (Figure 3.6). The Testcode program analyzes local nonrandomness at every third base in sequence in a frame-independent way, and it produces a plot that allows gene localization. Both methods revealed three

open reading frames (*orf2*, *orf3* (*corA*), *orf4*), two partial open reading frames at the ends of the insert (*orf1* and *orf5*), and 984-bp, 205-bp, and 247-bp regions without a distinguishable area of polypeptide coding (Figure 3.4).

The 695-bp fragment, *orf3*, was recognized as *corA*, since it contained a region coding for the N-terminal sequence of CorA. Based on the DNA sequence and its translation, it appears that CorA contains 695 residues, and it has a molecular mass of 21,860 Da. The discrepancy between the mass, estimated based on the amino acid sequence (21,860 Da), and the approximate mass of the polypeptide, predicted from the SDS-PAGE screening (28,500 Da), is probably because addition of the dye to polypeptides for SDS-PAGE electrophoresis sometimes causes them to migrate differently than their true molecular weights. Therefore, the mass of 21,860 Da was presumed to be the true mass of CorA. CorA was found in the membrane fraction of the cells (Figure 3.1) and this finding is supported by the presence of a leader sequence of 30 residues (Figure 3.5) and by hydropathy plots that indicate that CorA should be a membrane polypeptide (Figure 3.7). Eight possible membrane-spanning regions were identified in CorA by using the residue specific hydrophobicity index of Kyte and Doolittle (Figure 3.7). A search of both DNA and protein data bases revealed some homology of CorA (17.5% identity in 126 aa overlap) to rabbit and human calcium release channel protein (Takeshima *et al.* 1989) (Figure 3.8). No specific copper-binding domains were found in CorA. It is possible, however, that CorA is a metal porin (which can be involved in the transport of several metals, including copper), and it is induced

under conditions of a nutrient metal starvation. To provide more direct information about the function of CorA, mutants defective in *corA* were generated (see below).

The sequences of the other open reading frames (Figure 3.4) and their corresponding polypeptides were compared with DNA and protein data banks (SwissProtein Bank, GenBank). Only one of these, the 221-amino-acid-long polypeptide encoded by *orf1* (665 bp), demonstrated high similarity to a known protein. A 29-kDa extragenic suppressor protein (268 amino acids) that is involved in facilitating the function of heat shock proteins (Yano *et al.* 1990) had 50.7% identity in 221 aa with the product of *orf1* translation (Figure 3.9). No significant amino acid sequence similarity was found between the products of *orf2*, *orf4*, *orf5* and any known proteins (SwissProtein Bank, GenBank). Hydropathy analysis (Figure 3.10) suggests that all open reading frames in the insert encode membrane polypeptides, however a recognizable leader sequence was found only in *orf2* (22 residues). The second open reading frame, *orf2*, of 539 bases is located downstream of *orf1*, and it encodes a polypeptide of 180 amino acids. The fourth, 455-bp, open reading frame, *orf4*, encodes a polypeptide of 152 aa. The fifth, partial, open reading frame, *orf5*, (329 bp) codes for 113 residues of the N-terminus of a polypeptide. The open reading frames *orf1* and *orf5* are transcribed in the same direction as *corA*, while *orf2* and *orf4* are transcribed in the opposite direction.

3.3.4. Mutant Characterization

To obtain information on the function of *corA*, an insertion mutant defective in the gene was constructed. Mutants were generated by homologous recombination

between *M. albus* BG8 chromosome and the mutated gene in a plasmid. A 3.3-kb *Sall*-*SphI* fragment containing the *corA* gene (695 bp) was cloned into plasmid pUC19 to produce pOB12. The unique *BstEII* site is located 463 bp upstream from the end of *corA* and 780 bp upstream from the end of the 3.3-kb insert in pOB12 (Figure 3.4). The *BstEII* site was used to introduce Km^r cassette into pOB12. The plasmid, carrying the Km^r gene transcribed in the same direction as *corA* (pOB16), was identified by plating the transformants on LB plates containing both Amp and Km, and by the restriction analysis of these clones with *SphI* and *XhoI*. The *EcoRI* site was used to ligate pOB16 with the suicide vector pAYC61 (Chistoserdov *et al.* 1994). The size of the constructed plasmid (pOB17) in selected clones was checked by digestion with *EcoRI* (Figure 3.11). The phenotype of these mutants was checked by growing them on NMS plates containing Amp or Kan. The double crossovers should be Km^r/Amp^s , whereas single crossovers are expected to be Km^r/Amp^r , since they carry an insertion of the entire plasmid (Figure 3.12). DNA from one mutant (OB12.7) with a Kan^r/Amp^s phenotype was isolated and analyzed by PCR amplification with primers PR12-F6 and PR12-R1 located at the ends of the gene. The PCR product amplified from OB12.7 mutant was about 1.4 kb longer than those generated from wild type (Figure 3.13). These data suggested that this mutant contained the disrupted *corA* in the chromosome and was the result of the desired double crossover recombination event. This mutant grew very poorly on agar plates.

An attempt was made to determine the relationship between copper concentrations in the medium and growth of the OB12.7 mutant. The mutant and w.t. were inoculated into preequilibrated NMS medium with no copper added, 10 μ M, or 50

μM copper added. While w.t. cells grew best at $10\mu\text{M}$ and grew with longer lag phases at no copper added and $50\mu\text{M}$ copper added, the mutant did not grow at all under these conditions, after 6 days of incubation. This result implies that *corA* is vital for growth of *M. albus* BG8.

3.4. Conclusions

Circumstantial evidence suggests that CorA might be involved in copper uptake. The polypeptide was isolated as a copper-repressible polypeptide, which implies a regulatory effect of copper on CorA. The product of translation of *corA* shows similarity with calcium release channel proteins, which suggests that CorA might belong to a family of divalent metal porins induced under conditions of metal starvation. It is possible that such a porin is not specific for copper, but rather works with a range of divalent metals. The mutant analysis indicates the importance of *corA* for normal physiology of *M. albus* BG8. However, the inability to characterize copper uptake in the CorA mutant due to its poor growth makes it impossible to draw a definite conclusion about the role of CorA in copper transport/metabolism.

3.5. References

- Apte, S. C., M. J. Gardner, J. E. Ravenscroft, and J. A. Turrell.** 1990. Examination of the range of copper complexing ligands in natural waters using a combination of cathodic stripping voltammetry and computer simulation. *Anal. Chim. Acta* **235**:287-297.
- Berggren, D.** 1989. Speciation of aluminum, cadmium, copper, and lead in humic soil solutions - a comparison of the ion-exchange column procedure and equilibrium dialysis. *Intern. J. Environ. Anal. Chem.* **35**:1-15.
- Berson, O., M.E. Lidstrom.** 1996. Study of copper accumulation by the type I methanotroph *Methylobacterium albus* BG8. *Environ.Sci.Technol.* **30**:802-809.
- Boyle, E. A. and J. M. Edmond.** 1975. Copper in surface waters south of New Zealand. *Nature* **253**:107-109.
- Bruland, K. W.** 1980. Oceanographic distributions of cadmium, zinc, nickel, and copper in the North Pacific. *Earth and Planetary Science Letters* **47**:176-198.
- Bruland, K. W., J. R. Donat, and D. A. Hutchins.** 1991. Interactive influences of bioactive trace metals on biological production in oceanic waters. *Limnol. Oceanogr.* **36**:1555-1577.
- Chan, S.I., H.H.T. Nguyen, A.K. Shiemke, and M.E. Lidstrom.** 1993. Biochemical and biophysical studies toward characterization of the membrane-associated methane monooxygenase, p.93-107. *In* Murrell, J.C. and D.P. Kelly (eds.), *Microbial Growth on C1 Compounds*. Intercept, Andover.
- Chistoserdov, A. Y., L. V. Chistoserdova, W. S. McIntire, and M. E. Lidstrom.** 1994. Genetic organization of the *mau* gene cluster in *Methylobacterium extorquens* AM1: complete nucleotide sequence and generation and characteristics of *mau* mutants. *Journal of Bacteriology* **176**:4052-4065.
- Chistoserdova, L. V. and M. E. Lidstrom.** 1994. Genetics of the serine cycle in *Methylobacterium extorquens* AM1: identification, sequence, and mutation of three new genes involved in C₁ assimilation, *orf4*, *mtkA*, and *mtkB*. *Journal of Bacteriology* **176**:7398-7404.
- Coale, K. H. and K. W. Bruland.** 1988. Copper complexation in the Northeast Pacific. *Limnol. Oceanogr.* **33**:1084-1101.
- Coale, K. H. and K. W. Bruland.** 1990. Spatial and temporal variability in copper complexation in the north pacific. *Deep-Sea Research* **37**:317-336.

Fitch, M. W., D. W. Graham, R. G. Arnold, S. K. Agarwal, P. Phelps, G. E. Speitel, and G. Georgiou. 1993. Phenotypic characterization of copper-resistant mutants of *Methylosinus trichosporium* OB3b. *Appl. Environ. Microbiol.* **59(9)**:2771-2776.

Gutteridge, J.M.C., and S. Wilkins. 1983. Copper salt-dependent hydroxyl radical formation damage to proteins acting as antioxidants. *Biochim. Biophys. Acta.* **759**:38-41.

Hanson, R.S., A. I. Netrusov, K. Tsuji. 1990. The obligate methanotrophic bacteria *Methylococcus*, *Methylomonas*, and *Methylosinus*, p.2350-2364. *In* Balows, A., H.G. Truper, M. Dworkin, W. Harder, and K.H. Schleifer (eds.), *The Prokaryotes*. Springer-Verlag, New York.

Halden, K. and H.A. Chase. 1991. Methanotrophs for cleanup of polluted aquifers. *Wat.Sci.Tech.* **24**:9-17.

Hering, J. G. and F. M. M. Morel. 1988. Humic-acid complexation of calcium and copper. *Environ. Sci. Technol.* **22**:1234-1237.

Hodgson, J.F., H.R. Geering, and W.A. Norvell. 1965. Micronutrient cation complexes in soil solution: partition between complexed and uncomplexed forms by solvent extraction. *Soil Sci. Society Proceedings.* 665-669.

Hughes, M. N. and R. K. Poole. 1991. Metal speciation and microbial growth - the hard (and soft) facts. *J. Gen. Microbiol.* **137**:725-734.

Maniatis, T., E. F. Fritsch, and J. Sambrook. 1982. *Molecular cloning: a laboratory manual*. Cold Spring Harbor Laboratory. Cold Spring Harbor, N.Y.

Moffett, J. W., R. G. Zika, and L. E. Brand. 1990. Distribution and potential sources and sinks of copper chelators in the Sargasso Sea. *Deep-Sea Research* **37**:27-36.

Park, S., M.L. Hanna, R.T. Taylor, and M.W. Droege. 1991. Batch cultivation of *Methylosinus trichosporium* OB3b. I: production of soluble methane monooxygenase. *Biotechnology and Bioengineering* **38**:423-433.

Ruvkun, G. B. and F. M. Ausubel. 1981. A general method for site-specific mutagenesis in prokaryotes. *Nature* **289**:85-88.

Satio, H. and K.-I. Miura. 1963. Preparation of transforming deoxyribonucleic acid by phenol treatment. *Biochim. Biophys. Acta* **72**:619-629.

Silver, S. and M. Walderhaug. 1992. Gene regulation of plasmid- and chromosome-determined inorganic ion transport in bacteria. *Microbiological Reviews* **56(1)**:195-228.

- Simon, R., U. Priefer, and A. Puhler.** 1983. Vector plasmids for in vivo manipulations of gram-negative bacteria. p. 98-106. In A. Puhler (ed.), *Molecular genetics of the bacteria-plant interactions*. Springer-Verlag, Berlin.
- Sunda, W. G. and A. K. Hanson.** 1987. Measurement of free cupric ion concentration in seawater by a ligand competition technique involving copper sorption onto C₁₈ SEP-PAK cartridges. *Limnol. Oceanogr.* **32**:537-551.
- Takehima, H., Nishimura, S., Matsumoto, T., Ishida, H., Kangawa, K.** 1989 Primary structure and expression from complementary DNA of skeletal muscle ryanodine receptor. *Nature.* **339**: 439-445.
- Tsien, H. C. and R. S. Hanson.** 1992. Soluble methane monooxygenase component B gene probe for identification of methanotrophs that rapidly degrade trichloroethylene. *Appl. Environ. Microbiol.* **58**:953-960.
- Vandenberg, C. M. G. and J. R. Donat.** 1992. Determination and data evaluation of copper complexation by organic ligands in sea water using cathodic stripping voltammetry at varying detection windows. *Anal. Chim. Acta* **257**:281-291.
- Vandenberg, C. M. G., M. Nimmo, P. Daily, and D. R. Turner.** 1990. Effects of the detection window on the determination of organic copper speciation in estuarine waters. *Anal. Chim. Acta* **232**:149-159.
- Vulpe, C., B. Levinson, S. Whitney, S. Packman, and J. Gitschier.** 1993. Isolation of a candidate gene for Menkens disease and evidence that it encodes a copper-transporting ATPase. *Nature.* **3**:7-13.
- Yano, R., H. Nagai, K. Shiba, and Y. Yura.** 1990. A mutation that enhances synthesis of σ^{32} and suppresses temperature-sensitive growth of the *rpoH15* mutant of *Escherichia coli*. *J. Bacteriol.* **72**(4):2124-2130.
- Whittenbury, R., K. C. Phillips, and J. F. Wilkinson.** 1970. Enrichment, isolation and some properties of methane-utilizing bacteria. *J. Gen. Microbiol.* **61**:205-218.

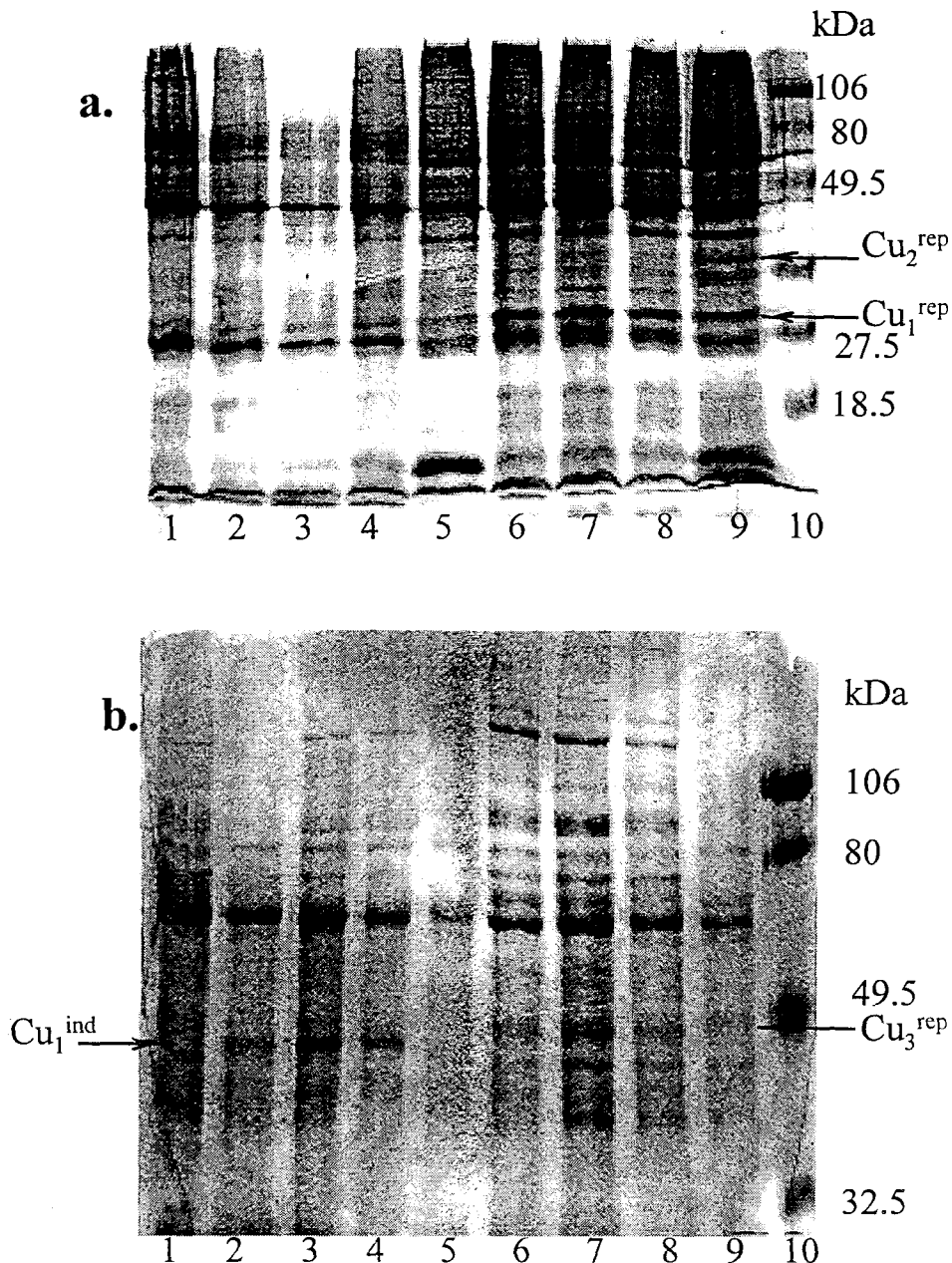


Figure 3.1 Identification of copper-repressible and copper-inducible polypeptides in particulate (a) and soluble (b) fractions of *Methylobacterium albus* BG8 by sodium dodecyl sulfate-polyacrylamide [14% (a) and 10% (b)] gel electrophoresis. Cell extracts of *M. albus* BG8 were grown with 10 μ M (lane 1); 20 μ M (lanes 2, 3, 5), 40 μ M (lane 4), and no copper (lanes 6-9) added to the medium. Samples in lanes 2-5 were prepared from poorly growing cells; samples in lanes 1, 6-9 were prepared from cultures with normal growth. Two copper-repressible polypeptides were identified in the particulate fractions: Cu_1^{rep} (~28.5 kDa) and Cu_2^{rep} (~33 kDa). A copper-repressible polypeptide Cu_3^{rep} (~49.5 kDa) and a copper-inducible polypeptide Cu_1^{ind} (~49 kDa) were identified in the soluble fraction.

A.

```

                10      19
Cu3rep      MKKILDVVKPGVVTGEDVQ
                | |:| |:| ||||| |||||
Alf_Ha      MAKLLDIVKPGVVTGEDVQKVFAYA
                10      20

```

84.2% homology in 19 aa overlap**B.**

```

Cu3rep      MKKILDVVKPGVVTGEDVQ
                ||:| |||||:|:| |
Alf_Ec      MSKIFDFVKPGVITGDDVQKVFQVAKENNF
                10    20    30    40    50

```

76.5% homology in 17 aa overlap

Figure 3.2. Comparison of the N-terminal amino acid sequence of Cu₃^f with the N-terminal part of fructose biphosphate aldolases.

A. Alf_Ha, fructose biphosphate aldolase from *Haemophilus influenzae*; SwissProt Data Base Accession number P44429.

B. Alf_Ec, fructose biphosphate aldolase from *Escherichia coli*; SwissProt Data Base Accession number P11604.

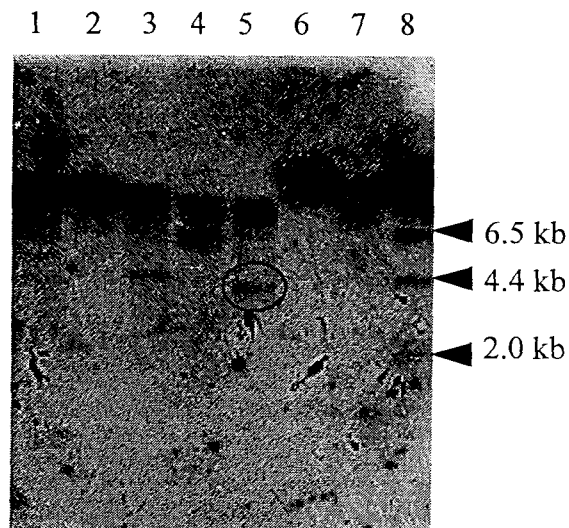


Figure 3.3 Hybridization of oligonucleotide probe OB1 to restriction enzyme digests of *Methylobacterium albus* BG8.

Lanes: 1, molecular weight standard (1 kb ladder, not labeled); 2, *SacI* digest; 3, *PstI* digest; 4, *SphI* digest; 5, *SalI* digest; 6, *XbaI* digest; 7, *BamHI* digest; 8, molecular weight standard (P^{32} -labeled λ DNA/*HindIII* fragments). A 4.2-kb band of *SalI*-digested chromosome is circled.

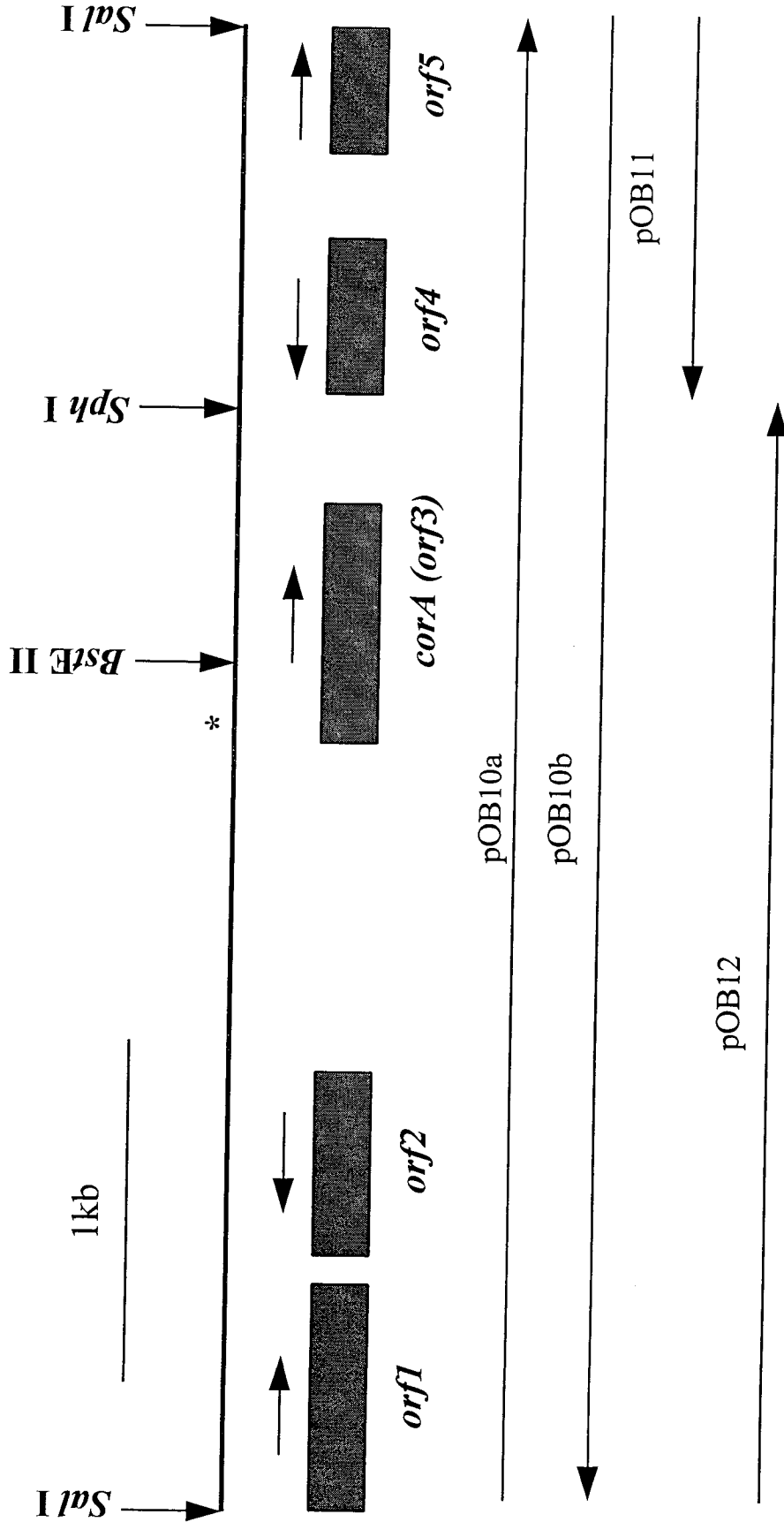


Figure 3.4 Physical map of the 4.2-kb *Methylobacterium albus* BG8 chromosomal region containing *orf1*, *orf2*, *orf3* (*corA*), *orf4*, *orf5*. Plasmids containing the whole region (pOB10a and pOB10b) or its fragments (pOB11 and pOB12) are shown below the map. The directions of the orfs transcription are indicated by the arrows above the orfs, and the direction of cloning with respect to direction of *corA* transcription is shown by the arrows on the inserts. The asterisk shows the beginning of the sequence hybridizing with OBI probe.

a
l
I

orf1 ⇒ GTCGACCGCAAGCGGAACGGAAATCATCAACATCATCCGCACGGCCTATCCCGATCATGC

S T A S G T E I I N I I R T A Y P D H A

61 GATCCTGGCCGAAGAAAGCGGCGCGCACCAAGGCAACGAGTTCGTCTGGGTGATCGACCC

I L A E E S G A H Q G N E F V W V I D P

121 GCTGGACGGCACGACCAATTTTCTGCACGGTTTTCCGCAGTTTGC GGTTTCGATTGC GTT

L D G T T N F L H G F P Q F A V S I A L

181 GAAACACAAAGGTCGGCTCGAAGTGGCCGTGATTTACGATCCGCTGCGCGACGAATTGTT

K H K G R L E V A V I Y D P L R D E L F

241 TACCGCCAAACGCGGCGGGCGCGATGCTGAACAACCGGAGGATTTCGCGTGACCAAACA

T A K R G G G A M L N N R R I R V T K Q

301 AAGCGCGATGAAAGGCGCGCTGATCGGCACCGTTTTTCCGTTCAAGACCGACCGGCATCT

S A M K G A L I G T G F P F K T D R H L

361 GGACGCCTACGTAGGGATGTTCAAAGCGATGACGACCGACTCCGCCGGCATCCGCCGGGC

D A Y V G M F K A M T T D S A G I R R A

421 CGGCTCCGCGGCGCTCGACCTGGCCTATGTCGCCCGGACGCCTGGACGGCTTCTGGGA

G S A A L D L A Y V A A G R L D G F W E

481 AATCGGATTGATGGAATGGGATATGGCGGCCGGGTCTTGCTGATCAAGGAAGCCGGCGG

I G L M E W D M A A G V L L I K E A G G

541 TGTCGTGACCGATTTTTTCGTTCAACGACGGCTATCTGCAAAACGGCAACCTGATCGCCGG

V V T D F S F N D G Y L Q N G N L I A G

Figure 3.5 Nucleotide sequence and deduced amino acid sequence of the 4.2-kb *M. albus* BG8 chromosome region containing *orf2*, *orf3* (*corA*), *orf4*, and partially *orf1*, *orf5*.

Asterisks indicate stop codons. Putative Shine-Dalgarno sequences are shown in bold, putative leader sequences are underlined. The amino acids that were determined by sequencing of the blotted protein band are shown in bold italic.

601 CAATCCGAAAATGCATCAGGTCATGTACAAGCTGATCGAGCCTCATGTGACCGACAGCTT
 N P K M H Q V M Y K L I E P H V T D S L

661 GCGATAAAAGGCAGTATTTGGCGGTTTTTTTCAAATTAAGGGCGGAAAGATTCCGCCCTT
 R *

721 TTTTCGTTTTAGGGATTGTGGACGCGCTACAGCGGGCGGCAGCTTGCAGGAATGCCGGGAT
 -----+-----+-----+-----+-----+-----+
 AAAGCAAATCCCTAACACCTGCGCGATGTCGCCGCCCGTTCGAACGTCCTTACGGCCCTA
 * L P P C S A P I G P

781 CGGCGGTATCGGCCAACCTGAAAATCCATCGGCAGCGCGTGACTIONCGGGTCTGTCTGTTGG
 -----+-----+-----+-----+-----+-----+
 GCCGCCATAGCCGGTTGGACTTTTAGGTAGCCGTCGCGCACTGAAGCCAGACAGCAACC
 D A T D A L R F I W R C R T V E P R D N

841 GGTGTGGGGTTCGTCGGTCTGATCGGTGTAGATGGACAGGCCGGTCAATGAACCGGTGC
 -----+-----+-----+-----+-----+-----+
 CCAACAACCCAGCAGCCAGACTAGCCACATCTACCTGTCCGGCCAGTTACTTGGCCACG
 P N N P D D T Q D T Y I S L G T L S G T

901 CTCTGTTTGGGTTTACGACCGGTTTCAGGTCCGGTAATCTCGGAAACGCCGGACGTAATAT
 -----+-----+-----+-----+-----+-----+
 GAGACAAACCCAAATGCTGGCGCAAGTCCAGCCATTAGAGCCTTTGCGGCCTGCATTATA
 G R N P N V V A N L D T I E S V G S T I

961 CCGCCTTGGTTGCGCAGTCGGCGATCGCGGCATGGCCCCGGGTGGTCCGGCCGGGTAATAC
 -----+-----+-----+-----+-----+-----+
 GGCGGAACCAACGCGTCAGCCGCTAGCGCCGTACCGGGGCCACCAGCCGGCCATTATG
 D A K T A C D A I A A H G R T T P R T I

1021 TGTCGATGGTGAAACCGGTGAAAGTGGCCGCCAGCTCTTCACCATCGAGCCATTGAACGG
 -----+-----+-----+-----+-----+-----+
 ACAGCTACCACTTTGGCCACTTTCACCGCGGTCGAGAAGTGGTAGCTCGGTAACTTGCC
 S D I T F G T F T A A L E E G D L W Q V

1081 ATAAGCGGCTGCCATCCGGTGGCTGGCTGATTCTCAGGCTTTGGGGCGGCTGGCTTCTGT
 -----+-----+-----+-----+-----+-----+
 TATTCGCCGACGGTAGGCCACCGACCGACTAAGAGTCCGAAACCCCGCCGACCGAAGACA
 S L R S G D P P Q S I R L S Q P P Q S R

Figure 3.5 (continued)

H S N W G F V K L K K G K P V T I A L T
 2521 ACGGAAGTCAGCGGTTTGCACCCGTCAATCACGGTATGGTACCGGGCGGGAGCCAAAAAT
 T E V S G L H P S I T V W Y R A G A K N
 2581 CCAAAGACGCTTCCTTATATGAACGGCCACGCCTACAAGCAGTTCGGCGATATTTACGAG
 P K T L P Y M N G H A Y K Q F G D I Y E
 2641 CCGAACGCCGAAGCCACCGATGCCGAGAACAACCCGGTCAAGGTCGGCAATATCATCATG
 P N A E A T D A E N N P V K V G N I I M -
 2701 AAGTTTATTACCAACGGGTTTGACCGCGACGGAATGGGCGACGCCTTACCGGCTGAGTAC
 K F I T N G F D R D G M G D A L P A E Y
 2761 GACCAGTCTCAGTTGTACCGGGTGATGGACGGTGTGCCAGGAAAGCTGGCGATTACCTTT
 D Q S Q L Y R V M D G V P G K L A I T F
 2821 ACCCCGCTGAAAACGGCTGGTATCAATTCGTCGTTGGGGCGATCAATCCGGATATCGAT
 T P P E N G W Y Q F V V G A I N P D I D
 TCGACGGCTTACGGTTCCGGCCCAGGTTCCGGCGCCGGTCCC GCGACTGCGCATACTGTC
 S T A Y G S G P G S G A G P A T A H T V
 2941 CATGTAGAAGTCAGTATCCCGTAAACGAGATCGTAAAAAGGGATTACCTCGCCACAGGGA
 H V E V S I P *
 3001 GGAGGCCGGGAGGCCTCCTCCTTTTTTATTTTGAATCATCATGTTCTGCTTCATCCAAA
 3061 AAGTTTTATCCGGTATTGCCCATGTGTTTATGCGTTAATTCTGTTATGTGCCTTAGCCG
 ATGCCGTATTTGCCACGGCGCACTGTCCGATCAAGTCATGAAAGGCTTTAAGGTTCCGA
 3121 -----+-----+-----+-----+-----+-----+-----+
 TACGGCATAAACGGGTGCCGCGTGACAGGCTAGTTCAGTACTTTCCGAAATCCAAGGCT
 * P E S
 CGACGCCCAAGTTGATCGGGAAGTCGGCAATCGTCGTCGATCAACAGGCCGCCGTCCAGC
 3181 -----+-----+-----+-----+-----+-----+-----+
 GCTGCGGGTTCAACTAGCCCTTCAGCCGTTAGCAGCAGCTAGTTGTCCGGCGGCAGGTCG
 S A W T S R S T P L R R R D V P R R G A

Figure 3.5 (continued)

P
h
I

3241 TCGCAAAGCCCTGTTTTGGGACGGAAACGTCGGCAGCACGGAACCGCATGCGCTTCGTGC
-----+-----+-----+-----+-----+-----+
AGCGTTTTCGGGACAAAACCTGCCTTTGCAGCCGTCGTGCCCTGGCGTACGCGAAGCAGC
R L A R N Q S P F T P L V S G C A S R A

3301 CATTTCATGCCGGATCGGATATTCGCCATATTAACCAGCTGAATCCCGGTCAAGCGCAC
-----+-----+-----+-----+-----+-----+
GTAAAAGTACGGCCTAGCCTATAAGCGGTATAATTGGTCGACTTAGGGCCAGTTCGCGTG
M K M G S R I N A M N V L Q I G T L R V -

3361 ACCGCCAATGCCGGCGGCACCGCGAAAACCTTTCGAATTGCCATCGGGCAATGACGCCGGG
-----+-----+-----+-----+-----+-----+
TGGCGGTTACGGCCCGCGTGGCGCTTTTGAAAGCTTAACGGTAGCCCGTACTGCGGCC
G G I G A A G R F S E F Q W R A I V G P

3421 CCGGACTATGAATTGAAAGCCGGCGATTTTCCGTTTTTCCGCTTTGCCGATGTGGACGAC
-----+-----+-----+-----+-----+-----+
GGCCTGATACTTAACTTTTCGGCCGCTAAAAGGCAAAAAGGCGAAACGGCTACACCTGCTG
R V I F Q F G A I K R K E A K G I H V V

3481 ATCGCCACGTTGACGGCATCGACCGACGACGTGGCCGGTTCTTCCGGAGAGCCACAGCAG
-----+-----+-----+-----+-----+-----+
TAGCGGTGCAACTGCCGTAGCTGGCTGCTGCACCGGCCAAGAAGGCCTCTCGGTGTCGTC
D G R Q R C R G V V H G T R G S L W L L

3541 CAATTTGTGGCGGTTGATGCGACGGGCATTAATGCGGGCATTAAATAACGATCAATGCGAT
-----+-----+-----+-----+-----+-----+
GTTAAACACCGCCAACCTACGCTGCCCCTAATTACGCCCCTAATTATTGCTAGTTACGCTA
L K H R N I R R A N I R A N I V I L A I

3601 TCCGAGTTGAGCGCGGTCTTTTCATGCGGGTAGTCTGAATACCCGCCAGGTCACCAAGCGC
-----+-----+-----+-----+-----+-----+
AGGCTCAACTCGCGCCAGAAAGTACGCCCAT**CAGACT**TATGGGCGGTCCAGTGGTTTCGCG
G L Q A R D K M ← *orf4*

3661 AATGCGCCGACGGTAATCAATGCCGCATTCAACTTCCGCAATTTTTGGGACGGCCGCGCA
3721 AATAACGTATTCAATGGCCAATCGCCGTTCCGATTGCGCGATACAGGCGCCAAAATCTGG
3781 CTTGCGAAAGGCACGAAAAGGTTAAGGCTGCGCGGTTGGCGCTGGAAAACGCCTCGCTG
3841 GCATCCC**AGG**CCGTCGGTCCTCCTCTAGATATGGTGGAATGTCCTGCAAGGGGCGCAGT

Figure 3.5 (continued)

orf5 ⇒ M V E M S C K G R S

3901 TCGCCGACATCGGCCGAAAATTGCTGCGGCGCAGGGCGCTGGAGTCGCAGGCGGTGCGAT
 F A D I G R K L L R R R A L E S Q A V H

3961 CCCGAAGACAGCGTGCTTGCCGGTCTGCGCGACCCGTCGCGCACCGGTTTGACGTTAACCC
 P E D S V L A G L R D P S G T G L T L T

4021 TACGACGAATTGATCAAAAAGGCGTTTAAACAAGAAATATTGGAGGAGTGCCGCTGCCATC
 Y D E L I K K A F N K K Y W R S A A A I

4081 GAGCTGGTGAAGGATTCGGGGCAATTCTATTCGCAAATGGAAGCTAATTTTGCATGTTTC
 E L V K D S G Q F Y S Q M E A N F A M F

4141 TTTGGCCTGGCTATCCAACAATACGAGAATACTTTGATTTCCGACGATGCGTTGTTTCGAC
 F G L A I Q Q Y E N T L I S D D A L F D
 S
 a
 l
 I

4201 CGGGAGGTCGAC
 R E V D

Figure 3.5 (continued)

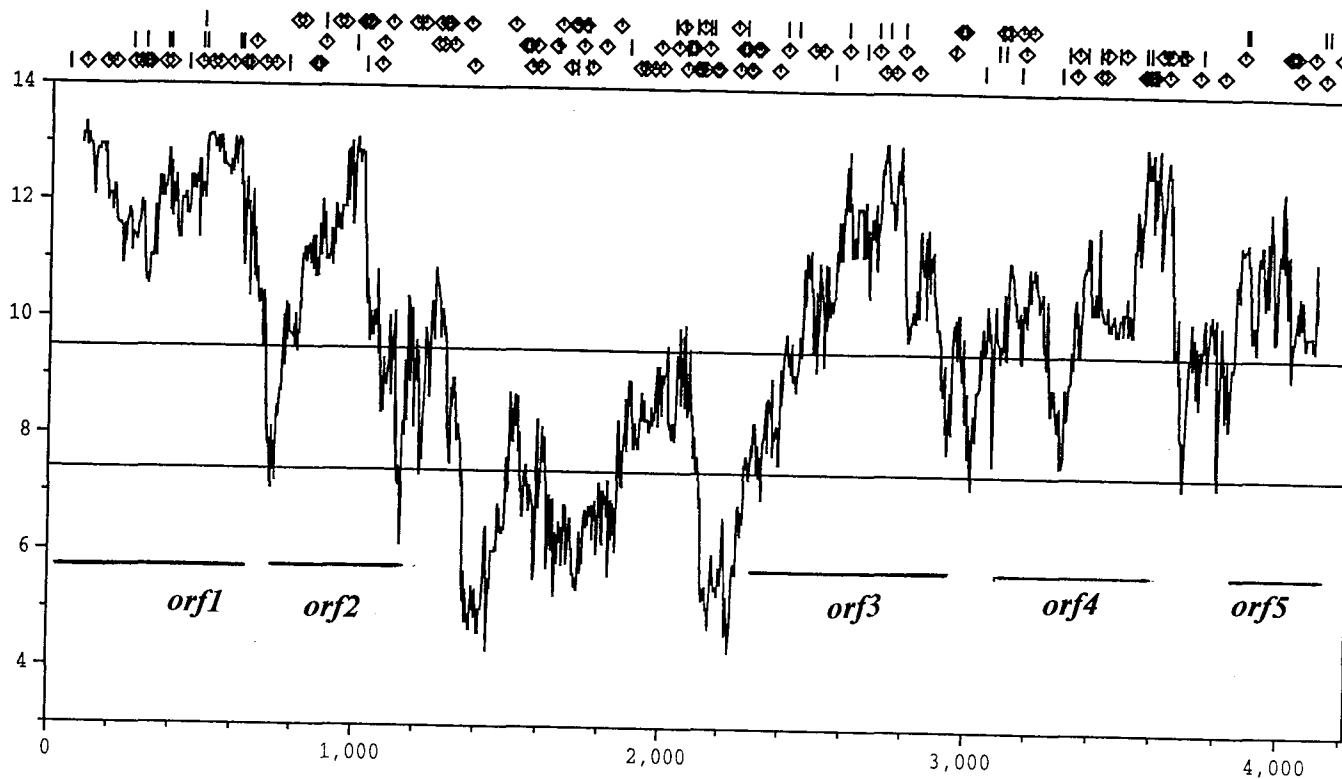


Figure 3.6 Frame-independent gene localization using the TestCode Program from the GCG Package.

The plot produced by the program is shown. X axis shows the number of residues in a sequence. The top horizontal line shows bias in the composition of bases found in the third positions of the codons. The lower horizontal line is the codon preference curve. Larger values of the testcode statistic (above the top horizontal line) correspond to regions with a greater likelihood of encoding a protein. The predicted open reading frames are indicated by the bars.

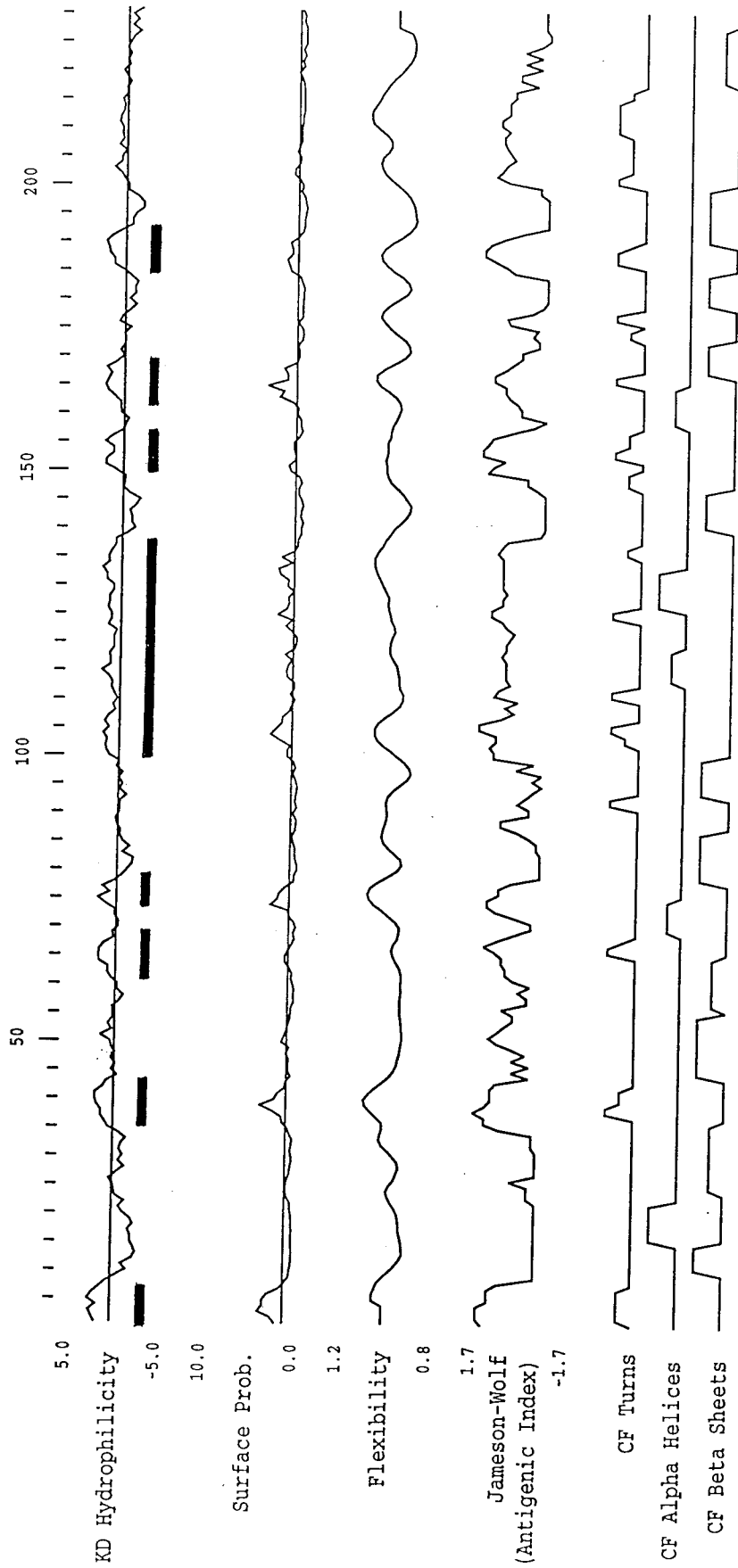


Figure 3.7 Predicted structure of *corA* gene product.

The hydrophobicity of CorA was predicted by the Kyte-Doolittle algorithm. Thick bars show potential membrane-spanning domains. Below is a plot which indicates probability of finding an amino acid residue on the surface of the protein molecule. The third panel shows flexibility of the peptide backbone. Next is antigenic index, surface probability and chain flexibility combined. The probability of the peptide chain to form secondary structures (α -helices, β -sheets, β -turns) are shown next.


```

          30          40          50          60          70          80
Orf3.P  FANPLQAATAISGTFDFDKNNTSADMTVRAYSWYNLSMGYLGWTHHSNWGFVKKLKKGPVT
          :|| : |: || |::|: |: : ::
Rynr_H  GLLTWLMSIDVKYQIWKFGVIFTDNSFLYLGWY-MVMSLLG--HYNFFFAAHLDDIAMG
          4760          4770          4780          4790          4800          4810

          90          100         110         120         130
Orf3.P  I-ALTTEVSGLHPSITVWYRAGAKNPKTLPYMNGHAYKQFGDIYEPNAEATDAENN-PVK
          : :| | :|:: : : : : : : : : : |:: | ::|: :::::::::: : :
Rynr_H  VKTLRTLSSVTHNGKQLVMTVGLLAVVVYLYTVVAFNFFRKFYNKSEDEDEPDMKCDDM
          4820          4830          4840          4850          4860          4870

          140         150         160         170         180         190
Orf3.P  VGNIIMKFITNGFDRDGMGDAL-PAEYDQSQLYRVMDGVPGKLAITFTPPENGWYQFVVG
          :: :::: :: : :|:| |: : :|:| |:
Rynr_H  MTCYLFHMYVGVVRAGGGIGDEIEDPAGDEYELYRVVFDITFFFFVIVILLAIQGLIIDA
          4880          4890          4900          4910          4920          4930

          200         210         220         230
Orf3.P  AINPDIDSTAYGSGPGSGAGPATAHTVHVEVSIPX

Rynr_H  FGELRDQQEQVKEDMETKCFICGIGSDYFDITPHGFETHLEEHNLANYMFFLMYLINKD
          4940          4950          4960          4970          4980          4990

```

Figure 3.8 Comparison of the deduced amino acid sequence of CorA with the sequence of calcium release protein (SwissProt Data Base Accession number P05838).

Identical residues are indicated by vertical lines, conserved substitutions are shown by dots.

```

Orf1.P                               STASGTEIINIIRTAYPDHAILAEESGAHQG-
                                     |::: ||::||::||:|:|:|:|:|:|:|:|:|:|
Suhb_E GNLIAKNYETPDAVEASQKGSNDFVTNVDKAAEAVIIDTIRKSYPQHTIITEESGELEGT
      20          30          40          50          60          70

      40          50          60          70          80          90
Orf1.P -NEFVWVIDPLDGTTFNHLHGFPQFAVSIALKHKGRLEVAVIYDPLRDELFTAKRGGGAML
      :: |||:|:|:|:|:|:|:|:|:|:|:|:|:|:|:|:|:|:|:|:|:|:|:|:|:|:|:|:|
Suhb_E DQDVQWVIDPLDGTTFIKRLPHFAVSIIVRIKGRTEVAVVYDEPMRNELFTATRGGQAQL
      80          90          100         110         120         130

      100         110         120         130         140         150
Orf1.P NNRRIRVTKQSAMKIGLIGTGFPFKTDRHLDAYVGMFKAMTTDSAGIRRAGSAALDLAYV
      |: |: ::::|:|:|:|:|:|:|:|:|:|:|:|:|:|:|:|:|:|:|:|:|:|:|:|:|:|
Suhb_E NGYRLLGSTARDLDGTILATGFPFKAKQYATTYINIVGKLFNECADFRRTGSAALDLAYV
      140         150         160         170         180         190

      160         170         180         190         200         210
Orf1.P AAGRLDGFWEIGLMEWDMAAGVLLIKEAGGVVTDFFSFDNGYLQNGNLIAGNPKMHQVMYK
      |||:|:|:|:|:|:|:|:|:|:|:|:|:|:|:|:|:|:|:|:|:|:|:|:|:|:|:|:|
Suhb_E AAGRVDGFFEIGLRPWDFAAAGELLVREAGGIVSDFTGGHNYMLTGNIVAGNPRVVKAMLA
      200         210         220         230         240         250

      220
Orf1.P LIEPHVTDSLRLX
      : :::|:|:|:|:|:|:|:|:|:|:|:|:|:|:|:|:|:|:|:|:|:|:|:|:|:|
Suhb_E NMRDELSDALKR
      260

```

Figure 3.9 Sequence comparison of predicted amino acid sequence of *orf1* and *suhB*, extragenic suppressor protein (SwissProt Data Base Accession number P22783).

Identical residues are indicated by vertical lines, conserved substitutions are shown by dots.

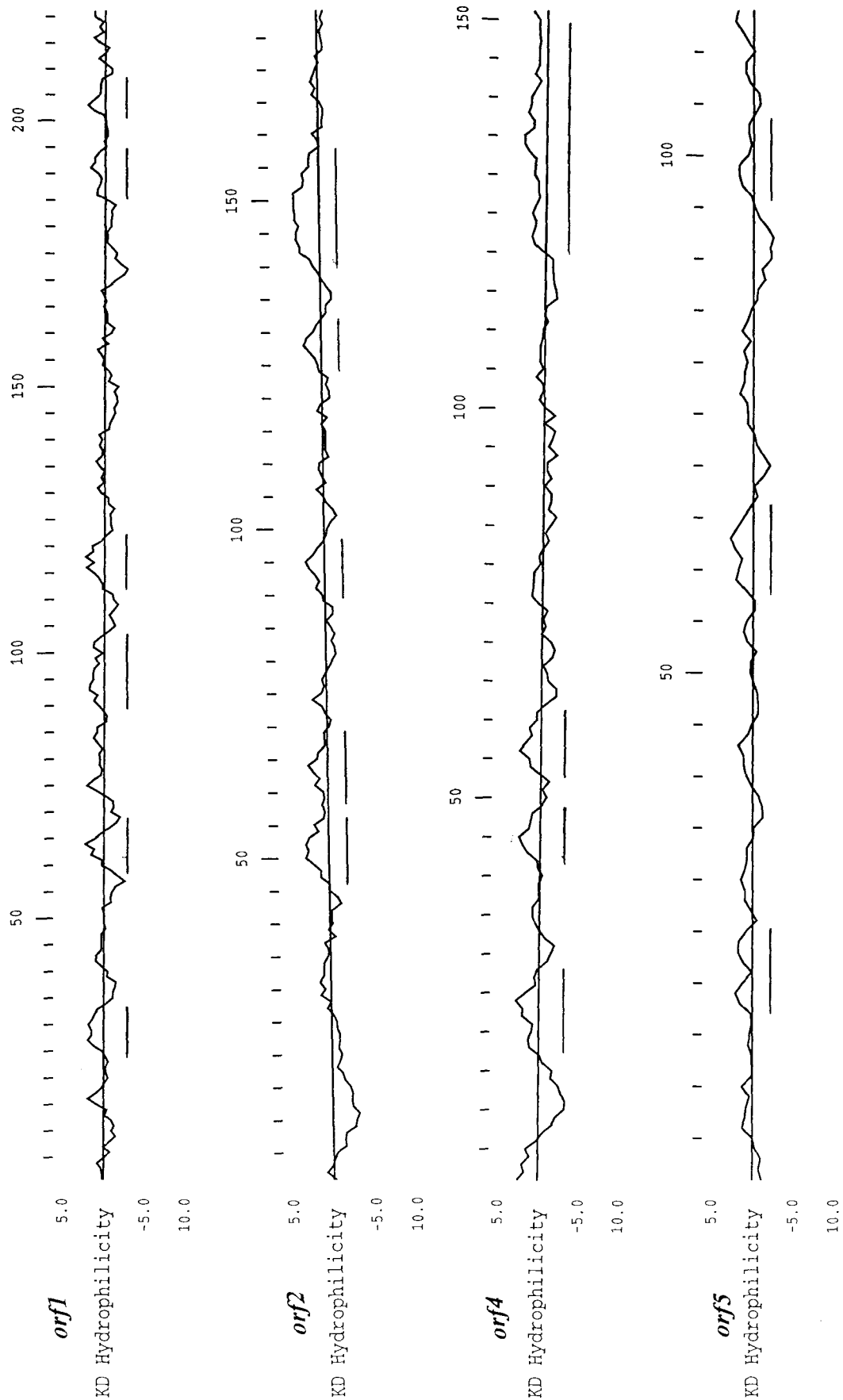


Figure 3.10 Predicted hydrophobicity plots of *orf1*, *orf2*, *orf4* and *orf5* gene products by the Kyte-Doolittle algorithm. Probable membrane-spanning domains are indicated with bars. Scales above the plots show the number of residues in a sequence.

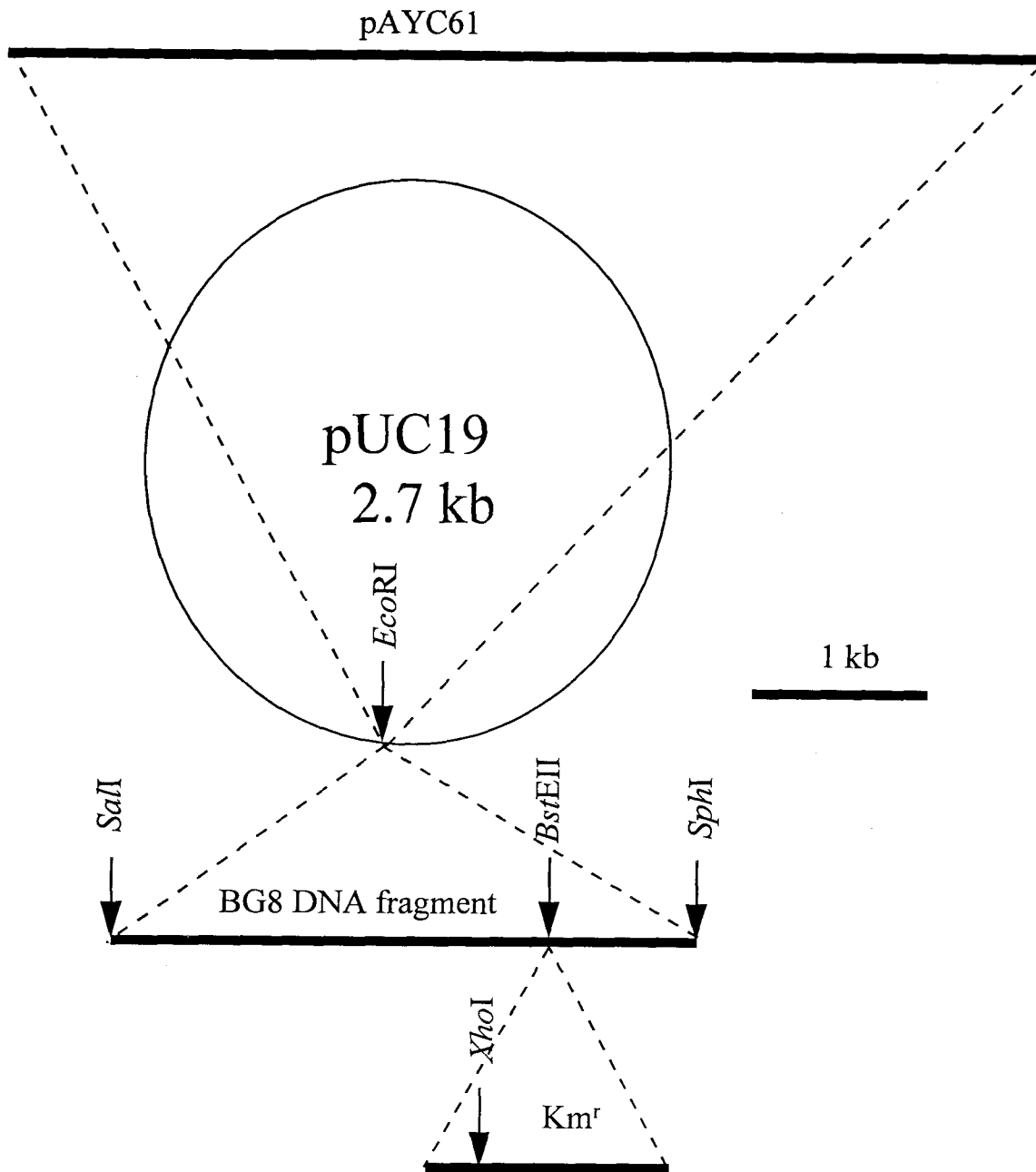


Figure 3.11 Construction of plasmids pOB16 and pOB17 carrying the mutated *corA* gene.

First, the 3.3-kb *M. albus* BG8 DNA fragment containing *corA* was inserted into pUC19, then, *corA* was disrupted by the insertion of a kanamycin resistance gene (Km^r) to produce pOB16. pOB16 was ligated with the suicide vector pAYC61 to yield pOB17.

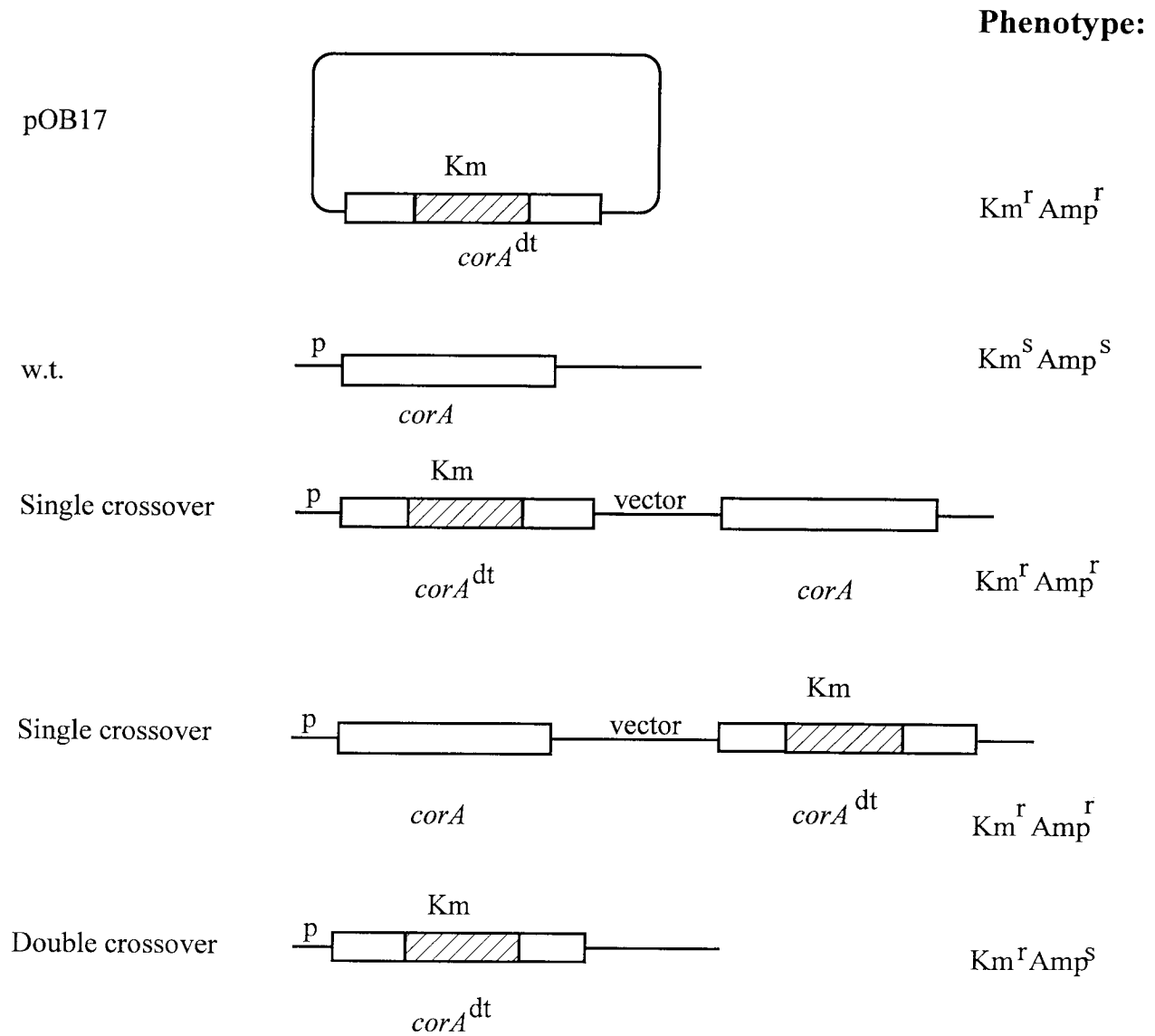


Figure 3.12 The phenotypes of wild-type (w.t.), single and double crossover *corA* mutants of *M. albus* BG8.

p, a promoter; *corA*, gene encoding copper-repressible polypeptide; *corA*^{dt}, *corA* deleted by an insertion of kanamycin resistance cassette (Km).

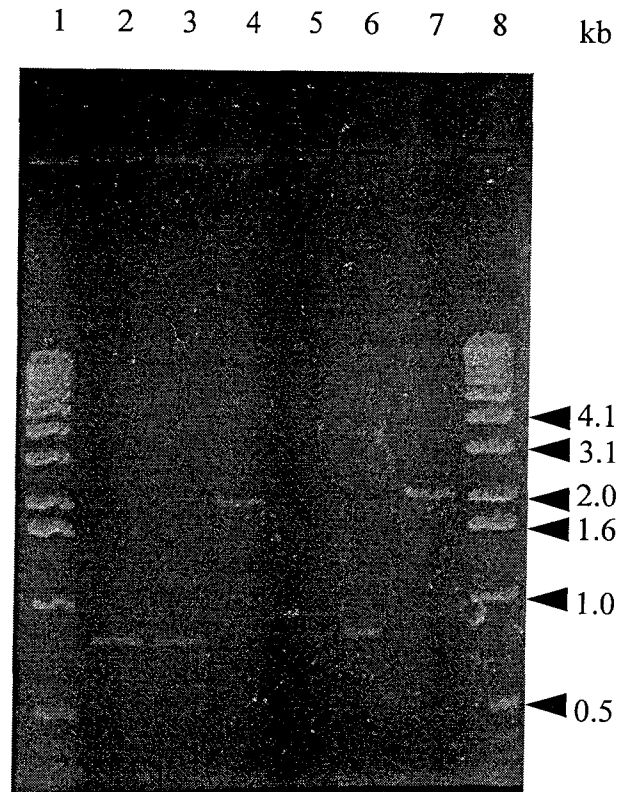


Figure 3.13 Characterization of OB12.7 mutant.

PCR-amplified products were separated on an agarose gel. Lanes 1 and 8, 1kb DNA Ladder DNA size standard. The following PCR products were loaded: lanes 2, 3, 5, 6, PCR with wild type *M. albus* BG8; lanes 4 and 7, PCR with OB12.7. Lanes 2-3, annealing at 50°C; lanes 5-8, annealing at 55°C. Samples of w.t. DNA were prepared from two batches: 2 and 5, cells grown under copper limitation, 3 and 6, cells grown with sufficient copper.

Appendix

To optimize separation of the polypeptide bands by electrophoresis several polyacrylamide concentrations in the gels were tested. In this appendix the results of sodium dodecyl sulfate-polyacrylamide gel electrophoresis with 10% (membranes) and 14% (soluble fraction) (Figure A3.1), 12% (Figure A3-2), and 16% (Figure A3-3) polyacrylamide in the base gels are shown. However, the best separation of the membrane bands was achieved with 14% polyacrylamide in the base gel, while the soluble fraction was better separated on a 10% polyacrylamide gel (Figure 3.1).

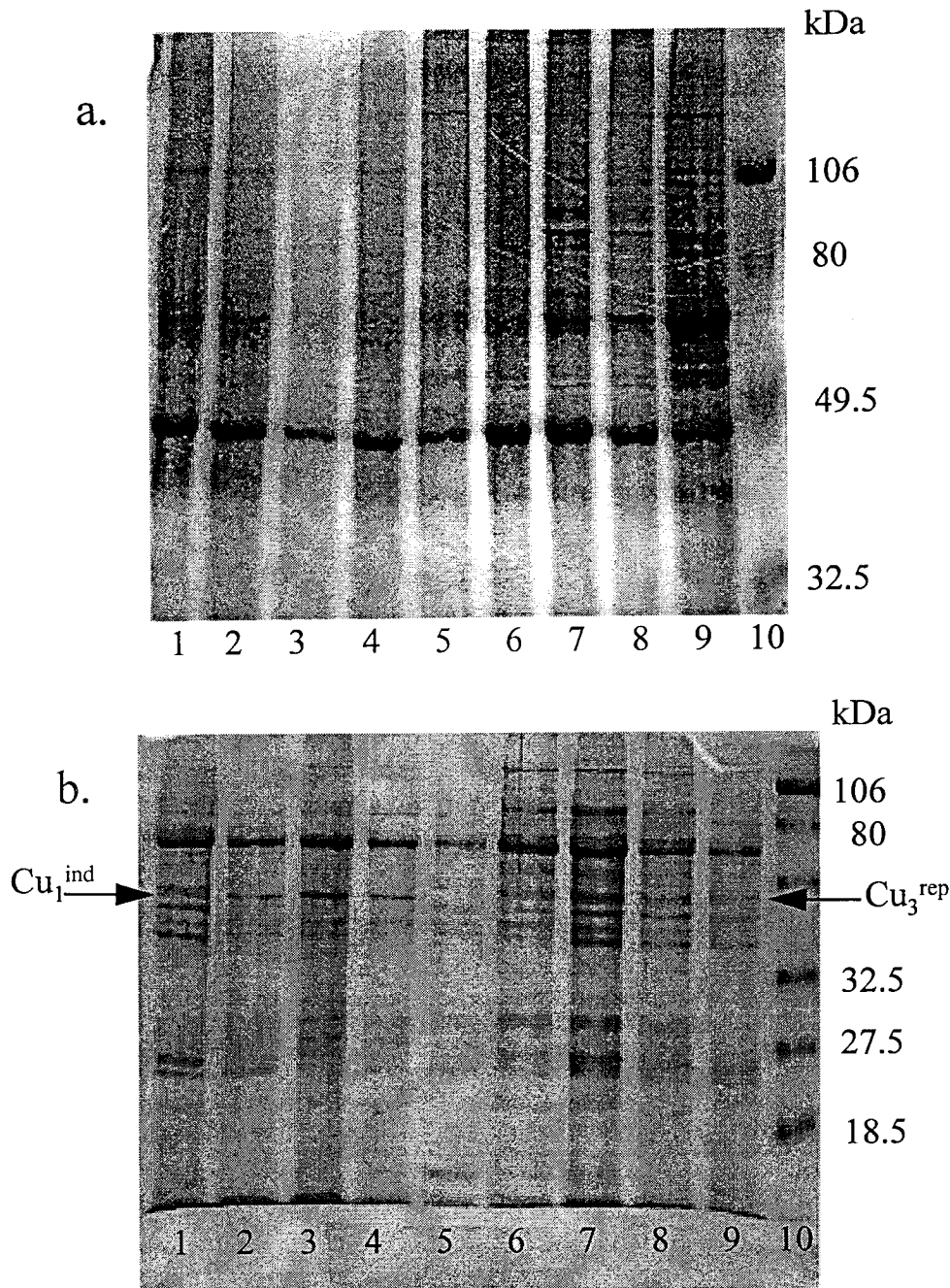


Figure A3.1 Identification of copper-repressible and copper-inducible polypeptides in particulate (a) and soluble (b) fractions of *Methylobacterium albus* BG8 by sodium dodecyl sulfate-polyacrylamide [10% (a) and 14% (b)] gel electrophoresis.

Cell extracts of *M. albus* BG8 were grown with 10 μM (lane 1); 20 μM (lanes 2, 3, 5), 40 μM (lane 4), and no copper (6-9) added to the medium. Lanes 2-5, cells grew poorly; lanes 1, 6-9, normal growth of cultures. A copper-repressible polypeptide Cu_3^{rep} (~49.5 kDa) and a copper-inducible polypeptide Cu_1^{ind} (~49 kDa) were identified in the soluble fraction.

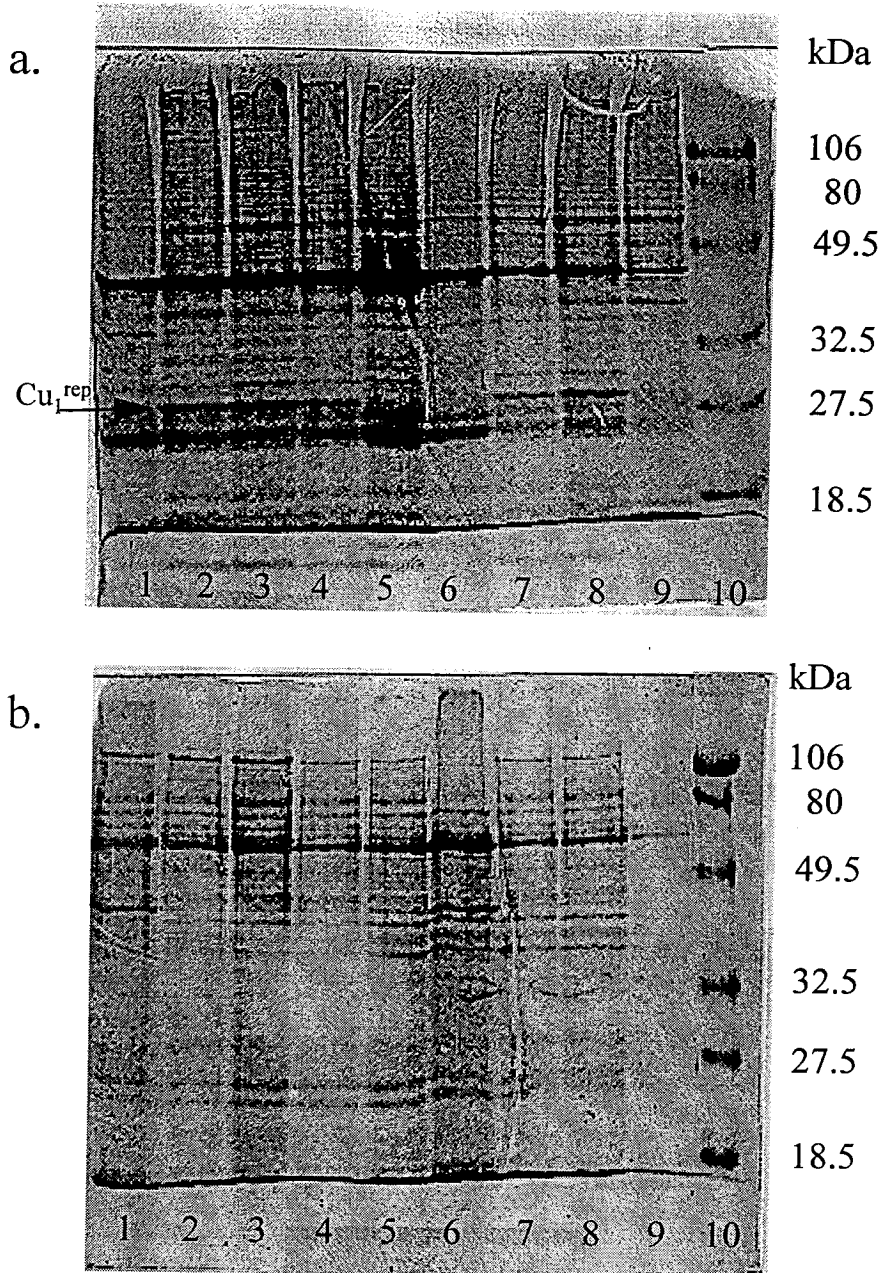


Figure A3.2 Identification of a copper-repressible polypeptides in particulate (a) and soluble (b) fractions of *Methylobacterium albus* BG8 by sodium dodecyl sulfate-polyacrylamide [12%] gel electrophoresis.

Cell extracts of *M. albus* BG8 were grown with 20 μ M (lanes 1, 6, 9); 10 μ M (lane 5), and no copper (lanes 2-4, 7, 8) copper added to the medium. Samples in lanes 3 and 8 were grown in medium with 20 μ M and 40 μ M EDTA added. Samples in lanes 1 and 6 were from poorly growing cultures, all other samples were from normally growing cultures. A copper-repressible, Cu_1^{rep} (~28.5 kDa), polypeptide was identified in the particulate fraction.

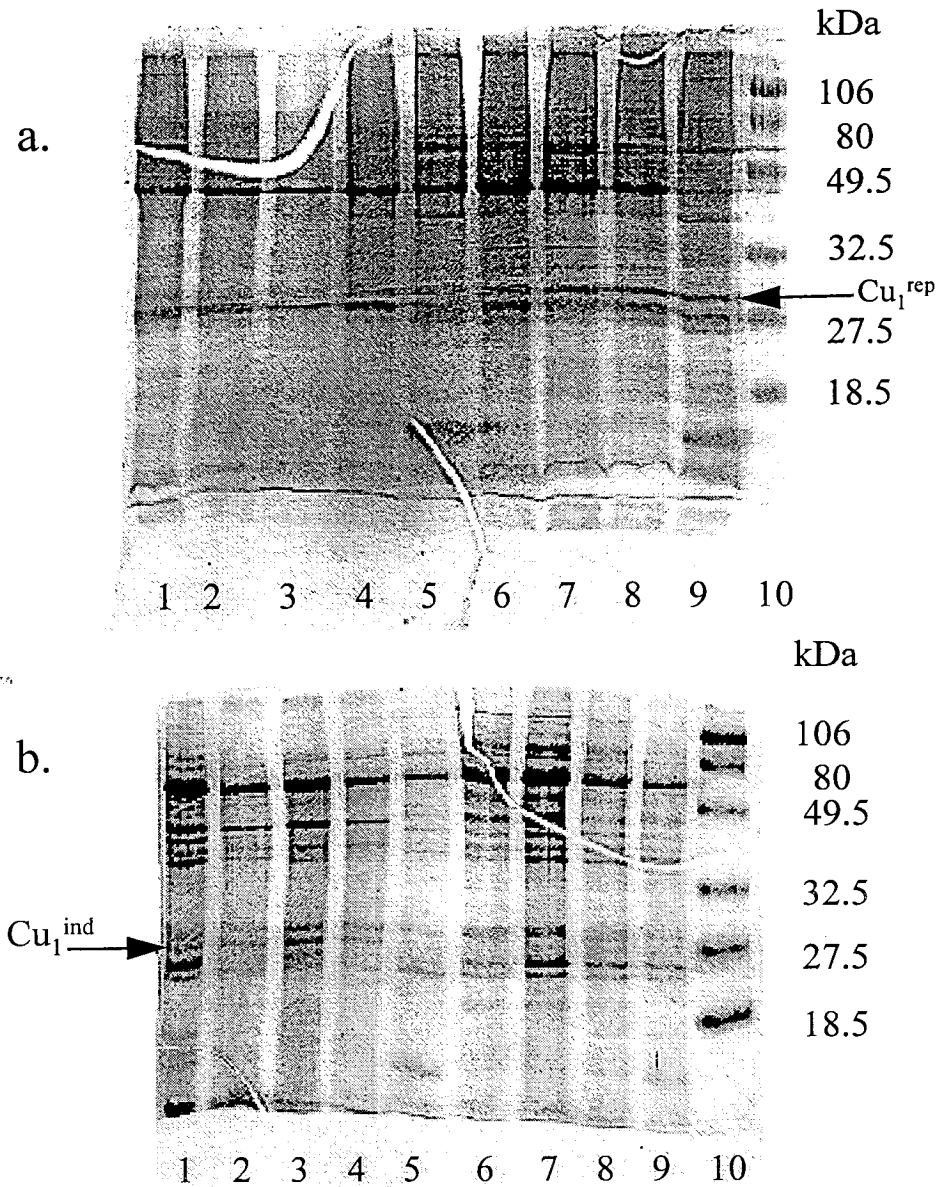


Figure A3.3 Identification of copper-repressible and copper-inducible polypeptides in particulate (a) and soluble (b) fractions of *Methylobacterium albus* BG8 by sodium dodecyl sulfate-polyacrylamide [16%] gel electrophoresis.

Cell extracts of *M. albus* BG8 were grown with 10 μM (lane 1); 20 μM (lanes 2, 3, 5), 40 μM (lane 4), and no copper (6-9) added to the medium. Lanes 2-5, cells grew poorly; lanes 1, 6-9, normal growth of cultures. A copper-repressible, Cu_1^{rep} (~28.5 kDa), polypeptide was identified in the particulate fraction. A copper-inducible polypeptide, Cu_1^{ind} (~49 kDa), was identified in the soluble fraction.

Chapter Four

Cloning and Sequencing of a Putative Copper Transporting P-type ATPase.

4.1. Introduction

Copper is an essential nutrient due to its role as a cofactor of many oxygenases and electron-transport proteins. Yet in excess, copper can cause extensive cellular damage. Consequently, the regulation of intracellular copper activity is required in all cells. Two mechanisms for the homeostasis of copper have been studied in bacteria: copper resistance/uptake in *Escherichia coli* and in *Pseudomonas syringae*. In *E. coli* four plasmid-encoded genes (*pcoARBC*) are required for copper resistance and seven chromosomal genes (*cutA-cutF*) are involved in copper metabolism. In *P. syringae* four structural plasmid-encoded genes (*copABCD*) constitute the copper-resistance system. Both copper resistance systems are regulated by a pair of regulatory genes (*pcoSR* (*E. coli*) and *copCR* (*P. syringae*)) (Butt *et al.* 1984; Ecker *et al.* 1986; Mellano 1988; Harwood-Sears and Gordon 1990; Lee *et al.* 1990; Cha and Cooksey 1991; Rogers *et al.* 1991; Cooksey and Azad 1992; Silver and Walderhaug 1992; Cha and Cooksey 1993; Cervantes and Gutierrez-Corona 1994; Gupta *et al.* 1995, etc.). However, recent studies have identified P-type ATPases as a new class of copper transporting proteins involved in the control of intracellular copper both in prokaryotic and eukaryotic cells (Odermatt *et*

al. 1993; Silver *et al.* 1993; Tanzi *et al.* 1993; Kanamaru *et al.* 1994; Rad *et al.* 1994; Vulpe *et al.* 1994; Fu *et al.* 1995; Ge *et al.* 1995). All P-type ATPases are involved in translocation of a specific cation (H^+ , Na^+ , K^+ , Ca^{2+} , Mg^{2+} , Cd^{2+} or Cu^{2+}), including uptake (movement into the cell), e.g., K^+ -ATPase (Hesse *et al.* 1984), efflux (movement out of the cell), e.g., Ca^{2+} -ATPase (Brandl *et al.* 1986), and cation exchange (one moving in, one moving out), e.g. Na^+/K^+ -ATPase (Shull *et al.* 1985). All known P-type ATPases, from bacteria to human, contain several highly conserved functional domains, such as a phosphatase motif, TGES (Figure 4.1A); a conserved proline in the transduction region, XPX (Figure 4.1B); a phosphorylation region, DKTGT(L or I)T (Figure 4.1C); and an ATP-binding domain, GDG(I or V)ND(A or S)P(A or S)L (Figure 4.1D). It is postulated that the conserved aspartate residue in the ATP-binding domain is phosphorylated by ATP during an intermediate step of cation transport, then, the phosphatase domain removes the phosphate from the aspartic acid during the reaction cycle (see Chapter One for details). The transduction domain is thought to transfer intracellular protein-bound cation to the membrane channel region (Silver and Ji 1994).

There are several unique features found only in copper and cadmium transporting ATPases that set them apart from the rest of the P-type ATPases. One is the cysteine residues flanking the conserved proline in the transduction domain (except for one of the two copper transporting ATPases in *Enterococcus hirae*, CopB, that has only one cysteine next to the proline) and the presence of a second proline six to eight positions downstream (Figure 4B). Another unique feature is a putative metal binding motif, GMXCXXC. This motif is repeated six times in the copper efflux ATPase that is thought

to be defective in the copper-related Menkes disease, Mc1 (Vulpe *et al.* 1993), and it is repeated five times in WD, a copper-ATPase associated with Wilson's disease of copper deficiency (Tanzi *et al.* 1993). The motif is present in CopA, the copper uptake ATPase of *Enterococcus hirae* (Odermatt *et al.* 1993), and CadA, the cadmium-transporting ATPase of *Staphylococcus aureus* (Nucifora *et al.* 1989) (Figure 4.1E). The same motif was previously noted in other proteins that transport or bind heavy metals, such as MerA, mercuric reductase, and in MerP, a periplasmic mercury binding protein (Silver *et al.* 1989), and can be a general heavy metal binding site.

Methanotrophs, aerobic bacteria that grow on methane as a sole source of carbon and energy, are expected to have a tightly regulated copper uptake/efflux system since the key enzyme of methane oxidation, particulate methane monooxygenase (pMMO), requires copper, but on the other hand, high levels of copper (above 50 μM) are toxic to methanotrophs. The presence of a specific copper uptake system(s) in methanotrophs is supported by the results of copper accumulation experiments with a type I methanotroph *M. albus* BG8 (Berson and Lidstrom 1996). In analogy to other bacteria, it seemed possible that a P-type copper-transporting ATPase(s) could be involved in copper transport in methanotrophs. This chapter describes cloning of three putative copper ATPase genes, *atpA*, *atpB* and *atpC*, their sequencing (complete sequence of *atpA* has been obtained, *atpB* and *atpC* were sequenced only partially), and an attempt to make a mutant in *atpB*.

4.2. Materials and Methods

4.2.1. Bacterial Strains, Culture Conditions, and Preparation of DNA.

Methylobacterium albus BG8 (Whittenbury *et al.* 1970), a type I methanotroph, was grown with 10 μ M copper nitrate added to nitrate mineral salts (NMS) medium (Whittenbury *et al.* 1981) as described in Chapter Three (3.2.1) to the late exponential phase and harvested. Chromosomal DNA was extracted from *M.albus* BG8 by the slightly modified procedure of Satio and Miura (1963) as described in detail in Chapter Three (3.2.3). Plasmid DNA was prepared by the method outlined in Chapter Three (3.2.3).

All enzymes used were purchased from New England Biolabs, Inc. (Beverly, Ma) unless stated otherwise. Restriction enzyme digestions were performed as described by Maniatis (*et al.*, 1982). DNA separation by electrophoresis, all ligations, transformations, DNA-DNA hybridizations with dried gels and with nitrocellulose filters, oligonucleotide probe labeling were carried out following the protocols described in Chapter Three.

4.2.2. Polymerase Chain Reaction.

The polymerase chain reaction (PCR) method was used to generate a probe for screening fragments of *M. albus* BG8 chromosome obtained by digestion with restriction enzymes. Amino acid sequences of CopA, a copper uptake protein of the Gram-positive bacterium *Enterococcus hirae* (Odermatt *et al.* 1993) and MC1, a putative human copper-ATPase (Vulpe *et al.* 1993) were aligned (Figure 4.1) to identify

consensus regions. Conserved regions, DKTGTIT (positions 425-431 in the amino acid sequence of CopA and positions 1044-1050 in the amino acid sequence of MC1) (Figure 4.1 C) and MVGDGIND (positions 618-625 in CopA and positions 1298-1305 in MC1) (Figure 4.1D) were identified. Primers P1-A and P2-A were generated, which were identical to the fragments of DNA sequence from *copA* of *E. hirae* that corresponded to the two consensus amino acid sequences. The other primers were backtranslated from the amino acid sequences based on *M. albus* BG8 codon usage frequencies (Table 4.1). The following degenerate primers were designed and synthesized at the Microchemical Facility at the California Institute of Technology: forward primers P1-A (5'-GAT-AAA-ACT-GGA-ACG-ATT-AC-3'), P1-B (5'-GAC-AAA-ACC-GGC-ACC-ATC-AC-3'), P1-C (5'-GA(C or T)-AA(A or G)-AC(C or G or T)-GG(A or C or T)-AC(C or G or T)-AT (C or T)-AC (C or G or T)-3'), and reverse primers, which were designed as reverse complements to the translated amino acid sequence MVGDGIND, P2-A (5'-TCA-TTG-ATT-CCA-TCA-CCG-ACC-3'), P2-B (5'-TCG-TTG-ATG-CCG-TCG-CCG-ACC-3'). For each primer, the temperature of hybridization was calculated based on the following formula (Maniatis *et al.* 1982): $T_{\text{hybr}} = T_m - 10 \text{ }^\circ\text{C} = [69.3 + 0.441(\text{GC}\%) - (650/L)] - 10^\circ\text{C}$, where T_{hybr} , hybridization temperature; T_m , oligo melting temperature; GC%, the percent of G and C in the oligo; L, number of base pairs in the oligo. The following hybridization temperatures were obtained: P1-A, 42.2°C; P1-B, 51.1°C; P1-C, 46.6°C; P2-A, 49.3°C; P2-B, 57.7°C. Each primer was end labeled with 5'-[γ ³²P]ATP, denatured and hybridized with dried agarose gels that contained *M. albus* BG8 chromosomal DNA digested with the following restriction enzymes: *Pst*I, *Sph*I, *Sal*I, *Eco*RI, *Bam*HI, *Hind*III. Only P1-C

and P2-B gave positive hybridization with the chromosomal DNA [up to 7 hybridizing bands were identified for each restriction (results are not shown due to high background)] and, therefore, this pair was used in PCR reactions.

The PCR reactions were carried out in 100 μ L volumes under the following conditions: approximately 20ng template DNA, PCR buffer (10 mM Tris-HCl, 50 mM KCl), 0.2 mM each dNTP, 1U of *Taq* polymerase (Boehringer, Germany), 100 pmol each primer, and in some cases, 5% [vol/vol] DMSO. The PCR reactions were performed with five concentrations of $MgCl_2$: 0.5 mM, 1 mM, 1.5 mM, 2 mM, or 2.5 mM. A Hybaid thermal cycler (Combi TR-2) was used for 25-cycle amplification with the following reaction conditions: denaturation, 94°C for 1 min.; annealing, 55°C or 50°C or 44°C for 1 min.; polymerization, 72°C for 2 min.

PCR products obtained were separated by electrophoresis on 1.4% agarose gels. The combination of 1mM $MgCl_2$, DMSO, and an annealing temperature of 44°C gave the best resolution of three major PCR products: *pcrA*, 340 bp, *pcrB*, 620 bp and *pcrC*, 900 bp) on the gel (Figure 4.2). It appeared that the presence of DMSO increased production of the main PCR products, while bringing down the background (Figure 4.2), so DMSO was added to all subsequent PCR reactions. Two additional PCR reactions were carried out with only one primer added, as controls. Two of the major PCR products *pcrB* and *pcrC*, were in the approximate size range expected, and they were chosen for further study.

The optimized PCR reaction was run once more, PCR products were separated on 1.4% agarose gels, DNA bands of *pcrB* and *pcrC* were excised from the gel and purified

using a GeneClean II[®] kit (Bio 101 Inc., La Jolla, Ca). The purified DNA was then cloned into the pCRTMII (Invitrogen, San Diego, CA) vector that was used to transform INV α F' *E. coli* cells (Invitrogen, San Diego, CA) using the protocol recommended by the manufacturer. The transformants were plated on Luria-Bertani (LB) agar with 50 μ g/ml ampicillin (Amp) and with 2.5% [wt/vol] X-gal (5-bromo-4-chloro-3-indolyl- β -D-galactoside) added. X-gal is a color indicator for the cells containing plasmids with inserts, which remain white on plates with X-gal. To determine the orientation of the inserts, 12 white clones per each insert were picked, grown overnight in LB broth containing 50 μ g/ml of Amp, and were used for plasmid DNA isolation. The plasmid DNA samples obtained were digested with *Eco*RI, which cuts the vector 9 bp up- and downstream of the PCR insert, and electrophoresed on 1.6% agarose gels. Two bands were observed in each case: one, of approximately 4 kb, corresponding to the pCRTMII vector, and another band, of either about 600 bp or 900 bp. Four different sizes of the second band were identified among the 620-bp inserts, 2.3, 2.5, 2.8, and 2.9, and three sizes of the second band were seen among 900-bp inserts, 3.1, 3.3, and 3.4 (not shown). These clones were grown overnight in LB with Amp, and the plasmid DNA was isolated using a Qiagen-tip 20 kit (Qiagen, Los Angeles, CA). DNA sequencing was performed with an Applied Biosystems automated sequencer at the California Institute of Technology, Pasadena, Sequencing Facility, for both strands with M13 Forward and M13 Reverse sequencing primers (New England Biolabs, Inc., Beverly, MA).

Clones 2.5 and 2.9 were found to contain plasmids with the same DNA fragment inserted in either the forward or reverse direction. The recombinant plasmids from *E. coli*

strains 2.3, 2.5, and 2.8 were called pOB18, pOB19, and pOB20 correspondingly, and were assumed to encode portions of ATPase-like genes. In order to obtain more complete information, these plasmids were used as probes for screening *M. albus* BG8 genes.

4.2.3. Cloning and Sequencing of ATPase genes

DNA was isolated from pOB18, pOB19, and pOB20 and digested with *EcoRI* and the DNA fragments obtained were separated on agarose gels. Two bands were observed in each case: one, of 3.9 kb, corresponding to the pCRTMII vector, the other, approximately 620-bp, of the inserts. The 620-bp band was excised from each agarose gel, purified using a GeneClean II[®] kit (Bio 101 Inc., La Jolla, Ca), and randomly labeled with [α -³²P]dCTP as described by Maniatis (Maniatis *et al.* 1982).

Chromosomal DNA of *M. albus* BG8 was digested with *PstI*, *SphI*, *SalI*, *EcoRI*, *BamHI*, and *HindIII*. The DNA fragments obtained were separated by electrophoresis on 0.7% agarose gels (three such gels were prepared). The gels were dried and hybridized with the labeled 620-bp fragment of the 2.3, 2.5, and 2.8 clones at 68°C as described in Chapter Three. These fragments will be called by the name of the clone from which they were isolated, e.g. clone 2.3 will mean 620-bp DNA fragment isolated from clone 2.3. A 1.8-kb *EcoRI* band, hybridizing to clone 2.5, and a 2.5-kb *SalI* band, hybridizing to clone 2.8 were chosen for subsequent cloning. Hybridization with clone 2.3 did not produce any convenient fragments for cloning (not shown), and, therefore, restriction of *M. albus* BG8 chromosomal DNA with different enzymes (*ApoI*, *KpnI*, *SacI*, *XbaI*, and *BspMI*) was

performed. The hybridization of the dried gel with clone 2.3 identified a 3-kb *KpnI* fragment that was used for further cloning.

The 1.8-kb *EcoRI*, 2.5-kb *SalI*, and 3-kb *KpnI* fragments were cloned into the pUC19 vector (New England Biolabs, Inc., Beverly, Ma) using the protocols described in Chapter Three to generate pOB21 (contains partial *atpB*), pOB22 (contains partial *atpC*), and pOB31 (contains complete *atpA*). These recombinant plasmids were used for sequencing of the *EcoRI*, *SalI*, and *KpnI* fragments on both strands at the Sequencing Facility at the California Institute of Technology, Pasadena. At the beginning, sequencing was performed with M13 Forward and M13 Reverse sequencing primers (New England Biolabs, Inc., Beverly, Ma). After the initial sequences were obtained, synthetic oligodeoxynucleotide primers complementary or identical to previously sequenced DNA fragments were synthesized at the Microchemical Facility at the California Institute of Technology, and they were used for sequencing. To translate and to analyze the DNA sequence programs supplied by the Genetic Computer Group (GCG), University of Wisconsin, were used.

4.2.4. Construction of Insertion Mutations in *atpB*.

An insertion mutant defective in *atpB* was obtained by homologous recombination as described in Chapter Three using the kanamycin resistance cassette (Km^r) as a selecting inactivating marker. In short, the 611-bp fragment from pOB19 (pCRTMII vector containing Km^r and ampicillin resistance (Amp^r)) was recloned into pAYC63 (Chistoserdov, personal communication) containing Amp^r and chloromphenicol

resistance (Cm^r) using LB agar plates with 50 mg/ml [wt/vol] Cm (in ethanol) to select recombinants. This clone was called pOB24. The *AvaI* site in pOB24 appeared to be the most promising for the insertional mutation since it is located almost in the middle of the 611-bp fragment, 270 bp downstream from the beginning of the insert. However, the site was not unique in pOB24, since pAYC63 (3.3 kb) also contains an *AvaI* site in the polylinker. Therefore, prior to the introduction of the Km^r cassette, the site was removed from the vector by standard methods described by Maniatis (1982) to generate pOB25 with the unique *AvaI* site in the middle of *atpB*. The plasmid carrying the Km^r gene transcribed in the same direction as *atpB* (pOB26) was ligated with the suicide vector pAYC61 (Chistoserdov *et al.* 1994), and the resulting plasmid (pOB30, Figure 4.3) was transformed into *E. coli* S17-1 (Simon *et al.* 1983). The resulting *E. coli* strain was employed as a donor in homologous recombination with *M. albus* BG8. The mutants were selected on NMS agar plates with 15 $\mu\text{g/ml}$ Km added grown under a methane/air atmosphere.

4.3. Results and Discussion

4.3.1. Isolation and Cloning of Three Putative Atpase Genes, *atpA*, *atpB* and *atpC*.

In order to determine whether *M. albus* BG8 might contain one or more genes encoding P-type ATPases, the consensus amino acid sequences, DKTGTIT and MVGDGIND, found in two known copper transporters, [CopA, the copper uptake protein of the Gram-

positive bacterium *Enterococcus hirae* (Odermatt *et al.* 1993) and MC1, a putative human copper-ATPase (Vulpe *et al.* 1993) (Figure 4.1 C and D)], were used to generate three forward primers and two reverse primers for PCR amplification. The redundancy of these primers was minimized by choosing the most prevalent of *M.albus* BG8 codons (Table 4.1). Only two of these primers, the forward primer P1-C and the reverse primer P2-B, hybridized to *M. albus* BG8 DNA. Several (up to 7) bands were seen in each case, suggesting the possibility that multiple ATPase-like genes might be present. This hypothesis was studied further by cloning and sequencing putative ATPase genes. Three PCR products, *pcrA*, *pcrB*, and *pcrC* of approximately 340, 620, and 900 nucleotides correspondingly, were generated by PCR. A PCR product of approximately 600 bp was expected from the PCR reaction with primers P1-C and P2-B since the primers were created based on the highly conserved regions separated by approximately 600 bp in bacterial ATPases. The PCR reaction with only one primer did not give any products in case of P1-C, but the reaction with P2-B produced two small DNA fragments, one of which was the same size as *pcrA* (Figure 4.2), which implied that *pcrA* was the result of an incomplete PCR reaction, and, therefore, it was not studied further.

The PCR products *pcrB* and *pcrC* were cloned into pCRTMII (Invitrogen, San Diego, CA) vector. The restriction analysis of the generated clones revealed three independent clones containing inserts of approximately 620-bp, and three independent clones containing inserts of approximately 900-bp. DNA fragments purified from all six clones were sequenced on both strands. The sequences obtained(not shown) were translated into amino acid sequences, and the obtained polypeptides were compared with

known proteins from the data base (SwissProt) by using GCG (University of Wisconsin) programs. All three sequenced 620-bp fragments demonstrated high homology to cation transporting ATPases, with especially high identity to copper and cadmium ATPases: 31.9% identity in a 207 aa overlap for pOB20, 41.2% identity in a 204 aa overlap for pOB18, and 41.7% identity in a 204 aa overlap for pOB19 (not shown). The 900-bp fragments, however, were not significantly homologous to any of the genes encoding known proteins. These, probably, were generated as side-products of PCR reactions due to non-specific binding of the primers to the DNA template. They were not pursued further.

Radioactively labeled 620-bp DNA fragments from pOB18, pOB19, and pOB20 were used to screen chromosomal DNA of *M. albus* BG8 digested with restriction endonucleases. 1.8-kb *EcoRI*, 2.5-kb *SalI*, and 3-kb *KpnI* fragments were identified by clones 2.5, 2.8, and 2.3, respectively. These fragments were cloned into the pUC19 vector (New England Biolabs, Inc., Beverly, MA) to produce pOB21, pOB22, and pOB31 respectively and the inserts were sequenced on both strands.

4.3.2. Sequencing Results And Sequence Comparison With Known Copper ATPases.

The sequence analysis revealed the presence of one open reading frame (*atpA*), 2231 bp in length, in pOB31 (Figure 4.4), and partial open reading frames *atpB* (1866 bp) and *atpC* (689 bp) in pOB21 (Figure 4.5) and pOB22 (Figure 4.6) correspondingly. Both *atpB* and *atpC* encoded the C-terminal part of the polypeptides AtpB and AtpC.

The amino acid sequence derived from *atpA*, *atpB* and *atpC* were compared with each other and with sequences in the SwissProt data base. It appeared that the three polypeptides are closely related to each other: AtpA/AtpB, 48.5% identity and 71.8% similarity (when conserved substitutions are considered); AtpA/AtpC, 48.3% identity and 67.8% similarity; AtpB/AtpC, 44.3% identity and 69.1% similarity. The AtpA/AtpB/AtpC alignment results (Figure 4.7) show especially high homology at the C-terminus of the polypeptides. All three polypeptides exhibited strong homology to P-type ATPases, especially the copper-ATPase family (Table 4.2, results only for AtpA are shown). Since only *atpA* was completely sequenced and because *atpB* and *atpC* are very similar, further discussion will be focused on AtpA.

The product of *atpA* has the highest homology (45.7% identity in 742 aa overlap) to a cation-transporting ATPase found in the thylakoid membrane of the cyanobacterium *Synechococcus* sp. PCC7942, which was recently postulated to be a copper-transporting ATPase (Kanamaru *et al.* 1994). The next four proteins most closely related to AtpA were CopA from *Enterococcus hirae* (Odermatt *et al.* 1993), WD, human Wilson disease related ATPase (Tanzi *et al.* 1993), Mc1, human Menkes disease, associated ATPase (Vulpe *et al.* 1993), and CtaA, another P-type ATPase from the cyanobacterium *Synechococcus* 7942 (Phung, *et al.* 1994). These are all copper-transporting ATPases (Table 5.2). Potassium/copper transporting ATPase, CopA, is thought to be a copper-uptake ATPase, because disruption of the *copA* gene does not affect copper-sensitivity of the cells but causes dependency on higher added copper concentrations for growth (Odermatt *et al.* 1993). Wilson and Menkes diseases are human hereditary disorders of

copper transport. It has been suggested that Wilson's disease is related to a defect in the copper-efflux ATPase, WD, that results in an inability to excrete an excess of copper and causes toxic accumulation of copper in the liver and brain (Tanzi *et al.* 1993). Menkes disease is associated with copper deficiency caused by a disruption in the *Mcl* gene encoding a copper ATPase, which is believed to be involved in copper transport to tissues containing copper-requiring proteins (Tanzi *et al.* 1993, Vulpe *et al.* 1993). A mutation in the *ctaA* gene of *Synechococcus* 7942, encoding a P-type ATPase, increases tolerance of the cells to higher copper concentrations while it does not cause higher resistance to other cations, suggesting that the product of *ctaA* is a copper ATPase (Phung *et al.* 1994).

A lower level of identity was observed between AtpA and cation transporting ATPases A and B with unknown specificity from *Mycobacterium leprae* (Fsilu and Cole, 1995), CCC2, an uptake copper ATPase from the yeast *Saccharomyces cerevisiae* (Fu *et al.* 1995), and CopB, a potassium/copper efflux ATPase from *Enterococcus hirae* (Odermatt *et al.* 1993) (Table 4.2). Outside of the copper ATPase subfamily, significant similarity was seen between AtpA and CadA, a cadmium ATPase of *Staphylococcus aureus* (30.2% identity) (Nucifora *et al.* 1989). AtpA is not similar to other P-type ATPases outside of the highly conserved regions of phosphorylation and ATP binding, which results in overall lower similarity between them (21 to 28 % identity in the 742 aa overlap). The sequence alignment tree presented in Figure 4.8 summarizes similarity relationships of P-type ATPases, and places AtpA in the copper ATPase subfamily.

All key motifs of P-type ATPases such as those involved in phosphatase function, ion-transduction, phosphorylation, and ATP-binding are conserved in AtpA (Figures 4.1

and 4.6). The ion transduction region is highly conserved within the copper ATPase subfamily (Figure 4.1B). Both AtpA and AtpB show more similarity to copper ATPases than other ATPases in this domain (Figures 4.1B and 4.7). The motif, Cys-Pro-Cys-X(6)-Pro, which is thought to participate in cadmium and copper coordination (Phung *et al.* 1994) is also conserved in AtpA and AtpB (Figures 4.1B and 4.7). A putative copper/cadmium binding motif, Gly-Met-X-Cys-X-X-Cys previously noted in CopA, the copper ATPase of *Enterococcus hirae* (Odermatt *et al.* 1993), Mc1, Menkes copper ATPase (Vulpe *et al.* 1993), WD, Wilson's Disease copper ATPase (Tanzi *et al.* 1993), the copper ATPase from *Synechococcus* sp. PCC7942 (Kanamaru *et al.* 1994), and CadA, the cadmium ATPase of *Staphylococcus aureus* (Nucifora *et al.* 1989) was identified in the N-terminus of AtpA (Figure 4.1E), strongly suggesting a role of AtpA in copper transport.

Hydropathy plots of AtpA, AtpB, and AtpC were generated with the GCG package using the residue-specific hydrophobicity index of Kyte and Doolittle (1982) and a span of 20 residues (Figures 4.9-4.11). Nine highly hydrophobic regions were identified in AtpA (Figure 4.9). The same regions were identified within sequenced fragments of AtpB, 3rd-9th, (Figure 4.10) and AtpC, 8th and 9th, (Figure 4.11). It is thought that a hydrophobic but uncharged sequence has a high probability to be in a transmembrane domain (Tanzi *et al.* 1993). To identify membrane-spanning regions, the hydrophobicity profile of AtpA was overlapped with a profile of residue charges (Figure 4.12, only hydrophobic regions identified in Figure 4.9 are shown). All nine hydrophobic peaks corresponded to the regions of no or little charge (zero or one charged residue per 14 to

20 residues) and they were predicted (Peptidestructure Program, GCG, Chou-Fasman algorithm) to be α -helices. Therefore, it is plausible to conclude that there are nine transmembrane domains in AtpA, including the metal-binding domain, 1, and the ion transduction domain, 7. A similar membrane topology was proposed for other copper ATPases (Tanzi *et al.* 1993, Odermatt *et al.* 1993, Vulpe *et al.* 1993).

4.3.3. Mutant Characterization

To confirm a role of AtpA, AtpB and AtpC in copper transport in *M. albus* BG8, an attempt was made to construct insertion mutants by homologous recombination between the *M. albus* BG8 chromosome and plasmids containing insertions in the genes of the interest. No mutants were obtained in *atpA* and *atpC*. The phenotype of the *atpB* insertion mutants was checked on NMS plates containing Amp, and it was found to be Km^r/Amp^r for all colonies obtained. Therefore, only single crossovers, containing an insertion of the entire suicide plasmid, and generating an intact gene were identified among *atpB* mutants (Figure 4.13). The inability to obtain double crossover mutants suggests that *atpB* is required for growth of *M.albus* BG8.

In conclusion, the presence of a copper or cadmium binding motif in AtpA and the high identity of AtpA, AtpB and AtpC with the subfamily of copper ATPases suggests that the cloned genes might encode copper pumps. Further studies, including more mutant construction and copper uptake experiments, will be needed to clearly define the role of this protein copper uptake.

4.4. References

- Berson, O., M.E. Lidstrom.** Study of copper accumulation by the type I methanotroph *Methylomicrobium albus* BG8. Environ.Sci.Technol. **30**:802-809.
- Brock, T. D. and M. T. Madigan.** 1991. Biology of Microorganisms. Prentice Hall, Englewood Cliffs.
- Butt, T. R., E. J. Sternberg, J. A. Gorman, P. Clark, D. Hamer, M. Rosenberg, and S. Crooke.** 1984. Copper metallothionein of yeast, structure of the gene, and regulation of expression. Proc. Natl. Acad. Sci. **81**:3332-3336.
- Cervantes, C. and F. Gutierrez-Corona.** 1994. Copper resistance mechanisms in bacteria and fungi. FEMS microbiology reviews **14**:121-138.
- Cha, J. S. and D. A. Cooksey.** 1991. Copper resistance in pseudomonas-syringae mediated by periplasmic and outer-membrane proteins. Proceedings Of The National Academy Of Sciences Of The United States Of America **88**:8915-8919.
- Cha, J. S. and D. A. Cooksey.** 1993. Copper hypersensitivity and uptake in pseudomonas-syringae containing cloned components of the copper resistance operon. Appl. Environ. Microbiol. **59**:1671-1674.
- Chistoserdov, A. Y., L. V. Chistoserdova, W. S. McIntire, and M. E. Lidstrom.** 1994. Genetic organization of the *mau* gene cluster in *Methylobacterium extorquens* AM1: complete nucleotide sequence and generation and characteristics of *mau* mutants. Journal of Bacteriology **176**:4052-4065.
- Cooksey, D. A. and H. R. Azad.** 1992. Accumulation of copper and other metals by copper-resistant plant- pathogenic and saprophytic pseudomonads. Appl. Environ. Microbiol. **58**:274-278.
- Ecker, D. J., T. R. Butt, E. J. Sternberg, M. P. Neepser, C. Debouck, J. A. Gorman, and S. T. Crooke.** 1986. Yeast metallothionein function in metal ion detoxification. The Journal of Biological Chemistry **261**:16895-16900.
- Fu, D., T. J. Beeler, and T. Dunn.** 1995. Sequence, mapping and disruption of *CCC2*, a gene that cross complements the Ca^{2+} -sensitive phenotype of *csgI* mutants and encodes a P-type AYPase belonging to the Cu^{2+} -ATPase subfamily. Yeast **11**:283-292.
- Ge, Z., K. Hiratsuka, and D. E. Taylor.** 1995. Nucleotide sequence and mutational analysis indicate that two *Helicobacter pylori* genes encode a P-type ATPase and a cation-binding protein associated with copper transport. Molecular microbiology **15**:97-106.

- Gupta, S. D., B. T. O. Lee, J. Camakaris, and H. C. Wu.** 1995. Identification of *cutC* and *cutF (nlpE)* genes involved in copper tolerance in *Escherichia coli*. Journal of Bacteriology **177**:4207-4215.
- Harwood-Sears, V. and A. S. Gordon.** 1990. Copper-induced production of copper-binding supernatant proteins by the marine bacterium *Vibrio alginolyticus*. Appl. Environ. Microbiol. **56**:1327-1332.
- Hesse, J. E., L. Wieczorek, K. Altendorf, A. S. Reicin, D. Elizabeth, and W. Epstein.** 1984. Sequence homology between two membrane transport ATPases, the Kdp-ATPase of *Escherichia coli* and the Ca^{2+} -ATPase of sarcoplasmic reticulum. Proc. Natl. Acad. Sci. USA **81**:4746-4750.
- Kanamaru, K., S. Kashiwagi, and T. Mizuno.** 1994. A copper-transporting P-type ATPase found in the thylakoid membrane of the cyanobacterium *Synechococcus* species PCC7942. Molecular microbiology **13**:369-377.
- Kyte, J. and R. F. Doolittle.** 1982. A simple method for displaying the hydrophobic character of a protein. J. Mol. Biol. **157**:105-132.
- Lee, B. T. O., N. L. Brown, S. Rogers, A. Bergemann, J. Camakaris, and D. A. Rouch.** 1990. Bacterial response to copper in the environment:copper resistance in *Escherichia coli* as a model system. NATO ASI Series **G 23**:625-632.
- Maniatis, T., E. F. Fritsch, and J. Sambrook.** 1982. Molecular cloning: a laboratory manual. Cold Spring Harbor Laboratory. Cold Spring Harbor, N.Y.
- Mellano, M. A.** 1988. Nucleotide sequence and organization of copper resistance genes from *Pseudomonas syringae* pv. *tomato*. Journal of Bacteriology **170**:2879-2883.
- Nucifora, G., L. Chu, T. K. Misra, and S. Silver.** 1989. Cadmium resistance from *Staphylococcus aureus* plasmid p1258 *cadA* gene results from a cadmium-efflux ATPase. Proc. Natl. Acad. Sci. USA **86**:3544-3548.
- Oddermatt, A., H. Suter, R. Krapf, and M. Solioz.** 1993. Primary structure of two P-type ATPases involved in copper homeostasis in *Enterococcus hirae*. J. Biol. Chem. **268**:12775-12779.
- Phung, L.T., G. Ajlani, and R. Haselkorn.** 1994. P-type ATPase from the cyanobacterium *Synechococcus* 7942 related to the human Menkens and Wilson disease gene products. Proc. Natl. Acad. Sci. USA **91**:9651-9654.
- Rad, M. R., L. Kirchrath, and C. P. Hollenberg.** 1994. A putative P-type Cu^{2+} -transporting ATPase gene on chromosome II of *Saccharomyces cerevisiae*. Yeast **10**:1217-1225.

- Rogers, S. D., M. R. Bhave, J. F. B. Mercer, J. Camakaris, and B. T. O. Lee.** 1991. Cloning and characterization of *cutE*, a gene involved in copper transport in *Escherichia coli*. *Journal of Bacteriology* **173**:6742-6748.
- Satio, H. and K.-I. Miura.** 1963. Preparation of transforming deoxyribonucleic acid by phenol treatment. *Biochim. Biophys. Acta* **72**:619-629.
- Shull, G. E., A. Schwartz, and J. B. Lingrel.** 1985. Amino-acid sequence of the catalytic subunit of the (Na⁺ + K⁺)ATPase deduced from a complementary DNA. *Nature* **316**:691-695.
- Silver, S. and G. Ji.** 1994. Newer systems for bacterial resistance to toxic heavy metals. *Environmental Health Perspectives* **102**:107-113.
- Silver, S., G. Nucifora, L. Chu, and T. K. Misra.** 1989. Bacterial resistance ATPases: primary pumps for exporting toxic cations and anions. *Trends biochem. Sci.* **14**:76-80.
- Silver, S., G. Nucifora, and L. T. Phung.** 1993. Human menkens X-chromosome disease and the staphylococcal cadmium-resistance ATPase: a remarkable similarity in protein sequences. *Molecular microbiology* **10**:7-12.
- Silver, S. and M. Walderhaug.** 1992. Gene regulation of plasmid- and chromosome-determined inorganic ion transport in bacteria. *Microbiological Reviews* **56(1)**:195-228.
- Simon, R., U. Priefer, and A. Puhler.** 1983. Vector plasmids for in vivo manipulations of gram-negative bacteria. p. 98-106. In A. Puhler (ed.), *Molecular genetics of the bacteria-plant interactions*. Springer-Verlag, Berlin.
- Tanzi, R. I., K. Petrukhin, I. Chernov, J. L. Pellequer, W. Wasco, B. Ross, and D. M. Romano.** 1993. The wilson disease gene is a copper transporting ATPase with homology to the Menkes disease gene. *Nature genetics* **5**:344-350.
- Vulpe, C., B. Levinson, S. Whitney, S. Packman, and J. Gitschier.** 1993. Isolation of a candidate gene for Menkens disease and evidence that it encodes a copper-transporting ATPase. *Nature genetics* **3**:7-13.
- Whittenbury, R., K. C. Phillips, and J. F. Wilkinson.** 1970. Enrichment, isolation and some properties of methane-utilizing bacteria. *J. Gen. Microbiol.* **61**:205-218.

Table 4.1 Codon frequency statistics for *Methylomicrobium albus* BG8 calculated using the CodonPreference program of GCG Package.

AmAcid	Codon	Number	/1000	Fraction
Gly	GGG	7.00	8.97	0.10
Gly	GGA	11.00	14.10	0.16
Gly	GGT	14.00	17.95	0.20
Gly	GGC	37.00	47.44	0.54
Glu	GAG	11.00	14.10	0.37
Glu	GAA	19.00	24.36	0.63
Asp	GAT	17.00	21.79	0.35
Asp	GAC	31.00	39.74	0.65
Val	GTG	12.00	15.38	0.29
Val	GTA	6.00	7.69	0.14
Val	GTT	6.00	7.69	0.14
Val	GTC	18.00	23.08	0.43
Ala	GCG	29.00	37.18	0.38
Ala	GCA	4.00	5.13	0.05
Ala	GCT	12.00	15.38	0.16
Ala	GCC	32.00	41.03	0.42
Arg	AGG	6.00	7.69	0.13
Arg	AGA	5.00	6.41	0.11
Ser	AGT	6.00	7.69	0.11
Ser	AGC	11.00	14.10	0.20
Lys	AAG	16.00	20.51	0.48
Lys	AAA	17.00	21.79	0.52
Asn	AAT	9.00	11.54	0.24
Asn	AAC	29.00	37.18	0.76
Met	ATG	21.00	26.92	1.00
Ile	ATA	2.00	2.56	0.05
Ile	ATT	14.00	17.95	0.33
Ile	ATC	27.00	34.62	0.63
Thr	ACG	14.00	17.95	0.26
Thr	ACA	3.00	3.85	0.06
Thr	ACT	9.00	11.54	0.17
Thr	ACC	28.00	35.90	0.52
Trp	TGG	13.00	16.67	1.00
End	TGA	0.00	0.00	0.00
Cys	TGT	0.00	0.00	0.00
Cys	TGC	5.00	6.41	1.00

Table 4.1 (continued)

End	TAG	1.00	1.28	0.25
End	TAA	3.00	3.85	0.75
Tyr	TAT	9.00	11.54	0.39
Tyr	TAC	14.00	17.95	0.61
Leu	TTG	19.00	24.36	0.31
Leu	TTA	4.00	5.13	0.06
Phe	TTT	21.00	26.92	0.54
Phe	TTC	18.00	23.08	0.46
Ser	TCG	10.00	12.82	0.19
Ser	TCA	6.00	7.69	0.11
Ser	TCT	4.00	5.13	0.07
Ser	TCC	17.00	21.79	0.31
Arg	CGG	12.00	15.38	0.27
Arg	CGA	8.00	10.26	0.18
Arg	CGT	0.00	0.00	0.00
Arg	CGC	14.00	17.95	0.31
Gln	CAG	10.00	12.82	0.45
Gln	CAA	12.00	15.38	0.55
His	CAT	9.00	11.54	0.60
His	CAC	6.00	7.69	0.40
Leu	CTG	31.00	39.74	0.50
Leu	CTA	0.00	0.00	0.00
Leu	CTT	3.00	3.85	0.05
Leu	CTC	5.00	6.41	0.08
Pro	CCG	23.00	29.49	0.53
Pro	CCA	5.00	6.41	0.12
Pro	CCT	6.00	7.69	0.14
Pro	CCC	9.00	11.54	0.21

Table 4.2 The results of sequence comparison of AtpA with some other cation transporting ATPases.

AtpA sequence was compared with other ATPase sequences using the FASTa (GCG) algorithm. In the table below, sequences are displayed in the order of decreasing similarity to AtpA. Gaps were introduced into sequences to enhance their alignment, and the reported length of overlapping regions include these gaps.

ATPase	Cation specificity	Origin	Length, amino acids	Identity with AtpA, % (overlapping amino acids)	Accession numbers for SwissProt data base
PacS	Cu ²⁺	<i>Synechococcus</i> sp. strain 7942	747	45.7 (742)	P37279
CopA	K ⁺ /Cu ²⁺	<i>Enterococcus hirae</i>	727	41.7 (739)	P32113
WD	Cu ²⁺	human	1411	47.1 (700)	P35670
Mc1	Cu ²⁺	human	1500	41.8 (710)	Q04656
SynA	Cu ²⁺	<i>Synechococcus</i> sp. strain 7942	790	41.1 (740)	P37385
CCC2	Cu ²⁺	<i>Saccharomyces cerevisiae</i>	1004	33.7 (700)	P38995
CopB	K ⁺ /Cu ²⁺	<i>Enterococcus hirae</i>	745	35.5 (617)	P05425

Table 4.2 (continued).

CadA	Cd ²⁺	<i>Staphylococcus aureus</i>	727	33.3% (550)	P20021
CadD	Cd ²⁺	<i>Staphylococcus aureus</i>	804	33.6 (550)	P37386
CadA-Bac	Cd ²⁺	<i>Bacillus firmus</i>	723	33.9% (545)	P30336
ATC2	Ca ²⁺	<i>Saccharomyces cerevisiae</i>	723	29.9% (720)	P38360
KdpB	K ⁺	<i>Escherichia coli</i>	682	27.96% (740)	P03960
AtnA	Na ⁺ /K ⁺	<i>Artemia salina</i>	996	21.3% (580)	P17326
MgtB	Mg ²⁺	<i>Salmonella typhimurium</i>	908	20.3% (650)	P22036

A. Phosphatase Region

Mgtb	A	G	D	L	V	P	A	D	V	R	L	L	A	S	R	D	L	F	I	S	Q	S	I	L	S	G	E	S	L	P	V	E	K	232
Atna	F	G	D	R	I	P	A	D	I	R	I	T	S	C	Q	S	M	K	V	D	N	S	S	L	T	G	E	S	E	P	-	-	-	205
Cada	P	G	E	K	I	A	M	D	G	I	I	V	N	G	L	S	A	-	V	N	Q	A	A	I	T	G	E	S	V	P	V	S	K	280
Cadd	P	G	E	K	I	A	M	D	G	I	I	I	N	G	V	S	A	-	V	N	Q	A	A	I	T	G	E	S	V	P	V	A	K	357
Cada-Bac	P	G	Q	K	I	A	M	D	G	V	V	V	S	G	Y	S	A	-	V	N	Q	T	A	I	T	G	E	S	V	P	V	E	K	277
Wd	P	G	G	K	F	P	V	D	G	K	V	L	E	G	N	T	M	-	A	D	E	S	L	I	T	G	E	A	M	P	V	T	K	840
Mcl1	P	G	G	K	F	P	V	D	G	R	V	I	E	G	H	S	M	-	V	D	E	S	L	I	T	G	E	A	M	P	V	A	K	888
Atpa	P	G	E	K	I	A	V	D	G	V	L	I	E	G	H	S	S	-	V	D	E	S	M	L	T	G	E	P	M	P	A	E	K	296
Pacs	P	G	E	K	V	P	V	D	G	E	V	I	D	G	R	S	T	-	V	D	E	S	M	V	T	G	E	S	L	P	V	Q	K	300
Copa	P	G	E	Q	V	P	T	D	G	R	I	I	A	G	T	S	A	-	L	D	E	S	M	L	T	G	E	S	V	P	V	E	K	291
Syna	P	G	D	R	I	P	V	D	G	C	I	V	A	G	Q	S	T	-	L	D	T	A	M	L	T	G	E	P	L	P	Q	P	C	310
Ccc2	P	G	M	K	I	P	A	D	G	I	I	T	R	G	E	S	E	-	I	D	E	S	L	M	T	G	E	S	I	L	V	P	K	477
Copb	A	G	D	K	M	P	T	D	G	T	I	D	K	G	H	T	I	-	V	D	E	S	A	V	T	G	E	S	K	G	V	K	K	307
Atc2	P	D	S	R	I	P	T	D	G	T	V	I	S	G	S	S	E	-	V	D	E	A	L	I	T	G	E	S	M	P	V	P	K	760
Atkb	A	G	D	I	I	P	C	D	G	E	V	I	E	G	G	A	S	-	V	D	E	S	A	I	T	G	E	S	A	P	V	I	R	173

Figure 4.1 Conserved regions found in P-type ATPases.

The deduced amino acid sequence of the *M. albus* BG8 Atpase, AtpA, was aligned with the following ATPases (from top to bottom, SwissProt data base accession numbers are shown in the parentheses): Mgtb, Mg²⁺ transport ATPase, *Salmonella typhimurium* (P22036); Atna, Na⁺/K⁺ ATPase, *Artemia salina* (brine shrimp) (P17326); Cada, Cd²⁺ ATPase, *Staphylococcus aureus* (P20021); Cadd, Cd²⁺ ATPase, *Staphylococcus aureus*, (P37386); Cada-Bac, Cd²⁺ ATPase, *Bacillus firmus* (P30336); WD, Cu²⁺ efflux ATPase associated with human Wilson disease (P35670); Mcl1, Cu²⁺ uptake ATPase associated with human Menkes disease (Q04656); AtpA, cation ATPase from *M. albus* BG8, this study; Pacs, probably Cu²⁺-transporting ATPase, *Synechococcus* Sp. (P37279); Copa, K⁺/Cu²⁺-transporting ATPase A, probably involved in copper intake, *Enterococcus hirae* (P32113); Syna, Cu²⁺-transporting ATPase, *Synechococcus* sp. (P37385); Ccc2, Cu²⁺-transporting ATPase, *Saccharomyces cerevisiae* (P38995); Copb, K⁺/Cu²⁺-transporting ATPase B, probably involved in copper efflux, *Enterococcus hirae* (P05425); Atc2, Ca²⁺-transporting ATPase, *Saccharomyces cerevisiae* (P38360); Atkb, K⁺-transporting ATPase, *Escherichia coli* (P03960).

The putative metal binding motif (Part E) is shown only for copper and cadmium ATPases. The sequences were aligned and arranged according to amino acid similarity by Pileup program of GCG Group. Gaps (-) were introduced when needed for better alignment. The regions with identical sequences are boxed. The signature motifs are marked with asterisks.

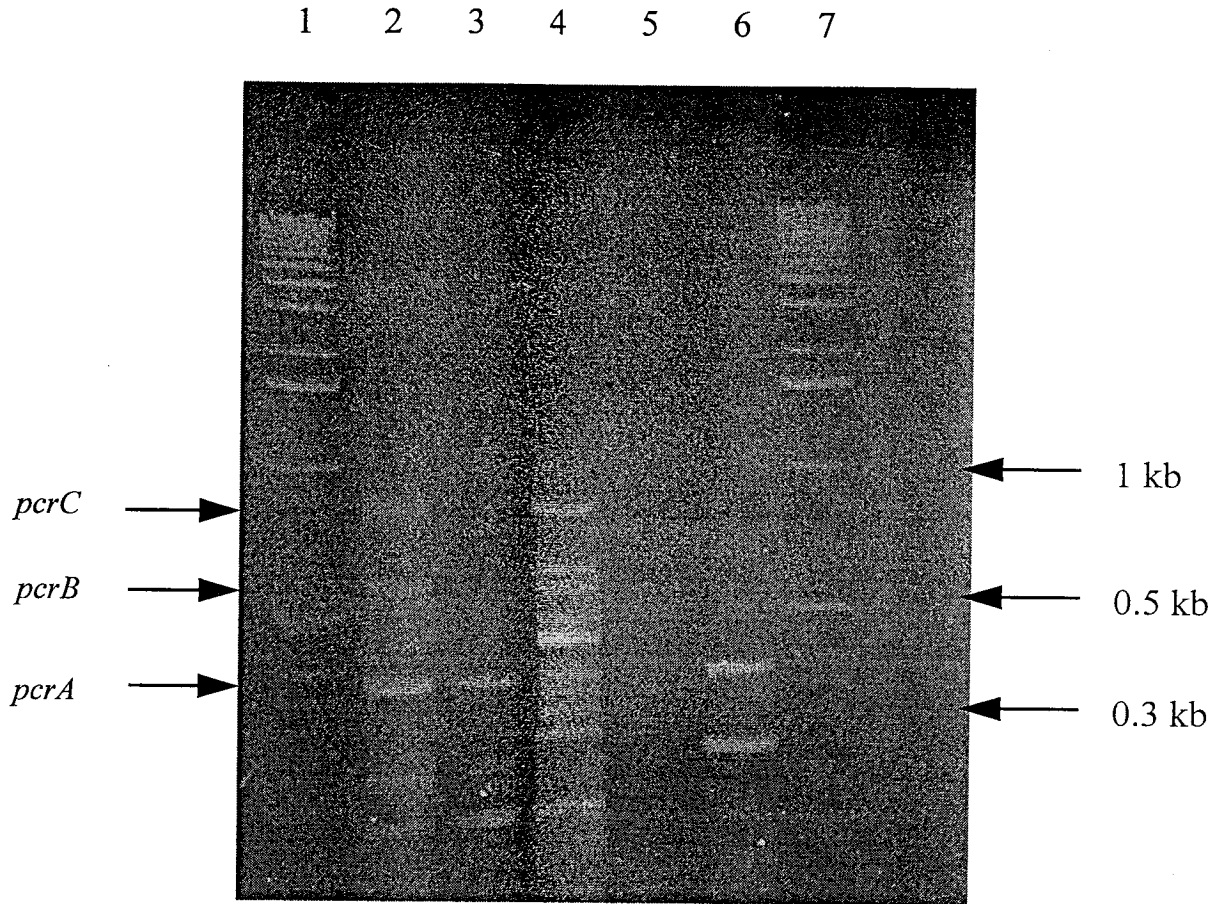


Figure 4.2 PCR-amplified products in an agarose gel.

1 kb ladder was used as DNA sizing standard, lanes 1 and 7. The reaction conditions were: denaturation, 94°C for 1 min.; annealing, 55°C or 50°C or 44°C for 1 min.; polymerization, 72°C for 2 min. The PCR reactions were carried out as follows: Lane 2, MgCl₂=1mM, +DMSO; lane 3, MgCl₂=1mM, -DMSO; lane 4, MgCl₂=2.5mM, -DMSO; lane 5, MgCl₂=1mM, +DMSO, only one primer added to the reaction, P1-C; lane 6, MgCl₂=1mM, +DMSO, only one primer added to the reaction, P2-B. Three major PCR products, *pcrA*, *pcrB*, *pcrC* are marked on the gel.

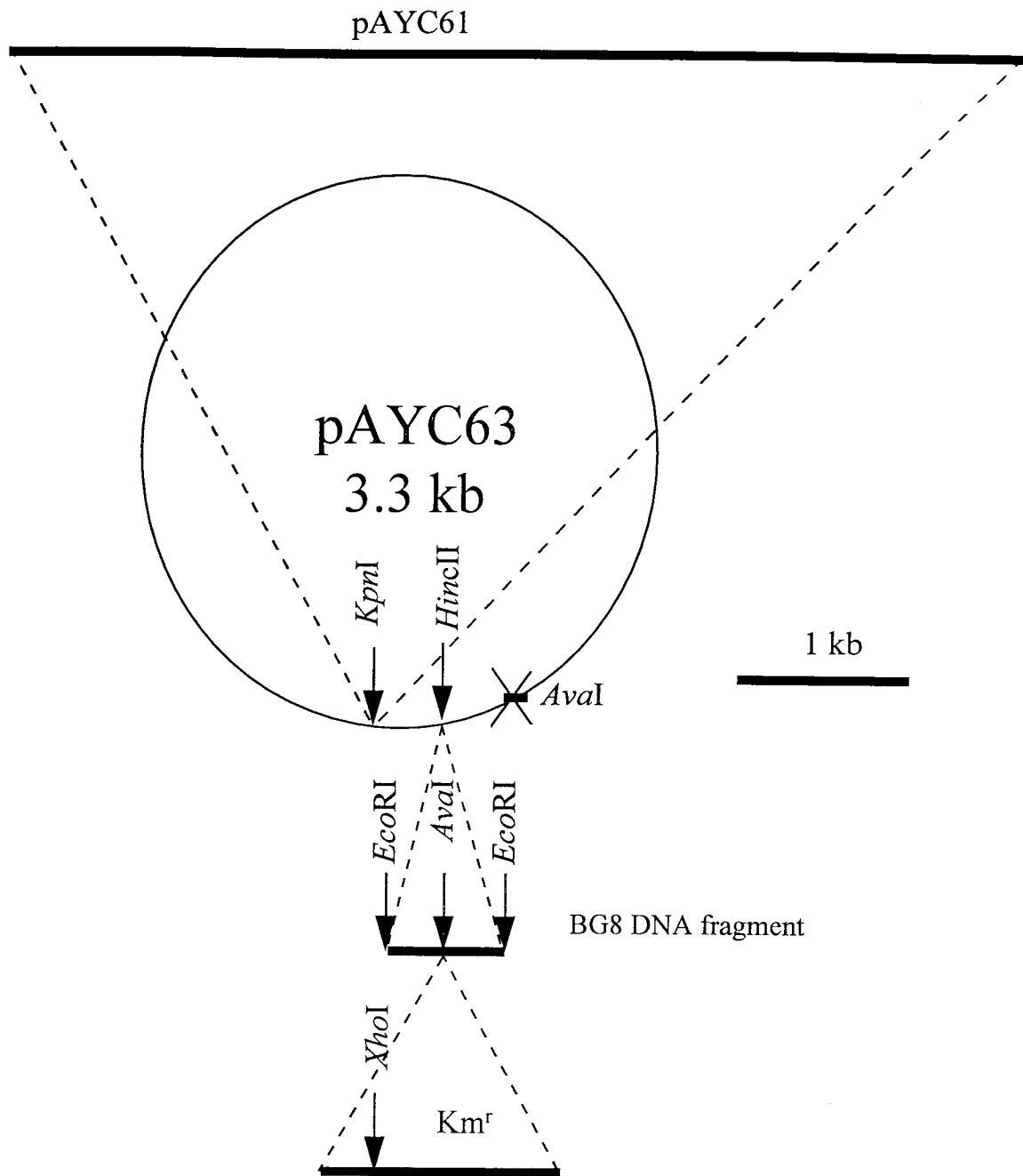


Figure 4.3 Construction of plasmid pOB30 carrying mutated *atpB* gene.

The 611-bp *M. albus* BG8 DNA fragment containing the middle part of *atpB* was cloned into pCRTMII to generate pOB19, then the fragment was recloned into pAYC63 to create pOB24. The *Ava*I site was removed from the polylinker to produce pOB25 with a unique *Ava*I site in *atpB*. Then, *atpB* was disturbed by the insertion of a kanamycin resistance gene (Km^r) to produce pOB26. pOB26 was ligated with the suicide vector pAYC61 to yield pOB30.

1 TGC GCG ACC CCT GCC AAT GCG AT GGG TTT GAT TGG TTAG TGT TTT TTA ATT CCAT GATT CGC
 61 GCAA AGGT GATT CACC AGGCAA AGCA AGCAG CGCC AGCT CCT CCTT ACTTT GCATT TATA
 121 TCAT GATT ATCC GGT TTT CAG TCG AGT ATG ATATA AACT TCG GGA AATTAC GCATAC GAGGA
 181 GAAT GAAT ATGG CTGA ATT CGT TGA ATT GAC AGT GACC GGA ATG AAAT GCG GAGG CTGCG
 241 AAG CCAAC GTCAA AAGCAA ACTGG GCGCG ATCG AC GGC GTGCT GTCG GTG ACC GCGT CGA
 301 GCAAG GAAAAA AAGT CGG CGT C GACT ATG ATGCC GCAAAA ACCG ACTGG CAGCG ATCG
 361 AGG CCGCG ATCG CCGAG GCGG TTT TTT CGG TCGA ATG ATCC GAAT CCG ATGG TAAT CGC
 421 GGAGAGACCTCATGAGCAAAGAAGAAACATCGAACGAACTGCGCTTGTTCGATTTTAGGGA

AtpA ⇒ M S K E E T S N E L R L S I L G M

481 TGAGCTGCGCCGGCTGCGTCAGCGTCTGTCGAAAGCGCGCTGAACGGCGTGCCCGCGTTA
S C A G C V S V V E S A L N G V P G V T

541 CCGAAGTCAGCGTCAACTTTGCGGACCATTCCGCGACCGTCAAAGGCGAGACCGATCCGG
 E V S V N F A D H S A T V K G E T D P E

601 AACGGTTGATCCGGGCCGTCAAGGATGCGGGCTACGAAGCGGCGTAATGGAAGGTTTCG
 R L I R A V K D A G Y E A A V M E G F E

661 AAAATCCGGCGGAACAGGAAGAACAGGAGCTGGCGCGTTACCGGATACTGCTGAAAAAAG
 N P A E Q E E Q E L A R Y R I L L K K A

721 CGGCGGTGCGCCGGTGGCGCCGGCGCCTTGCTGATGCTGCTGGAAATGGCGAACTGGCTGC
A V A G G A G A L L M L L E M A N W L P

781 CGGACATGGGCTCCGCCACCGGACGCTGGTTCTGGCCGGAAGTCGCGATATTGACCCTGG
 D M G S A T G R W F W P E V A I L T L A

841 CGGTACTGGTCTATTCCGGGCGCGCACATTTACCGGGGCGCGCTGAAGGCCCTGCTGTCCG
V L V Y S G A H I Y R G A L K A L L S G

Figure 4.4 Nucleotide sequence and deduced amino acid sequence of 2.2-kb *M. albus* BG8 chromosome region containing *atpA*.

Asterisks indicate stop codons. The nine putative transmembrane domains as predicted by a hydrophobicity plot are underlined. The signature motifs in phosphatase, ion transduction, phosphorylation, and ATP-binding regions are shown in bold. A putative copper binding motif is shown in bold italic. A putative Shine-Dalgarno sequence is double underlined.

901 GGCAGGCGAACATGGATAACCTGATCGCGGTCGGCACCGGCGCCGCCTGGCTCTATTCT
 Q A N M D T L I A V G T G A A W L Y S C

961 GCATCGTGATCGAGTATTACGGCAGCCTGCCGTCCCTGGCCAAGCACGCTTATTTCGAAG
 I V I E Y Y G S L P S L A K H A Y F E A

1021 CCGCAGTCGTGATCCTGGCGTTCATCAACCTGGGTTCGGGCCTCGAAACCCGGGCGCGCG
 A V V I L A F I N L G S G L E T R A R G

1081 GCAAGACTTCATCCGCGATCCGCCAATTGATCGGCCTGCAGCCGCGTACGGCCCGGGTTCG
 K T S S A I R Q L I G L Q P R T A R V V

1141 TTCGGAACGGCGCGGAACCTCGACGTGCCGATCGAGGAAGTCGGCCTCGGCGAAACGCTCA
 R N G A E L D V P I E E V G L G E T L R

1201 GGGTCCGCCCGGCGGAAAAAATCGCGGTCGACGGCGTACTGATCGAAGGCCACTCGTCCG
 V R P G E K I A V D G V L I E G H S S V

1261 TCGACGAATCGATGCTGACCGGCGAACCGATGCCGGCCGAAAAAATCGAAGGCTCCACGG
 D E S M L T G E P M P A E K I E G S T V

1321 TCGCCGCCGGTACGATCAATCAAAGCGGCAGTTTCTCTGTTCAAGGCGACCCGCATCGGCC
 A A G T I N Q S G S F L F K A T R I G R

1381 GCGATACCGCGCTCGCCCAGATCATTACAGCGTGCGCCAGGCGCAGAACAGCAAACCGG
 D T A L A Q I I H S V R Q A Q N S K P E

1441 AAATCGCGCGGCTGGCCGACCGGGTTTCCGCCGTCTTCGTGCCGGCCGTGATCGGCCTCG
 I A R L A D R V S A V F V P A V I G L A

1501 CGGTCTTACCTTTCTGGTCTGGTACGGCTTTGGCCCCGAACCGTCCCTGGGTTATGCGT
 V F T F L V W Y G F G P E P S L G Y A F

1561 TCGTCACTTCGATGACCGTGCTGGTAATCGCCTGCCCTTGC GCGCTGGGCCTTGCCACCC
 V T S M T V L V I A C P C A L G L A T P

Figure 4.4 (continued)

1621 CGATTTCCGGTGATGGTTTCGGTCCGGGAAGGCCGCGCAAACCGGCATACTGATCCGCCAAG
 I S V M V S V G K A A Q T G I L I R Q G
 1681 GCGACGCCTTGCAAACAGCCGGCAAACCTGACCTGCCTGGTGCTGGACAAGACCGGCACCG
 D A L Q T A G K L T C L V L D K T G T V
 1741 TCACTCAGGGCAAGCCGAAGGTCGTGTCGATCGAAGGCCGCCGGCGGTTTTTCCGAAACCG
 T Q G K P K V V S I E G A G G F S E T E
 1801 AAGTGCTGCAACTCGCGTCCAGCCTCGAAGCCGGCTCCGAGCATCCGCTGGCGGCGGCCG
 V L Q L A S S L E A G S E H P L A A A V
 1861 TGTTGACGGCGGCGCGGGAACACGCGGTCCAACCGAAAAAATGGCCCAATTCAAGGCGA
 L T A A R E H A V Q P K K M A Q F K A I
 1921 TCACCGGCCACGGCGTCAAGCGACGCAGGACGGCCGCCGCGTTCGTATTTCGGCAACCGGG
 T G H G V E A T Q D G R R V V F G N R A
 1981 CGCTCCTGGAGAAGGAAGGCATCGATCTCGCAAGCCATCAGGACAACCTCGCCAGACTCA
 L L E K E G I D L A S H Q D N L A R L S
 2041 GCGCCGAAGGCAAACGCCGATGCTGCTCGCGGTGACCGGCAGTTCGCCGGGATCGTTG
 A E G K T P M L L A V D R Q F A G I V A
 2101 CCGTCGCCGATCCGATCAAGCCCGATTCCGCCGCCGCGGTACAGCGGCTGCGCAACCTGG
 V A D P I K P D S A A A V Q R L R N L G
 2161 GCATCCGCGTACTGATGGTGACCGGCGACAATCCGATCACGGCCCGGGCGATCGCCCGGG
 I R V L M V T G D N P I T A R A I A R E
 2221 AAGCCGGCATTGCCGAAGTCAGGGCGCAAGTGCTGCCGCAGGATAAGGCGGCCGTGGTCA
 A G I A E V R A Q V L P Q D K A A V V R
 2281 GGGAAGTGCAGGCCCAAGGCGAAACGGTCCGGCATGGTCCGGCGACGGCATCAACGATGCGC
 E L Q A Q G E T V G M V G D G I N D A P

Figure 4.4 (continued)

2341 CGGCGCTCGCGCAGGCCGATGTCGGCCTCGCCATCGGGACCGGCACCGACGTGCCATCG
 A L A Q A D V G L A I G T G T D V A I E
 2401 AAAGCGCGGACGTGGTGATCCTGCAAGGTTGCTGATGAAAGTGCCGGAAGTGATCCGAC
 S A D V V I L Q G S L M K V P E V I R L
 2461 TGTCGCAGCTTACCGTGGCCAATATCAAACAAAACCTGTTGCGGCCTTTTTCTACAACA
 S Q L T V A N I K Q N L F G A F F Y N T
 2521 CGATCAGCATTCCGGTCGCCGCCGGCCTTTTGTATCCTTTCGCCGGCATCCTGCTGAATC
 I S I P V A A G L L Y P F A G I L L N P
 2581 CGATGATCGCGGGCGCGGCGATGGCGATGTCTTCGCTGACCGTGGTCAGCAATGCCAATC
 M I A G A A M A M S S L T V V S N A N R
 2641 GCCTGCGCTGGCAAAAACTTTGACCCCGCATTTCTTCCCCGAGACGGGCCCGTGCGCGC
 L R W Q K L *
 2701 AGAGCCAGGACCGTCTTCGATTCATCATCCGACGATTCCGGTGACTAGACGCTCCTGCGC
 2761 AAGGACCGGCTAAATTGCCCCATCGGAAAGCGATCACTTCGGCAATCGTTCGGCGGCTGCC
 2821 TGGGCTTGTGCCCCGTTTTCGCCCGGGGCGGCGGAAATCATCGTCAACGTCTCGGTCCCGT
 2881 CCGCGCATTACTCACGCGCCGATACCCGGGCAATCTTCGCGATGCATCTGAGGATCTGGC
 2941 CTAACGGCGAACCGATCAAGGTCTTTACGCTAACCGACGACAACCCGGTCCATAAAGACT
 3001 TCGTCAAGAACAGCCTGAACATGTTTCCGCACCAGTTCCGGCGCGTCTGGGACCGAATGA
 3061 TCTACTCCGGTA

Figure 4.4 (continued)

1 TGAATTCGCCCTGGCCACCCCCGTCGTGTTGTGGGGCGGCTGGCCTTTTTTTCAACGCGG

AtpB⇒E F A L A T P V V L W G G W P F F Q R G

61 AGGGTCTTCTGTGCTGACTCGCCGCCTGAATATGTTTACCTTGATTGCGTTGGGAATCGG

G S S V L T R R L N M F T L I A L G I G

121 CGTCGCCTGGATTTACAGTGTGCTGGCCTCCTTTCTGCCGCAGATCTTCCCGTCGTCGCT

V A W I Y S V L A S F L P Q I F P S S L

181 GCGGGATCAGCAGGGTFCGGGTGGCGGTGTATTTTGAAGCGGCGGCGGTGATCACGACGCT

R D Q Q G R V A V Y F E A A A V I T T L

241 GGTTTTACTCGGCCAAGTGCTGGAATTGCGGGCCAGAAGCCGAACCAGCGCGGCGATTAA

V L L G Q V L E L R A R S R T S A A I K

301 ACTGTTGCTGGGATTGGCGCCCAAGACCGCCCGGCTTCACCATGCCGACGGCAGCGAGAC

L L L G L A P K T A R L H H A D G S E T

361 GGATATTCCCTTGAGCAAGTGAAGCCCGCGATATTCTGCGGGTGCGGCCAGGCGAGAA

D I P L E Q V K P G D I L R V R P G E K

421 AATACCGGTGGACGGGATCGTGATCGAAGGCATCAGCGCGGTTGATGAATCGATGGTAAC

I P V D G I V I E G I S A V D E S M V T

481 GGGTGAGCCGGTGCCGGTTGAGAAATTGACGGATATGCCGCTGATCGGTGCGACGATTAA

G E P V P V E K L T D M P L I G A T I N

541 CGGCACCGGGAGCTTGCTGATGCGTGCCGAACCGTCCGGCAGCGAAACCTGCTTTCCCA

G T G S L L M R A E R V G S E T L L S Q

601 AATTGTGCACATGGTTCGGTGAAGCGCAACGCAGCCGGGCGCCGATTCAAAAATTGGCCGA

I V H M V G E A Q R S R A P I Q K L A D

Figure 4.5 Nucleotide sequence and deduced amino acid sequence of the 1.96-kb *M. albus* BG8 chromosome region containing a fragment of *atpB*.

Asterisks indicate stop codons. The six putative transmembrane domains as predicted by a hydrophobicity plot are underlined. The signature motifs in phosphatase, ion transduction, phosphorylation, and ATP-binding regions are shown in bold.

661 TACGGTTTCCGGCTACTTTGTTCCCGCAGTGGTGCTGACGGCCGCCATTACGCTTGTCGT
 T V S G Y F V P A V V L T A A I T L V V
 721 CTGGTGGCGTTGGGGGCCCCGAGCCCCGATTGGCCCACGCGGTCGTGAACGCGGTAGCGGT
 W W R W G P E P R L A H A V V N A V A V
 781 GTTGATTATCGCTTGTCCCTGTGCCCTGGGATTGGCCACCCCGATGTCGATCATGGTCGG
 L I I A C P C A L G L A T P M S I M V G
 841 TACCGGGCGCGGGGCGACGGCGGGTGTCTGATTAAAAATGCCGAAGCGCTGGAAGTAAT
 T G R G A T A G V L I K N A E A L E V M
 901 GGAAAAAGTGGACACCCTGGTTCGTTGATAAAAACCGGCACGCTCACCGAAGGCAAACCGCG
 E K V D T L V V D K T G T L T E G K P R
 961 ACTGATCACGGTCGAGGCGGCCAACGGCTTCACGAAGGAAGAGGTCTTGGCTTATGCGGC
 L I T V E A A N G F T K E E V L A Y A A
 1021 CGGTCTGGAACGGGCCAGCGAACATCCGCTTGGCGGGCGATCGGCAAAGGCGCAGAAGC
 G L E R A S E H P L A A A I G K G A E A
 1081 GCAGGGGCTAAAACCGCTGCCTGTGCGCCGAGTTTCAATCGCTGACCGGTAGAGGAGTGGT
 Q G L K P L P V A E F Q S L T G R G V V
 1141 CGGGATGATAAACGGCAGGAACGTGGCGTTGGGGAATGCGCAGTTGATGAAGGACTCGGG
 G M I N G R N V A L G N A Q L M K D S G
 1201 CATCGCGACGGACATTTTGACAAACTCGATGGAGACGTTGCGCCAACAAGGCCAAACGGT
 I A T D I L T N S M E T L R Q Q G Q T V
 1261 CGTAATGATCGGGATCGACGGTAAAGCGGCCGACTTCTCGGCGTAGCCGATCCGATCAA
 V M I G I D G K A A G L L G V A D P I K
 1321 GCCTACCGCCTTCAAAGCCTTGGCGGACTTGCATAAAGAAGGCATTTCGGGTGGTGTGTT
 P T A F K A L A D L H K E G I R V V M L

Figure 4.5 (continued)

1381 AACCGGCGACAATCGCACCCACGGCCGAGTTTGTGGCCAAAAGCCTGAGGATCGATCAACT
 T G D N R T T A E F V A K S L R I D Q L
 1441 GCAGGCGGAAGTGTTCGGGAGCAAAAAACCGAGGTGATCAAAAAATTACAGGGTGAAGG
 Q A E V L P E Q K T E V I K K L Q G E G
 1501 CCGTATCGTCGCGATGGCCGGCGACGGTATCAACGATGCGCCGGCCTTGGCGGCGGCCCA
 R I V A M A G D G I N D A P A L A A A H
 1561 CATCGGCATCGCGATGGGCACGGGCACGGACGTCGCGATGGAAAAGTTCCGGCATTACGCT
 I G I A M G T G T D V A M E S S G I T L
 1621 CGTGAAAGGGGATCTGATGGGGCTGGTCAAAGCCCGCCATTTAAGTCGGGCGACTTTGCG
 V K G D L M G L V K A R H L S R A T L R
 1681 TAATATCCGCCAGAACCTGTTTTTCGCGTTTTATCTACAATGCCCTGGGCGTGCCCGTTGC
 N I R Q N L F F A F I Y N A L G V P V A
 1741 CGCCGGCGCGCTCTATCCGTTTTTCGGTATTCTCTTGTCTCCGATGATTGCGGCGGCCGC
 A G A L Y P F F G I L L S P M I A A A A
 1801 GATGAGTCTCAGCTCGGTTTTTCGGTCAATCGGCAATGCGTTGCGGCTCAGGCGGGTGACATT
 M S L S S V S V I G N A L R L R R V T L
 1861 ATAAATAGAAAATACCTGGCAAGGTGTGTAGAAGAGAATCCTCTTGGGAGCGGCCAACCTT
 *
 1921 TTCAAACGATATGTCCCATGGACGAAGTAGGGGTAGCGGCAG

Figure 4.5 (continued)

661 GATCGCCTCCCTGGCGATGGCGTTGAGCTCGCTCTCGGTGGTGCTCAATTCGCTGCGCTT
I A S L A M A L S S L S V V L N S L R L
 721 GAGTAAAAAGTAGGTTTTTCGGCATGGATCATTTCGATGATGGATCACGCCGCGATGCAGGG
 S K K * *orf1* ⇒ M D H S M M D H A A M Q G
 781 CATGGCGGAGGCCGCTGCTGCAGCCGGCGGCTTCGATTACACACTCGCCTTCGTCGCGGG
 M A E A A A A A G G F D Y T L A F V A G
 841 TTTTTTGGGCAGTGGCCATTGCCTCGGCATGTGCGGCGCACTGGTGTCCGGCTATTTTCAT
 F L G S G H C L G M C G A L V S G Y F M
 901 GAACGCCGGCAAACAGCGCTCGTATTGGCCGTATCTGTTGTATCAGGCTGCGCGCATCTC
 N A G K Q R S Y W P Y L L Y Q A A R I S
 961 GGTTTACGGCCTGATCGGCATCGCCGCCGCGCTGCTCGGCCTGGTGTGGTGTGCGGGCGG
 V Y G L I G I A A A L L G V V L V S G G
 1021 AGTATTCGGCAAAAATCCAGAGCATTTTACAGATGCTGATCGGTCTTGTGGTGTGATCGGCCT
 V F G K I Q S I L Q M L I G L V V I G L
 1081 CGCGCTCGGCATTTTGGGCTGGCTGCCCGGCAAGGCGCGTTGCGCCTGTTGCCCGTGCA
 A L G I L G W L P R Q G A L R L L P V Q
 1141 ATGGCTGCGCAAAGGCTATGCGGCCTCCCGGCGGCAAGGCCCCCTCGGCGGTGCGCTCCT
 W L R K G Y A A S R R Q G P L G G A L L
 1201 GGCGGGCTTATTGAACGGCATGATGCCGTGCCCGTTGACCTTTGCGATGGCGGTAAAAGC
 A G L L N G M M P C P L T F A M A V K A
 1261 GGTCACCGCCCCGAACGTTCTCGGCGGCGGCACGCTGATGCTCGCGTTTCGGCGCCGGCAC
 V T A P N V L G G G T L M L A F G A G T
 1321 CCTGCCCATGATGCTGTTTATCACCTTGCTTTTCGGCAGAATCCAA
 L P M M L F I T L L S A E S

Figure 4.6 (continued)

```

Atpa M S K E E T S N E L R L S I D G M S C A G C V S V V E S A L N G V P G V T E V S V N F A D H S A T V K G E T D P P E R L I R A V K D A G Y E A A V M E G F E N P A E Q E E E Q E L A R Y 90
Atpb 0
Atpc 0

Atpa R I L L K K A A V A G G A G A L L M L L E M A N W L P D M G S A T G R W F W P P E X A I L L T L A V L V Y S G A H I Y I R G A L K A L L S G Q A N M D T L I A V G T G A A W I Y S C I V I 180
Atpb 50
Atpc 50

Atpa E Y Y C S L P S L A K H - - - - A Y F E A A V I L A F I N L G S G L E T R A R G K T S A I R Q L I G L Q P R T A R V V R - N G A E L D V P P I E V I G L G E T L R V R P P G E K 263
Atpb 140
Atpc 0

Atpa I A V D G V L I E G H S I S V D E S M L T G E P M P A E K I E G S T V A A G T I N Q S G S F L F K A T R I G R M D T A I A Q I I H S V R Q A C N S K P P E A R L A D R V S A V F V P A V 353
Atpb 230
Atpc 0

Atpa I G L A V T F L V W Y G F G P E P S L G Y A F V T S M T V L V I A C P C A L G L A T P I S V M V S V G K A A Q T G I L I R Q G D A L Q T A G K L T C L V L D K T G T V T Q G K P K 443
Atpb 320
Atpc 0

Atpa V V S I E G A G G F S E T E V L Q L A S S L E A G S E H P L A A A V L T A A R E H A V Q P K K M A Q F K A I T G H G V I E A T Q D C R R V V I F C N A L L E K E G T D L A S H Q D N D 533
Atpb 410
Atpc 28

Atpa A R L S A E C K T H M L L A V D R Q F A G T V A V A D P I K P D S A A A V Q R L R N L G I R V L M V T G D N P I T A R A I A R E A G I A E V R A A Q V L P Q D K K A A V V R E L Q A Q G 623
Atpb 500
Atpc 118

Atpa E T V G M V G D G I N D A P A L A Q A R D I V G L A I G T G T D V A I E S A D V V I L Q G S L M K V P E V I R L S Q L T V I A N I Y O N L F G A F P Y N T I S I P V A A G L L Y P P A G I 713
Atpb 590
Atpc 201

Atpa L L N P M I A G A A M A M S S T T V V S N A M R L R W Q K L I -
Atpb 743
Atpc 229

```

Figure 4.7 Sequence comparison of AtpA and partially sequenced AtpB and AtpC. The conserved regions are boxed. The ion transduction motif conserved in all heavy metal ATPases is indicated by asterisks. Dashes represent areas not sequenced. The amino acid sequences targeted by the primers are underlined.

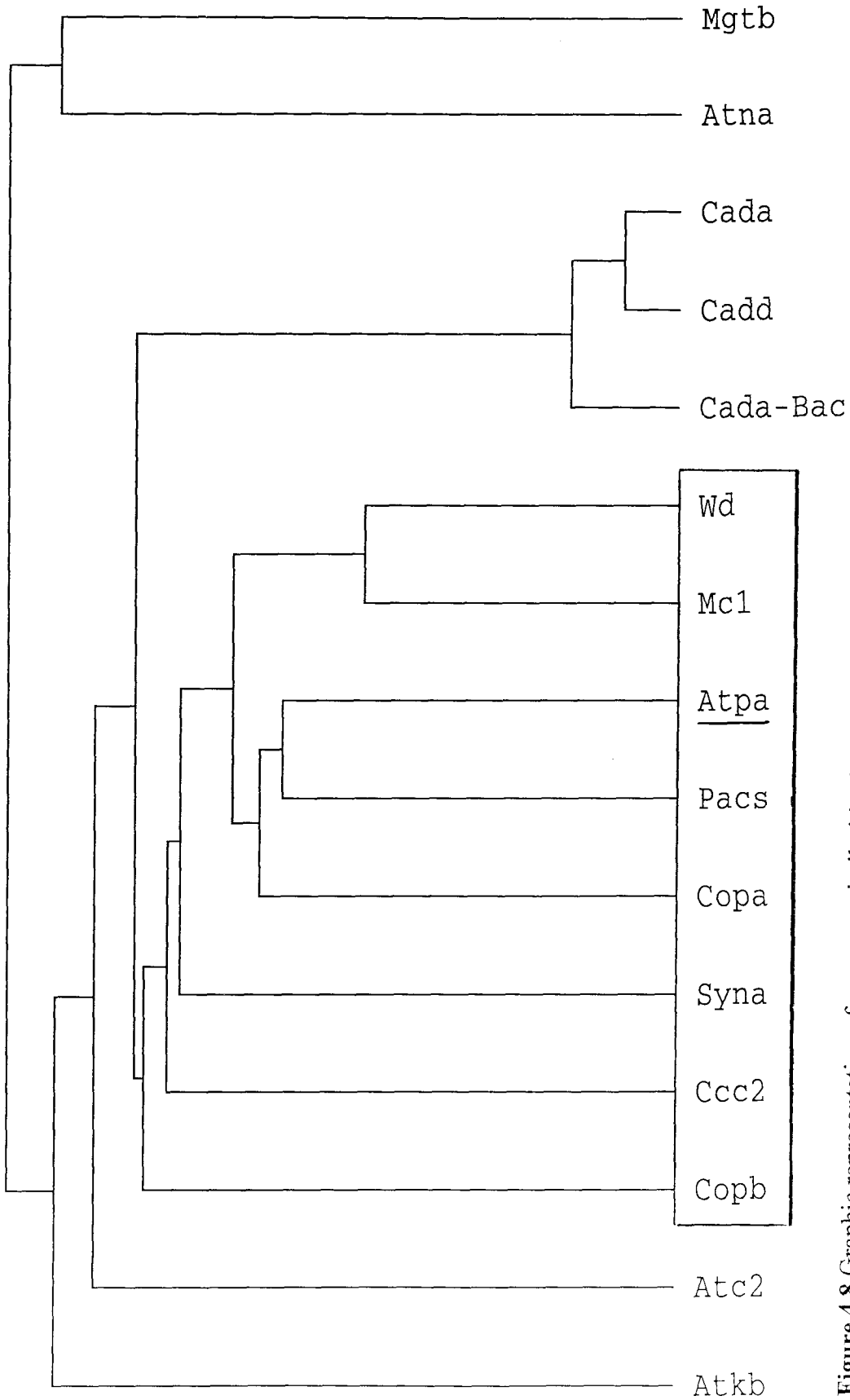


Figure 4.8 Graphic representation of sequence similarities between cation transporting ATPases.

The diagram was generated by the program Pileup of GCG Group. The shorter the branch length, the more closely related the sequences. The accession numbers for the sequences are the same as in Figure 4.1. Copper ATPase subfamily is boxed. AtpA (this study) is underlined.

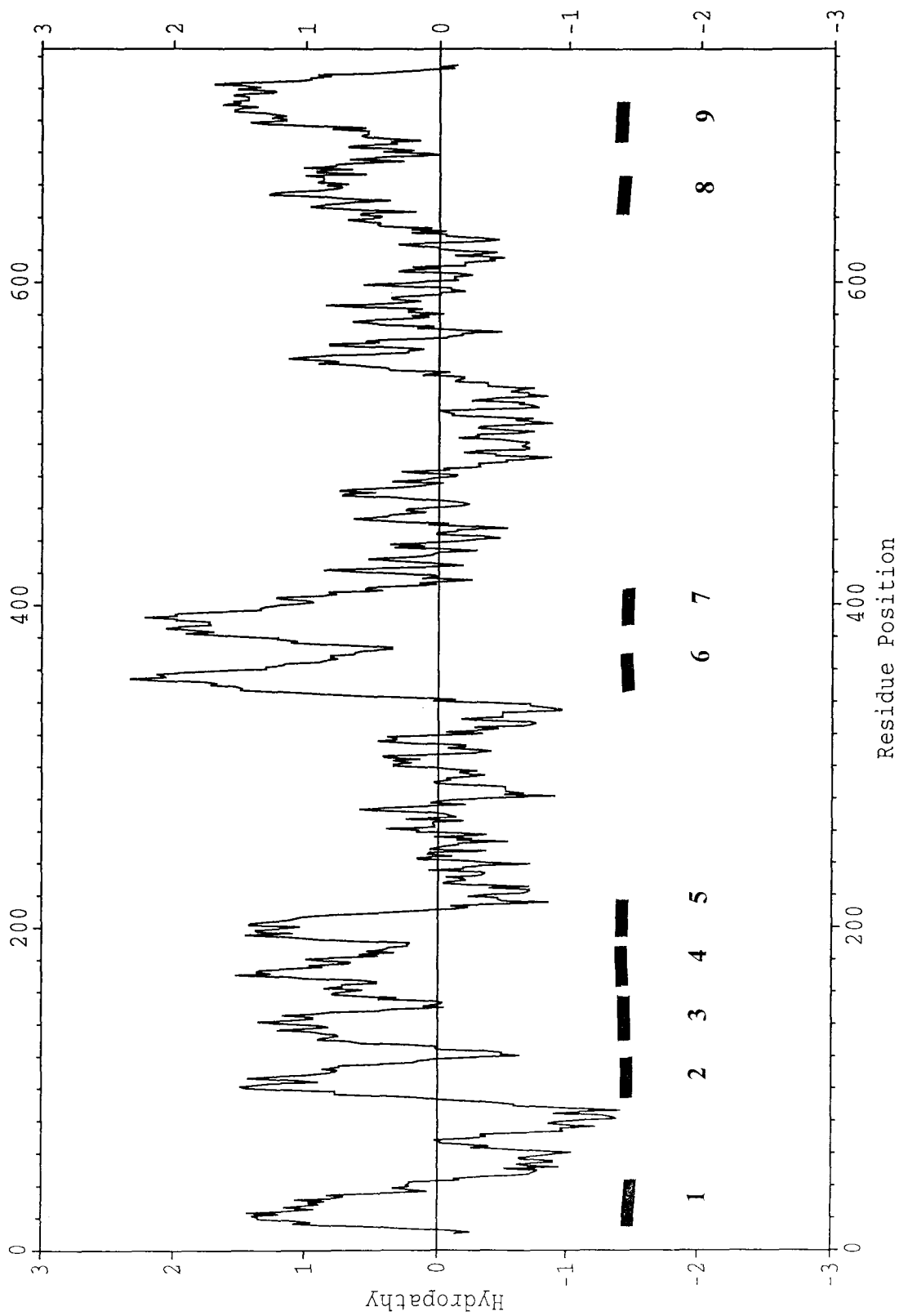


Figure 4.9 Predicted hydropathy plot of the *atpA* gene product using the Kyte and Doolittle algorithm (1982) over a span of 20 residues. The numbered bars indicate the polypeptide sequence fragments that have peaks of hydrophobicity and a length sufficient to form a putative transmembrane domain.

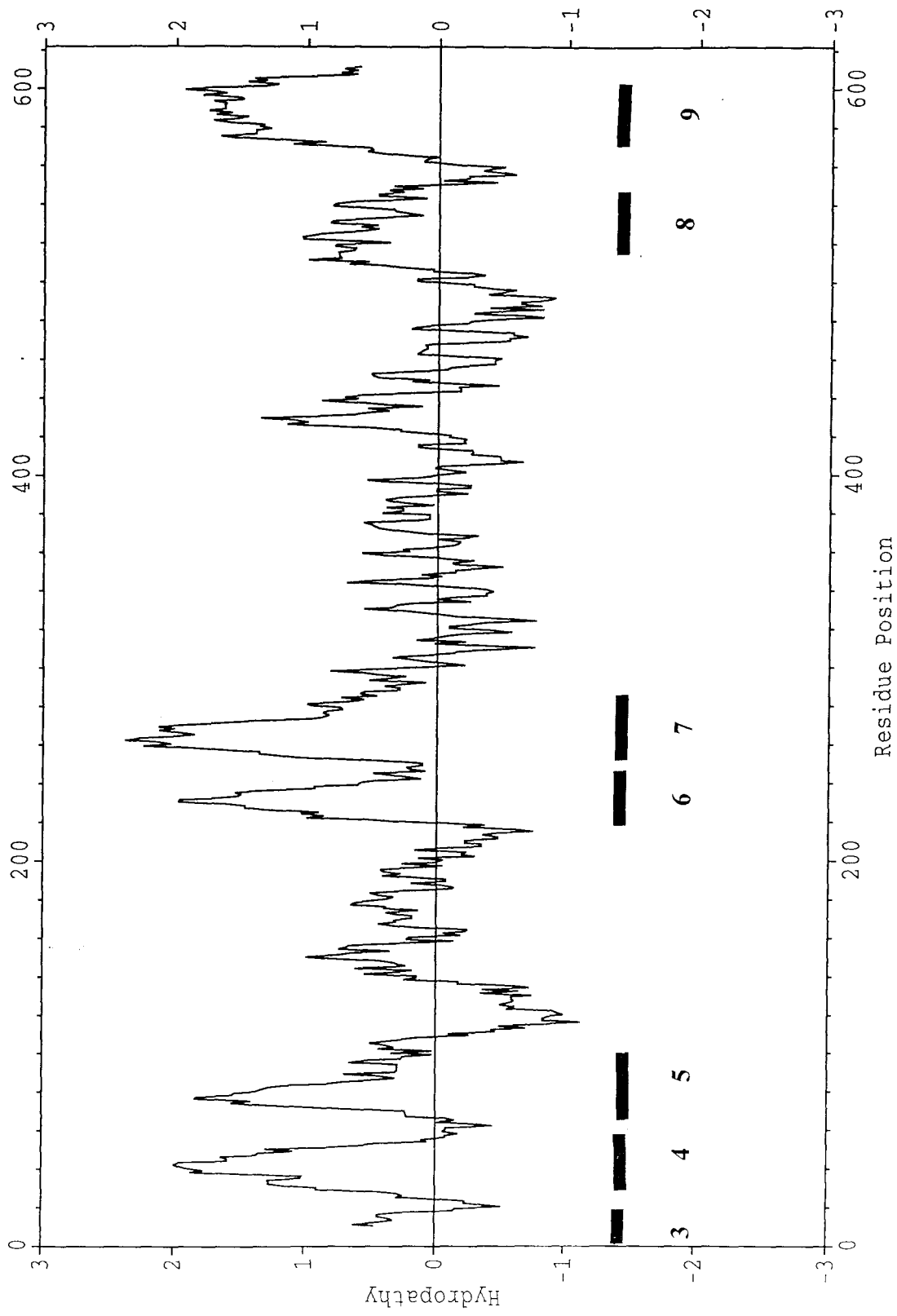


Figure 4.10 Predicted hydropathy plot of the C-terminal fragment of the *atpB* gene product using the Kyte and Doolittle algorithm (1982) over a span of 20 residues. The numbered bars indicate possible transmembrane domains.

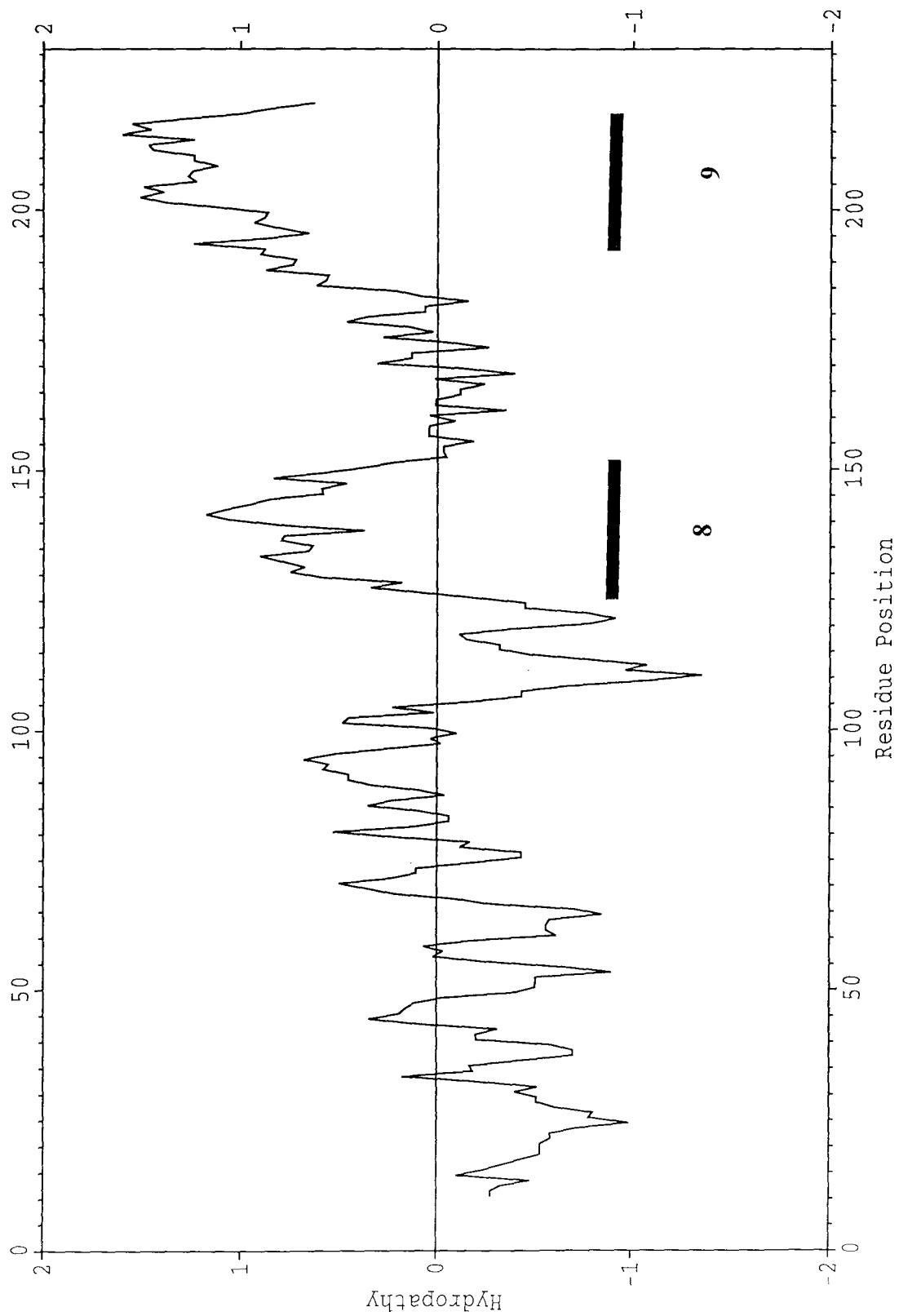


Figure 4.11 Predicted hydropathy plot of the C-terminal fragment of the *atpC* gene product using the Kyte and Doolittle algorithm (1982) over a span of 20 residues. The numbered bars indicate possible transmembrane domains.

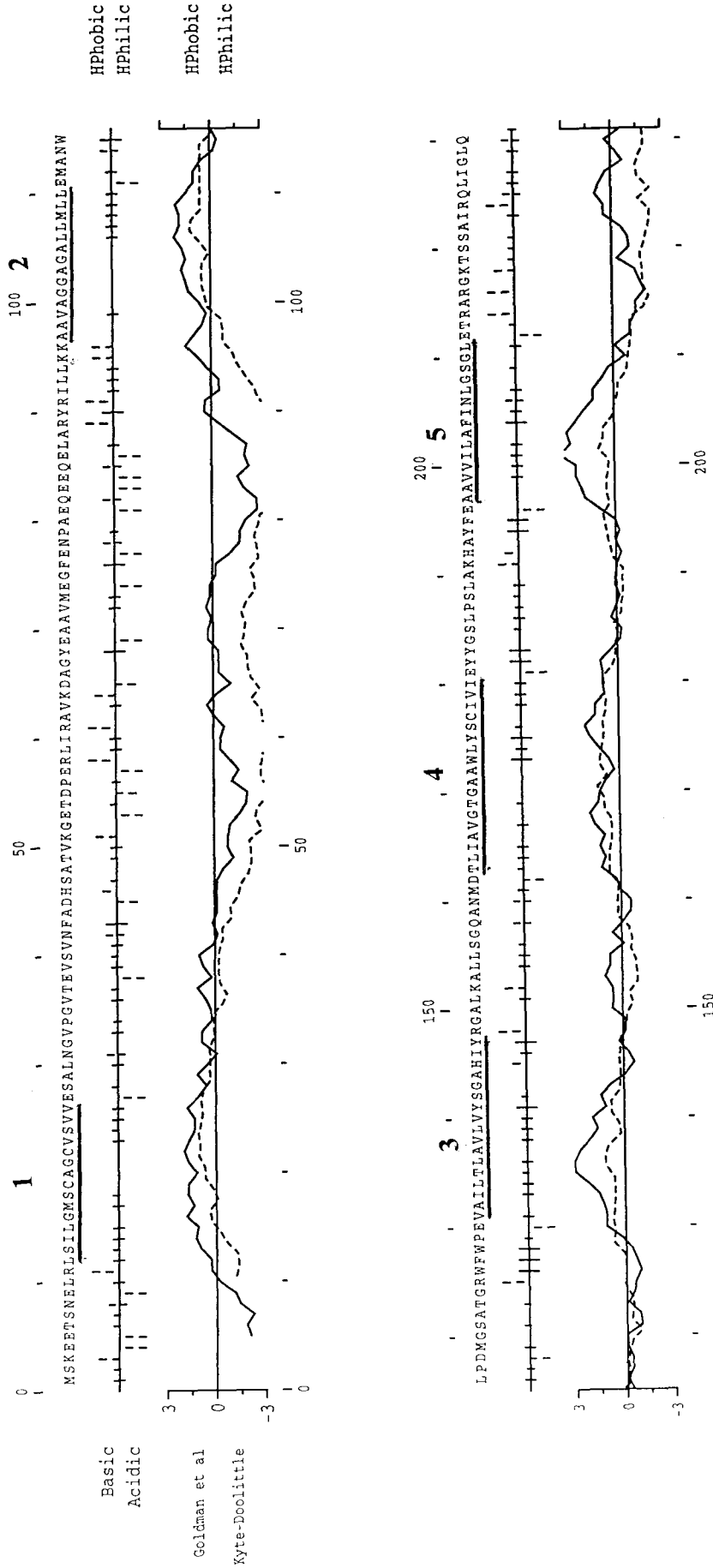


Figure 4.12 Charge (top) and hydrophobicity (bottom) profiles of AtpA. Hphobic, hydrophobic; Hphilic, hydrophilic. Putative membrane domains are underlined and numbered. Only the fragments of the sequence containing such domains are shown.

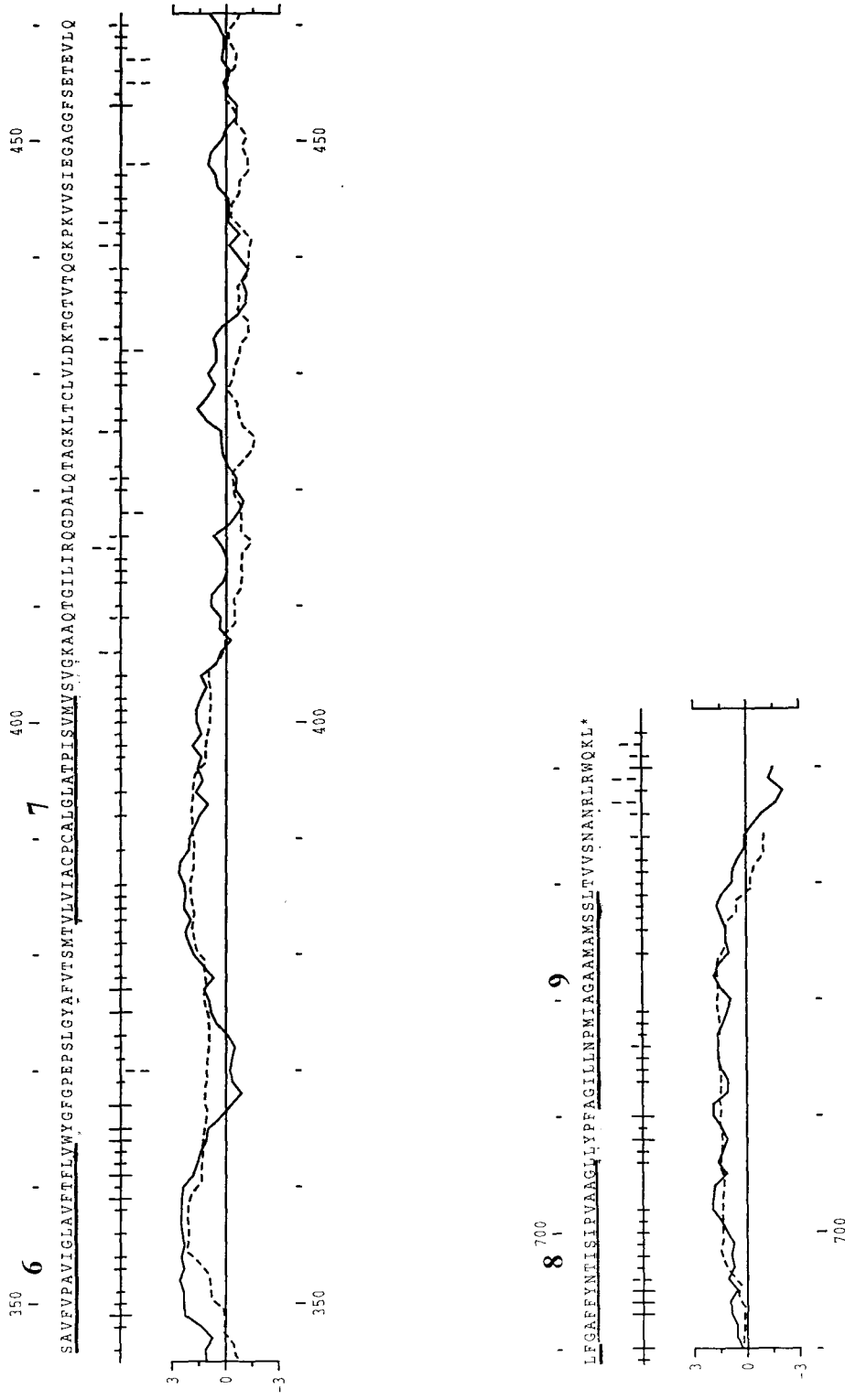


Figure 4.12(continued)

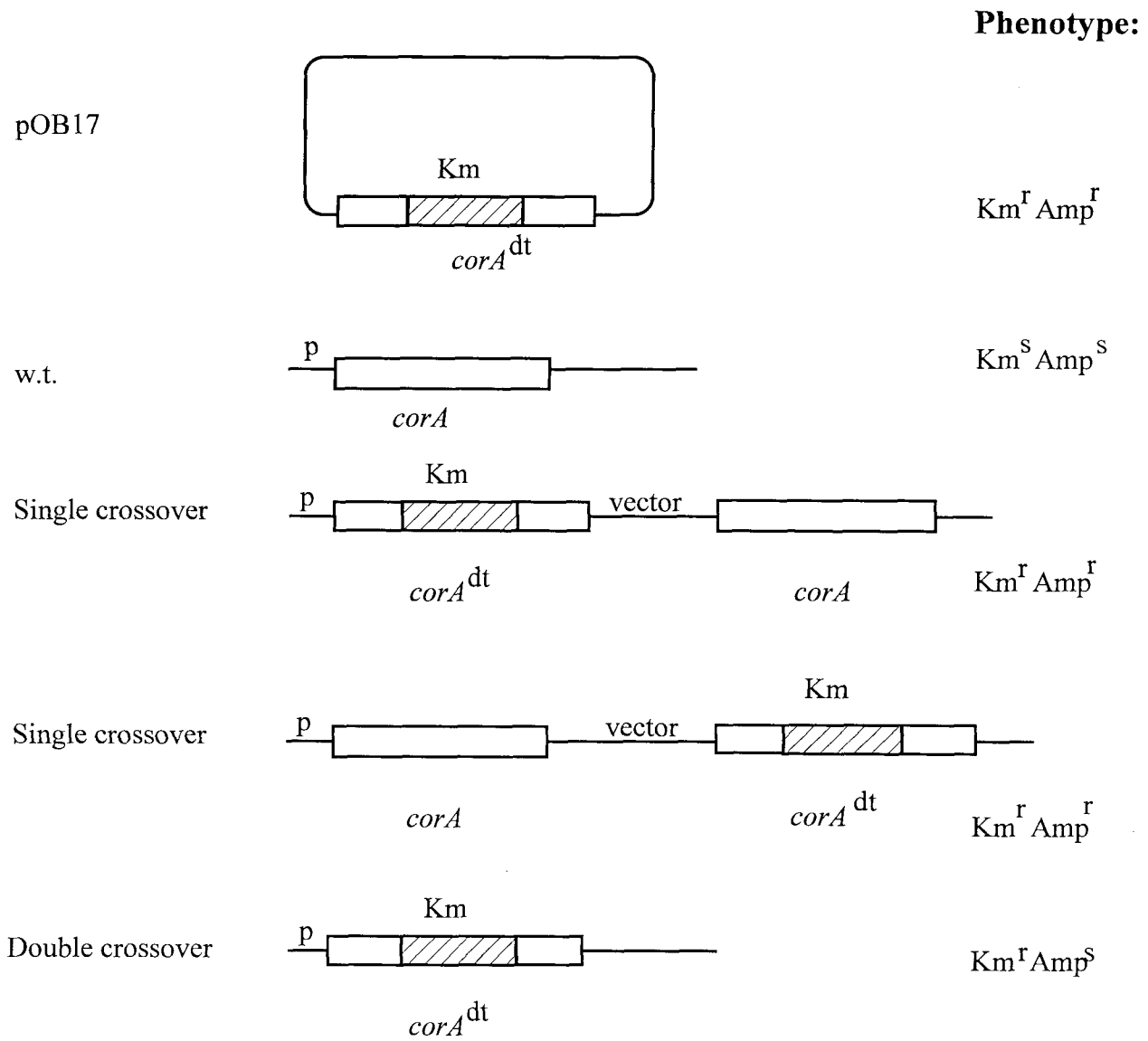


Figure 4.13 The phenotypes of wild-type (w.t.), single and double crossover *atpB* mutants of *M. albus* BG8.

p, a promoter; *atpB*, gene encoding a putative copper P-type ATPase; *atpB*^{dt}, *atpB* deleted by an insertion of kanamycin resistance cassette (Km).

Appendix

Polymerase Chain Reaction (PCR) Method for DNA Amplification *in vitro*.

The PCR method utilizes thermostable *Taq* polymerase, which catalyzes the addition of nucleotides to the growing chain of preexisting DNA. To use the method for obtaining sufficient amounts of desired gene(s) for cloning or other purposes it is necessary to know a portion of the gene sequence to create primers. Primers are 18-22 nucleotide sequences that are complementary to sequence of gene(s) of interest. A PCR cycle involves three steps: (1) heat denaturation of double-stranded DNA to split it into two separate molecules; (2) cooling of the PCR reaction to allow hybridization of the primers to the DNA template; (3) primer extension by synthesis of a new DNA molecule complementing the template; this step is catalyzed by *Taq* polymerase (Figure A4.1). A PCR cycle is usually repeated 20 to 30 times, yielding up to a billion-fold increase in the target DNA concentration (Brock and Madigan 1991)

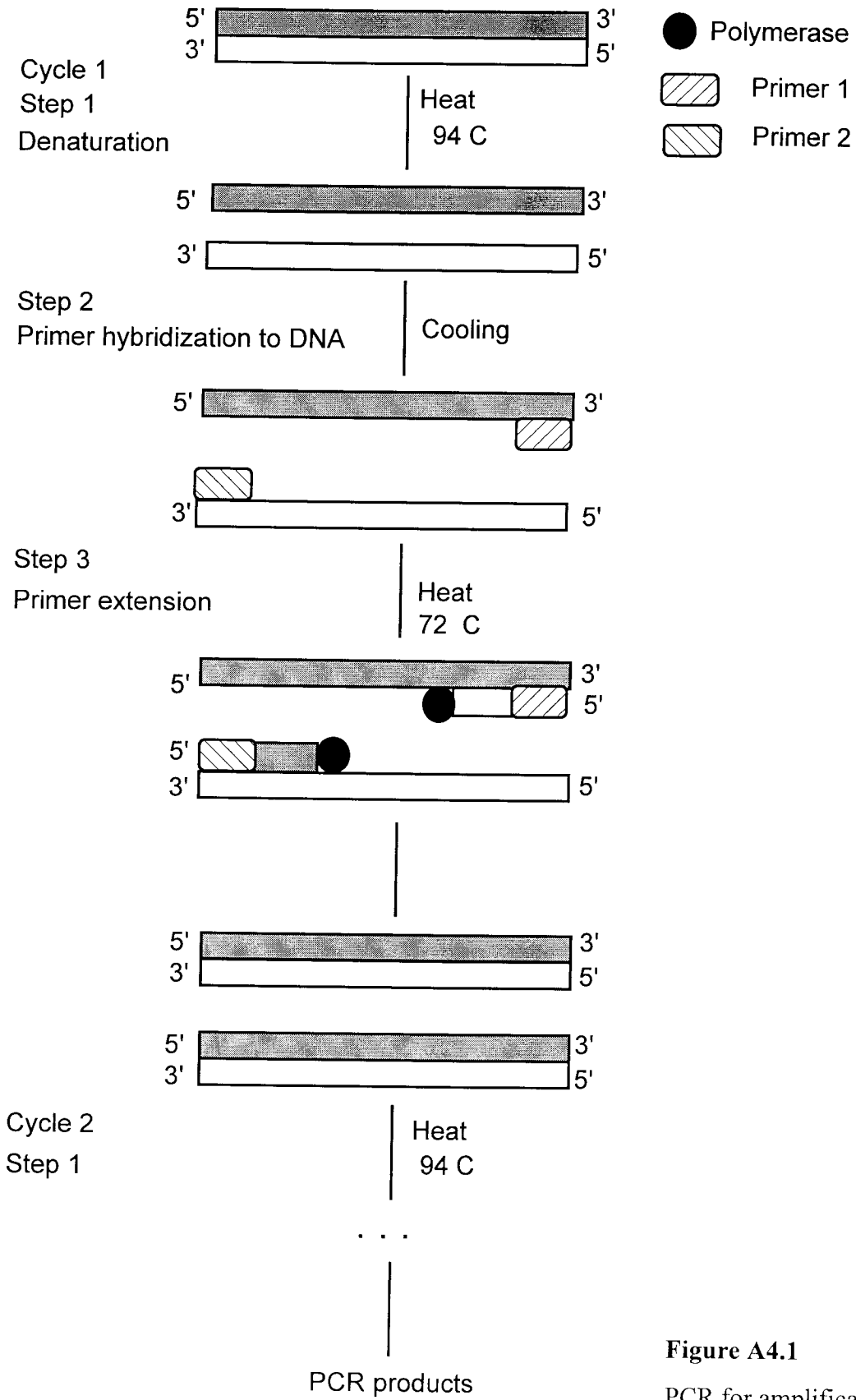


Figure A4.1
PCR for amplification of target genes.

Chapter Five

Conclusions

The possible future application of methanotrophs in biodegradation of trichloroethylene (TCE) depends on our understanding of all the major factors involved in the process. It is known that particulate methane monooxygenase (pMMO), found in all methanotrophs, can oxidize TCE and remove it to levels below the drinking water standard (DiSpirito *et al.* 1992). Recent studies (Chan *et al.* 1993; Nguyen *et al.* 1994) have identified trinuclear copper clusters in pMMO as the catalytic sites of the enzymatic activity. Moreover, it has been shown that the kinetics of TCE oxidation by pMMO are strongly affected by copper concentrations in the growth medium (Semrau 1995; Smith 1996). Therefore, an understanding of copper bioavailability and uptake in methanotrophs is important for optimization of *in situ* TCE bioremediation. This project has made significant progress in assessing the effect of copper speciation in the growth medium on copper accumulation by the type I methanotroph *Methylomicrobium albus* BG8 (Chapter Two), as well as in recognizing and evaluating possible copper uptake mechanisms in this microorganism (Chapters Three and Four).

5.1. Copper Speciation Affects Copper Uptake by *M.albus* BG8.

Copper is widely present in the environment, however, over 99% of the total copper is complexed by organic ligands, which results in cupric ion concentrations of

10^{-10} to 10^{-18} M (Hodgson *et al.* 1965; Sunda and Ferguson 1983; Sunda and Hanson 1987; Coale and Bruland 1988; Hering and Morel 1988; Berggren 1989; Coale and Bruland 1990; Moffett *et al.* 1990; Van den Berg *et al.* 1990, Bruland *et al.* 1991; Van den Berg and Donat 1992). Although several copper species can coexist in an environment, there is a general agreement in the literature on a key role of cupric ion in toxicity and in biological uptake of copper in all studied organisms, from bacteria to animals (Sunda and Guillard 1976; Anderson and Morel 1978; Zevenhuizen *et al.* 1979; Blust *et al.* 1986; Coale and Bruland 1990; Bruland *et al.* 1991; Langford and Guzman 1992).

In this research the relationship between copper accumulation and cupric ion concentration in the medium was investigated in the type I methanotroph *M. albus* BG8 at copper concentrations that were neither growth limiting nor toxic (Chapter Two). The disappearance of cupric ion from the growth medium was studied using a copper-selective electrode, and was compared with total copper accumulation by the cells assayed by inductively coupled plasma mass spectrometry. The amount of copper accumulated by the cells was related to the cupric ion concentration rather than to that of total copper added to the growth medium, as has been seen previously in other organisms. Copper accumulation demonstrated a hyperbolic dependence on cupric ion concentration, suggesting saturation of copper binding sites on the cell surface. A mean maximum binding capacity was estimated as $(1.54 \pm 0.06) \times 10^{-15}$ moles/cell, and an apparent half saturation constant as $(1.43 \pm 0.05) \times 10^{-7}$ moles/l. Sorption experiments established that most of the copper accumulated by the cells was nonspecifically sorbed

to external sites (e.g., amino acid, carboxylic, hydroxy groups, etc.). Copper that was not removed by EDTA during a 24-h treatment was assumed to be either inside the cells or bound to specific copper transport sites. The copper concentration measured in the cells after the EDTA wash was essentially constant at $1-3 \times 10^{-17}$ moles of copper per cell despite a 100-fold variation in medium total copper and cupric ion concentrations. This result implies the presence of a specific copper uptake system in *M. albus* BG8 regulated by the copper concentration in the medium.

5.2. Copper Uptake in *M. albus* BG8 Involves Membrane Proteins.

Several transport mechanisms described in Chapter One (1.5. and 1.6.) could be involved in copper uptake by methanotrophs, such as a periplasmic binding-protein dependent mechanism (Figure 5.1A); an active transport via a copper P-type ATPase (Figure 5.1B); a siderophore-type high-affinity system (similar to the one in iron uptake)(Figure 5.1C); and copper accumulation in a special periplasmic storage protein for pMMO assembly (Figure 5.1D). All except a siderophore type mechanism might involve an outer membrane component, such as a porin, which facilitates copper transport from the outside into the periplasm. It is not uncommon for the cells to have more than one transport system with different affinities for a substrate, therefore, a combination of several transport systems from Figure 5.1 might be employed in methanotrophs.

By analogy to other uptake systems in bacteria, it is expected that a specific copper uptake system would be copper-regulated. Therefore, membrane and soluble fractions of *M. albus* cells were screened for the presence of copper-regulated

polypeptides (Chapter Three). One such copper-repressible membrane polypeptide, CorA, was identified, and the corresponding gene, *corA*, was cloned and sequenced. An insertion mutant defective in the gene was constructed, but it grew very poorly on plates or in liquid culture. This result confirms the vital significance of CorA to *M. albus* cells. DNA and protein data base analysis revealed some homology of CorA to rabbit and human calcium release channel protein. This, together with the fact that the expression of CorA seems to be regulated by copper (it was isolated as a major copper-repressible polypeptide), makes it plausible that CorA might be a divalent metal porin. It was not possible to confirm the specificity of CorA because of the poor growth of the CorA mutant.

To study the hypothesis that P-type ATPases might be involved in copper uptake by *M. albus* BG8 cells, a partial clone library of *M. albus* BG8 chromosome was screened with a labeled PCR product obtained with a pair of primers designed from the consensus sequences of two known copper ATPases (Chapter Four). Three putative copper ATPase genes, *atpA*, *atpB*, *atpC*, were cloned and sequenced (*atpA* was completely sequenced, while *atpB* and *atpC* were sequenced only partially). From the sequences analysis and comparison with DNA and protein data bases it appears that all three cloned genes are closely related to each other and that they belong to the group of heavy metal transporting ATPases, possibly they are members of the copper ATPases subfamily. The fact that only single crossover mutants were obtained when an insertion mutation was attempted in one of the genes, suggests that this gene is required for normal growth of *M. albus* BG8.

A project in progress is focusing on the identification and study of extracellular compounds excreted by *M. albus* BG8 under conditions of copper limitation. The siderophores identified so far in the literature (mainly in iron acquisition) have been chemically classified as hydroxamates and catechols (Martinez *et al.* 1990). Copper has a high affinity for these ligands and possibly can be accumulated by some bacteria in the same way as iron (Hider 1984). Preliminary data from potentiometric titration experiments with *M. albus* BG8 have suggested that some extracellular copper-complexing material is excreted by the cells (Lloyd and Kwan, personal communication). The chemical nature of these compounds is currently under investigation, but preliminary qualitative tests identified the presence of hydroxamate functionality in media in which cells were grown under copper limitation (Lloyd and Kwan, personal communication). The possibility of siderophore-type copper uptake in *M. albus* BG8 is being pursued by Dr. Morgan's group.

The following hypothesis for copper uptake in *M. albus* BG8 is suggested by the data presented in this research. One or more copper P-type ATPase(s) appears to be involved in copper uptake and /or copper efflux in *M. albus* BG8. Since in all gram-negative bacteria P-type ATPases are situated in the inner membrane (Figure 5.1B), it is possible that the copper-repressible protein (CorA) described in Chapter Three may be an outer membrane porin that works in tandem with the putative copper ATPase(s) (Chapter Four). Such a porin would not necessarily be specific for copper, and might be overexpressed under conditions of any divalent metal limitation to facilitate the metal diffusion into periplasm. Such a scenario, however, does not exclude the possibility that

other uptake mechanisms presented in Figure 5.1 might be involved in copper transport in *M. albus* BG8.

This project has suggested a number of further studies into the mechanisms of copper transport in methanotrophs. First, the cellular location of CorA and the putative copper ATPases should be confirmed, by expression of the cloned genes in an alternative host, and the possible regulation of CorA by other metals should be investigated. Next, the sequences of *atpB* and *atpC* should be completed, and mutants should be generated that are defective in AtpA and AtpC, to test their phenotype. These genes should be tested for their ability to complement *E. coli* CopA and CopB mutants, to further investigate their functions. Finally, the existence of copper-binding siderophore-like compounds should be addressed, as well as the role of such compounds in copper uptake under different copper-related growth conditions.

5.3. Summary

- Cu accumulation by *M. albus* BG8 depends on the concentration of cupric ion $[\text{Cu}^{2+}(\text{H}_2\text{O})_6]$ in the growth medium.
- At high total copper concentrations in the growth medium, most of the accumulation is apparently due to non-specific sorption to outer cell layers.
- Total Cu/cell that is not removable by EDTA, presumably inside the cell, is relatively constant, indicating the presence of a specific homeostasis mechanism for copper.
- A membrane protein (CorA) that is over expressed in the absence of copper (copper-repressible) is required for significant growth of *M. albus* BG8, and may be a divalent metal porin.
- *M. albus* BG8 contains at least three genes whose products show homology to the protein subfamily of P-type copper ATPases.
- One of these genes was sequenced in its entirety, and it contains the P-type copper ATPase copper-binding signature sequence, suggesting that it does play a role in copper transport.

References

- Anderson, D. M. and F. M. M. Morel.** 1978. Copper sensitivity of *Gonyaulax tamarensis*. *Limnol. Oceanogr.* **23(2)**:283-295.
- Berggren, D.** 1989. Speciation of aluminum, cadmium, copper, and lead in humic soil solutions - a comparison of the ion-exchange column procedure and equilibrium dialysis. *Intern. J. Environ. Anal. Chem.* **35**:1-15.
- Blust, R., E. Verheyen, C. Doumen, and W. Decler.** 1986. Effect of complexation by organic ligands on the bioavailability of copper to the Brine Shrimp, *Artemia* sp. *Aquatic Toxicology* **8**:211-221.
- Bruland, K. W., J. R. Donat, and D. A. Hutchins.** 1991. Interactive influences of bioactive trace metals on biological production in oceanic waters. *Limnol. Oceanogr.* **36**:1555-1577.
- Chan, S. I., H. H. T. Nguyen, A. K. Shiemke, and M. E. Lidstrom.** 1993. Biochemical and biophysical studies toward characterization of the membrane-associated methane monooxygenase, p. 93-107. In J. C. Murrell and D. P. Kelly (eds.), *Microbial Growth on C1 Compounds*. Intercept, Andover.
- Coale, K. H. and K. W. Bruland.** 1988. Copper complexation in the Northeast Pacific. *Limnol. Oceanogr.* **33**:1084-1101.
- Coale, K. H. and K. W. Bruland.** 1990. Spatial and temporal variability in copper complexation in the north pacific. *Deep-Sea Research* **37**:317-336.
- Dispirito, A. A., J. Gullede, J. C. Murrell, A. K. Shiemke, M. E. Lidstrom, and C. L. Krema.** 1992. Trichloroethylene oxidation by the membrane associated methane monooxygenase in type I, type II and type X methanotrophs. *Biodegradation* **2**:151-164.
- Hering, J. G. and F. M. M. Morel.** 1988. Kinetics of trace-metal complexation: role of alkaline-earth metals. *Environ. Sci. Technol.* **22**:1469-1478.
- Hodgson, J. F., H. R. Geering, and W. A. Norvell.** 1965. Micronutrient cation complexes in soil solution: partition between complexed and uncomplexed forms by solvent extraction. *Soil Sci. Society Proceedings* 665-669.
- Martinez, J. L., A. Delgadoiribarren, and F. Baquero.** 1990. Mechanisms of iron acquisition and bacterial virulence. *Fems Microbiology Reviews* **75**:45-56.

Moffett, J. W., R. G. Zika, and L. E. Brand. 1990. Distribution and potential sources and sinks of copper chelators in the Sargasso Sea. *Deep-Sea Research* **37**:27-36.

Nguyen, H. H. T., A. K. Shiemke, S. J. Jacobs, B. J. Hales, M. E. Lidstrom, and S. I. Chan. 1994. The nature of the copper ions in the membranes containing the particulate methane monooxygenase from *Methylococcus capsulatus* (Bath). *J. Biol. Chem.* **269**(21):14995-15005.

Semrau, J.D. 1995. Kinetic, biochemical, and genetic analysis of the particulate methane monooxygenase. Ph.D. dissertation, Caltech, Pasadena.

Smith, K. S. 1996. Enrichment dynamics of a marine methanotrophic population and its kinetics of methane and TCE oxidation. Ph.D. dissertation, Caltech, Pasadena.

Sunda, W. and R. R. L. Guillard. 1976. The relationship between cupric ion activity and the toxicity of copper to phytoplankton. *J. Mar. Res.* **34**:511-529.

Sunda, W. G. and R. L. Ferguson. 1983. Sensitivity of natural bacterial communities to addition of copper and cupric ion activity: a bioassay of complexation in seawater. *Mar. Sci.* **4**:871-891.

Sunda, W. G. and A. K. Hanson. 1987. Measurement of free cupric ion concentration in seawater by a ligand competition technique involving copper sorption onto C₁₈ SEP-PAK cartridges. *Limnol. Oceanogr.* **32**:537-551.

Vandenberg, C. M. G. and J. R. Donat. 1992. Determination and data evaluation of copper complexation by organic ligands in sea water using cathodic stripping voltammetry at varying detection windows. *Anal. Chim. Acta* **257**:281-291.

Vandenberg, C. M. G., M. Nimmo, P. Daily, and D. R. Turner. 1990. Effects of the detection window on the determination of organic copper speciation in estuarine waters. *Anal. Chim. Acta* **232**:149-159.

Zevenhuizen, L. P. T. M., J. Dolfing, E. J. Eshuis, and I. J. Scholten-Koerselman. 1979. Inhibitory effects of copper on bacteria related to the free ion concentration. *Microbiol. Ecol.* **5**:139-146.

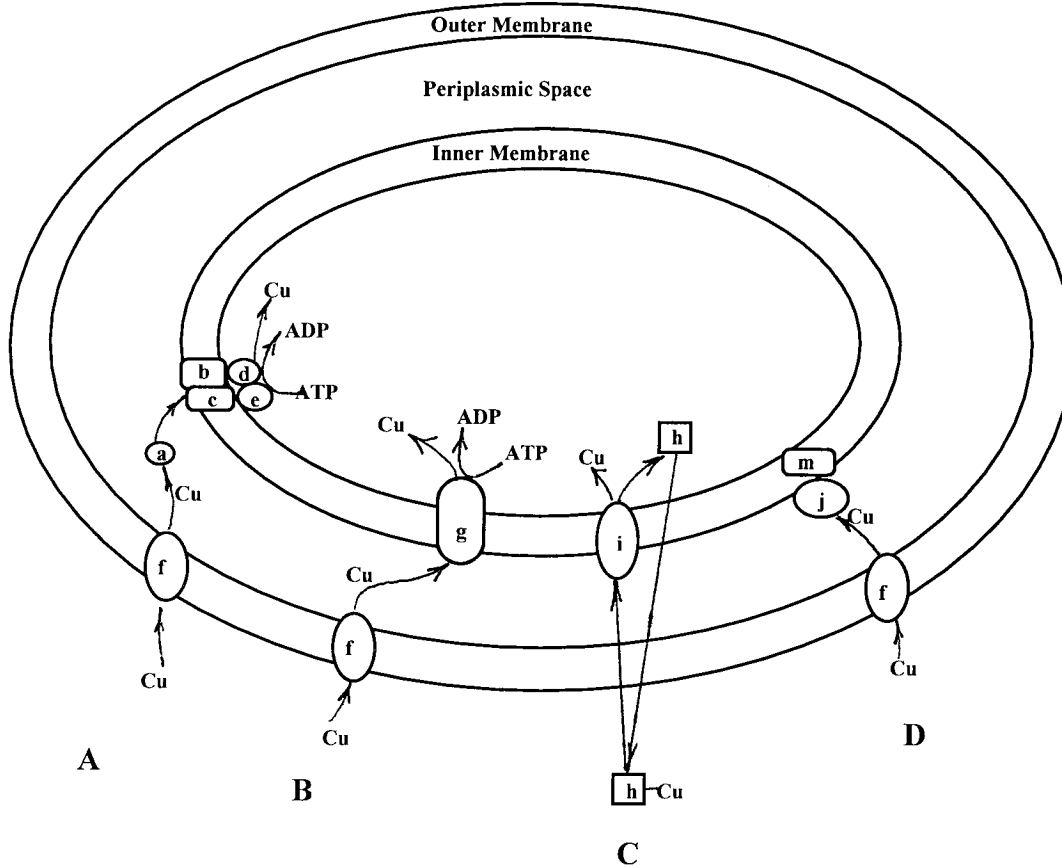


Figure 5.1 Schematic representation of the different types of transport systems that might be employed in copper uptake by *Methylomonas albus* BG8.

- A.** Binding-protein dependent mechanism. **a**, periplasmic substrate-binding protein; **b,c,d,e**, inner membrane-associated proteins. **d,e**, proteins that couple ATP hydrolysis to the transport. **f**, outer membrane porin
- B.** Copper transport via P-type ATPase (**g**) exposed to both cytoplasm and periplasm. Copper bound on the periplasmic side can be carried through the membrane by a conformational change of the protein.
- C.** A high-affinity system, consisting of low-molecular-weight copper chelator (**h**) and a specific membrane receptor (**i**).
- D.** Passive diffusion through porin (**f**) with further copper accumulation in a special periplasmic storage protein (**j**) for pMMO (**m**) assembly.